Analysis of $\Delta^0(1232)$ Production in $p+^{12}C$ and $d+^{12}C$ Collisions at 4.2 GeV/c Per Nucleon

By

Imran Khan

CIIT/FA10-PPH-002/ISB

PhD Thesis

In

Physics

COMSATS Institute of Information Technology
Islamabad-Pakistan
Spring 2013

COMSATS Institute of Information Technology

Analysis of $\Delta^0(1232)$ Production in $p+^{12}C$ and $d+^{12}C$ Collisions at 4.2 GeV/c Per Nucleon

A Thesis Presented to

COMSATS Institute of Information Technology, Islamabad

In partial fulfillment

Of the requirement for the degree of

PhD Physics

By

Imran Khan

CIIT/FA10-PPH-002/ISB

Spring, 2013

Analysis of $\Delta^0(1232)$ Production in $p+^{12}C$ and $d+^{12}C$ Collisions at 4.2 GeV/c Per Nucleon

A Post Graduate Thesis submitted to the Department of Physics as partial fulfillment of the requirement for the award of Degree of PhD (Physics)

Name	Registration Number
Imran Khan	**CIIT/FA10-PPH-002/ISB**

Supervisor
Dr. Khusniddin Olimov
HEC Foreign Professor
Department of Physics
COMSATS Institute of Information Technology, Islamabad

Co-Supervisor
Dr. Mahnaz Q. Haseeb
Professor
Department of Physics
COMSATS Institute of Information Technology, Islamabad

Final Approval

This thesis titled

Analysis of $\Delta^0(1232)$ Production in p+^{12}C and d+^{12}C Collisions at 4.2 GeV/c Per Nucleon

By

Imran Khan
CIIT/FA10-PPH-002/ISB
Has been approved
For the COMSATS Institute of Information Technology, Islamabad

External Examiner: _____
Dr. Mahmood-Ul-Hassan
Department of Physics, University of Punjab, Lahore

External Examiner: _____
Prof. Dr. Fayyazuddin
National Center for Physics, Quaid-i-Azam University, Islamabad

Supervisor: _____
Dr. Khusniddin Olimov
HEC Foreign Professor, Department of Physics
COMSATS Institute of Information Technology, Islamabad

HoD: _____
Prof. Dr. Arshad Saleem Bhatti
Head of Department of Physics
COMSATS Institute of Information Technology, Islamabad

Chairman: _____
Prof. Dr. Sajid Qamar
Chairman, Department of Physics
COMSATS Institute of Information Technology, Islamabad

Dean, Faculty of Sciences: _____
Prof. Dr. Arshad Saleem Bhatti
Dean, Faculty of Sciences
COMSATS Institute of Information Technology, Islamabad

Declaration

I **Imran Khan**, registration Number **CIIT/FA10-PPH-002/ISB,** hereby declare that I have produced the work presented in this thesis, during the scheduled period of study. I also declare that I have not taken any material from any source except referred to wherever due that amount of plagiarism is within acceptable range. If a violation of HEC rules on research has occurred in this thesis, I shall be liable to punishable action under the plagiarism rules of the HEC.

Date: _____

Signature of the Student:_____

Imran Khan

CIIT/FA10-PPH-002/ISB

Certificate

It is certified that **Imran Khan**, registration Number **CIIT/FA10-PPH-002/ISB**, has carried out all the work related to this thesis under my supervision at the Department of Physics, COMSATS Institute of Information Technology (CIIT), Islamabad and the work fulfills the requirement for award of PhD degree.

Date: _____

Supervisor:

_____

Dr. Khusniddin Olimov

HEC Foreign Professor
Department of Physics
COMSATS Institute of Information Technology, Islamabad

Head of Department:

_____

Prof. Dr. Arshad Saleem Bhatti

Head of Department of Physics,
COMSATS Institute of Information Technology, Islamabad

Dedicated To

My Family ...

Abbu, Amee,

Shakeel, Idrees, Tufail, Adnan

And Pyari Behna ...

They do their best for me...

ACKNOWLEDGEMENTS

All of my praises are running towards the Almighty ALLAH, the most Merciful and the most Beneficent. He blessed me the opportunity to take admission in PhD in the field of High Energy Physics and gave me enough strength and patience to complete it.

I feel pleasure to express my deep and sincere thanks to my supervisor, HEC Foreign Professor, Dr. Khusniddin Olimov from Department of Physics, COMSATS Institute of Information Technology, Islamabad, for his best guidance, continual help, and encouragement throughout the course of this research work. Without his careful attention and encouragement, this thesis would have never been completed. I am also very grateful to my co-supervisor Professor Dr. Mahnaz Q. Haseeb, Department of Physics, COMSATS Institute of Information Technology, Islamabad, for her tremendous help, valuable suggestions and affectionate guidance.

I wish to extend my sincere gratitude to Prof. Dr. Sajid Qamar, Chairman, Department of Physics, to Prof. Dr. Arshad Saleem Bhatti, HoD of Physics and Dean, Faculty of Sciences, and to Dr. S. M. Junaid Zaidi, Rector, COMSATS Institute of Information Technology, Islamabad, for providing me all the required facilities to complete my PhD studies and research in Physics at COMSATS Institute of Information Technology, Islamabad. I also wish to thank the staff and colleagues from the Department of Physics, COMSATS Institute of Information Technology, Islamabad, for their moral and practical help throughout this research work. I would like to give my special thanks to Prof. Dr. Mais Suleymanov, Dr. Ijaz Ahmad, and PhD students Ali Zaman and Akhtar Iqbal for their various support and encouragement.

I am also very thankful to the Higher Education Commission (HEC), Islamabad, for providing me the financial support under the “Indigenous MS Leading to PhD 5000 Scholarships Program” during the whole period of my studies. Without HEC assistance it would not be possible for me to continue my studies after getting M. Sc. in Physics.

I am very grateful to my friend Aamir Sohail Mughal and his family for their full cooperation during my MS and PhD studies. His sincere friendship has made it easier for me to complete my studies.

I have no words to pay thanks to my family members. How can I thank my Father, my Mother, and my Grand Father for their countless prayers and lots of hardships they suffered during my studies? My head is bowed before their sacrifices. I am very grateful to my dear brothers Muhammad Shakeel Ahmad, Muhammad Idrees Khan, Muhammad Tufail Khan, Muhammad Adnan Khan, my Sweet Sister and Uncle Muhammad Younas, and Muhammad Ismail for their full support during my studies.

I thank all my relatives, especially Zahid, Zubair, Israr, Daniyal, and friends: especially Liaqat Ali Khan, Muhammad Sameen, Khalil-ur-Rahman, Zahir Ahmad, Muhammad Sadeeq, Khalil Ahmad, and Rafi Ullah for their best wishes for me.

Imran Khan

ABSTRACT

Analysis of $\Delta^0(1232)$ Production in p+^{12}C and d+^{12}C Collisions at 4.2 GeV/c Per Nucleon

Production and various properties of $\Delta^0(1232)$ resonances in p+^{12}C and d+^{12}C collisions at a momentum of 4.2 GeV/c per nucleon were analyzed. The mass distributions of $\Delta^0(1232)$'s in both collision types were reconstructed by analyzing the experimental and background invariant mass distributions of proton and negative pion pairs with the help of angular criterion. The emission angle, rapidity, momentum, transverse momentum, and kinetic energy distributions of $\Delta^0(1232)$'s were reconstructed for both collision types and their mean values extracted. Analyzing the reconstructed transverse mass spectra of $\Delta^0(1232)$'s, the freeze-out temperatures of $\Delta^0(1232)$'s were estimated for both collision types. The parameters and various characteristics of $\Delta^0(1232)$ resonances produced in p+^{12}C and d+^{12}C collisions at the same incident momentum per nucleon were compared with each other to get the valuable information about the role of the weakly bound neutrons of projectile deuterons in $\Delta^0(1232)$ production. The spectral temperatures of $\Delta^0(1232)$'s produced in p+^{12}C and d+^{12}C interactions at 4.2 GeV/c per nucleon were extracted by analyzing the transverse momentum spectra of $\Delta^0(1232)$'s in the framework of Hagedorn Thermodynamic Model and compared with the corresponding temperatures of negative pions in p+^{12}C and d+^{12}C collisions.

TABLE OF CONTENTS

LIST OF FIGURES

LIST OF TABLES

LIST OF ABBREVIATIONS

JINR	Joint Institute for Nuclear Research (Dubna, Russia)
DCM	Dubna Cascade Model
QGSM	Quark-Gluon-String Model
c.m.s.	Center-of-mass system
d	deuteron (^{2}H nucleus)
hh	Hadron–Hadron
hA	Hadron–Nucleus
AA	Nucleus–Nucleus
NN	Nucleon–Nucleon
p_t	Transverse momentum
$\sqrt{s_{NN}}$	Total nucleon–nucleon center-of-mass energy
$\Delta^0(1232)$'s	$\Delta^0(1232)$ resonances

Chapter 1

Introduction

1.1 Introduction

Resonances with short lifetimes and their couplings to a nuclear medium have unique characteristics to examine various features of the medium created in relativistic hadron–nucleus and nucleus–nucleus interactions. Among these are the $\Delta(1232)$ resonances, which are the lowest excited states of nucleons having very short lifetimes of about 10^{-23} s. They belong to a class of nucleon or baryon resonances and play an important role in the particle physics. Baryon resonances are believed to be produced during the early compression phase of the interactions. The average values of mass (M_{Δ}) and width (Γ) of $\Delta(1232)$'s produced in collisions of nucleons with nucleons are 1232 and $115-120$ MeV$/c^2$ [1], respectively. It is believed that the main source of pion production in central heavy ion interactions at incident energies of the order of few GeV per nucleon is the decay of baryon resonances [2]. The $\Delta(1232)$ resonances decay in about 99% cases through the $\Delta \rightarrow N\pi$ channel producing nucleons and pions. To study the production of $\Delta(1232)$ resonances, much experimental and theoretical research work [2–22] has been done in the past. For this purpose, various strong and electromagnetic interactions triggered by pions, protons, photons, light nuclei, and heavy ions have been analyzed. The mass and width of $\Delta(1232)$ produced in dense media created in the high energy central collisions of hadrons and nuclei with nuclei were significantly lower as compared to the mass and width of $\Delta(1232)$ produced in free nucleon collisions. This decrease in the mass and width of $\Delta(1232)$ resonances generated in dense hadronic matter could be explained in the framework of thermal and isobar models [2, 3]. These modifications were also related to the value of hadronic density, temperature, and non-nucleon degrees of freedom (collective phenomena) in a nuclear matter [2–5]. However, still many experimental findings on $\Delta(1232)$ resonances are not understood completely, and not a single theoretical model is able to explain all the observed properties of $\Delta(1232)$ resonances produced in relativistic hadron–nucleus and nucleus–nucleus interactions [6, 7].

The $\Delta(1232)$ resonances control different phenomena related to nuclei at the energies beyond the threshold of pions production (280 MeV for π^0 mesons and 290 MeV for π^-

and π^+ mesons) [9, 23–26]. In cosmology, the CMB (cosmic microwave background) suppresses the flux of high energy cosmic rays and thus the "Greisen-Zatsepin-Kuzmin (GZK) cut-off" effect [27] occurs, and Δ(1232) resonances are believed to be mostly responsible for this effect. If the energies of the cosmic rays are adequate (energy threshold = 1.08 GeV) to yield Δ(1232) resonances in the processes of scatterings with the photons of the cosmic microwave background, then the rate of observed cosmic rays decreases suddenly [28]. The energies of the initial cosmic rays reaching from distances greater than many tens of Mpc (1Mpc ≈ 3.09 x 10^{22} m) get a cutoff at around about 10^{13} MeV due to this effect [9, 28].

The possibility of a phase transition of a nuclear matter into the state of quark gluon plasma has been discussed and researched extensively for a last few decades. The necessary conditions for creation of quark gluon plasma are either high temperatures or high baryonic densities, or both of them. It was predicted earlier [29] that the nuclear matter in an excited state passes through a phase transition from a hadronic matter to a de-confined state of quarks and gluons at sufficiently high baryon densities. In nature, it is believed that the state of quark gluon plasma occurs in neutron stars, while in the laboratories it could be achieved in the central collisions of ultra relativistic heavy nuclei. The nuclear matter spectrum on a border to a phase transition is expected to be complicated. It is believed that the lower states of this spectrum are connected with excitations of Δ(1232)'s and other resonances [6]. Hence, information on Δ(1232)'s produced in a nuclear medium can help to understand better the properties of a nuclear matter produced in ultra relativistic nuclear collisions [6, 7].

Structures identified in the invariant mass distributions of proton–pion pairs proved that nucleons are excited to baryon resonances [8]. The large combinatorial background of non correlated proton–pion pairs is a major obstacle in extracting the mass spectra of Δ(1232) resonances [8]. This problem of large combinatorial background has to be overcome in order to reproduce the mass distribution of Δ(1232) resonances [8]. The analysis of proton–pion pairs was done and mass distributions of the Δ(1232) resonances were reconstructed successfully for the very light projectiles, for example, in peripheral reactions induced by ^{1}H (proton) [9, 10] or ^{3}He [15] at about 2 GeV incident energies. The Δ(1232) mass was shifted by ≈ –25 MeV/c^2 on average

in collisions with different target nuclei, as compared to collisions with protons [9, 11, 12]. In p+A interactions (A = C, Nb, Pb) at incident energies of 0.8 GeV and 1.6 GeV, the masses of Δ(1232)'s were also decreased as compared to the mass of free nucleon Δ(1232) [11]. These mass reductions were related to the Fermi motion's effects, nucleon–nucleon scatterings, and re-absorption of pions in a nuclear matter [11].

In the simplest theoretical approach, the production of Δ(1232) is thought to take place mainly via the reaction $NN \to \Delta N$ (where N denotes a nucleon) in nucleus–nucleus collisions. In this model, the production of Δ^0(1232) is realized via the $NN \to \Delta^0 N + k\pi \quad (k = 0,1,...)$ reaction, followed by Δ^0(1232) decay through $\Delta^0 \to p\pi^-$ and $\Delta^0 \to n\pi^0$ channels.

The detected final particles, protons and π^- mesons, were used to analyze the Δ^0(1232) production in p+^{12}C and d+^{12}C interactions at incident momenta of 4.2 GeV/c per nucleon in the present work. The results extracted in the present thesis may help to understand better production and properties of Δ(1232)'s in the proton and deuteron induced reactions, and may also be useful to interpret the relevant data coming from relativistic heavy ion collisions.

1.2 Properties of Δ(1232) resonances

Delta resonances are baryon resonances having mean mass 1232 MeV/c^2 and width 115–120 MeV/c^2. The family of Δ(1232) resonances has four members with the different charges denoted by a superscript: Δ^{++}(1232), Δ^+(1232), Δ^-(1232), and Δ^0(1232). Each Δ(1232) resonance has a total spin (J) and isospin (I) equal to 3/2, and parity (P) equal to +1. Every Δ(1232) resonance is composed of three quarks. Their quark contents are as follows:

$$\Delta^{++}(1232) = uuu,\ \Delta^{+}(1232) = uud,\ \Delta^{0}(1232) = udd,\ \Delta^{-}(1232) = ddd\ .$$

Using the Clebsch-Gordan coefficients [1], one obtains the following probabilities of various decay channels of Δ(1232) resonances [30]:

- $\Delta^{++}(1232) \rightarrow 1(p+\pi^{+})$,
- $\Delta^{+}(1232) \rightarrow \frac{2}{3}(p+\pi^{0}) + \frac{1}{3}(n+\pi^{+})$,
- $\Delta^{0}(1232) \rightarrow \frac{2}{3}(n+\pi^{0}) + \frac{1}{3}(p+\pi^{-})$,
- $\Delta^{-}(1232) \rightarrow 1(n+\pi^{-})$.

Δ(1232) resonances can be involved in inelastic interactions as follows:

(a) $NN \rightarrow \Delta N$ (hard scattering - production of delta resonances);

(b) $\Delta \rightarrow N\pi$ (decay of delta resonance);

(c) $\Delta N \rightarrow NN$ (absorption of delta resonance);

(d) $N\pi \rightarrow \Delta$ (self – delta production).

1.3 Aims and outline of the thesis

The main aim of the present PhD thesis is to reconstruct the mass and kinematical distributions (momentum, transverse momentum, kinetic energy, rapidity, and emission angle distributions) and to extract the various physical properties (mass, width, production yields, spectral temperatures) of $\Delta^0(1232)$ resonances produced in p+^{12}C and d+^{12}C collisions at 4.2 GeV/c per nucleon. In particular, it is interesting to check whether the masses and widths of $\Delta^0(1232)$ produced in p+^{12}C and d+^{12}C interactions at 4.2 GeV/c per nucleon modify noticeably as compared to these parameters of $\Delta^0(1232)$'s produced in collisions of free nucleons. Comparison of the parameters and various characteristics of $\Delta^0(1232)$ resonances produced in d+^{12}C collisions with those of $\Delta^0(1232)$ excited in p+^{12}C interactions at the same initial momentum per nucleon could give us the valuable information about the role of the weakly bound neutrons of incident deuterons in $\Delta^0(1232)$ production. The further experimental information on $\Delta^0(1232)$ resonances is to be deduced from comparison of the rapidities, emission angles, momenta, and transverse momenta spectra and their

mean values for $\Delta^0(1232)$'s produced in p+^{12}C and d+^{12}C interactions at 4.2 GeV/c per nucleon. The extracted properties of $\Delta^0(1232)$ in p+^{12}C and d+^{12}C collisions will be compared systematically with the corresponding characteristics of $\Delta^0(1232)$ resonances produced with different sets of colliding nuclei at various initial energies, available in the published literature. The mean momenta, transverse momenta, and rapidities of protons and π^- mesons originating from the decay of $\Delta^0(1232)$ resonances in both collision types will be extracted and compared with the respective mean values for participant protons and π^- mesons [31–33] in experiment and estimated using Dubna Cascade Model (DCM) [34], FRITIOF model [35], and Quark-Gluon-String Model (QGSM) [36].

Also the spectral temperatures of $\Delta^0(1232)$ obtained in p+^{12}C and d+^{12}C interactions at 4.2 GeV/c per nucleon will be estimated by analyzing the transverse momentum spectra of $\Delta^0(1232)$ resonances in the framework of Hagedorn Thermodynamic Model [37, 38]. The extracted spectral temperatures of $\Delta^0(1232)$ resonances will be compared with the respective temperatures of π^- mesons in p+^{12}C and d+^{12}C interactions at 4.2 GeV/c per nucleon obtained in the same way from approximating the p_t distributions of π^- mesons by the Hagedorn Thermodynamic Model, and with the respective temperatures deduced from analysis of p_t distributions of $\Delta^0(1232)$ resonances and π^- mesons obtained using Modified FRITIOF model [39–41] adjusted for intermediate energies.

The thesis is arranged as follows. The experimental procedures and models are described in Chapter No. 2. Procedures of reconstruction of $\Delta^0(1232)$ mass distributions are described in Chapter No. 3. Chapter No. 4 contains comparison of kinematical spectra of $\Delta^0(1232)$ resonances produced in p+^{12}C and d+^{12}C collisions. Chapter No. 5 presents the procedures of extraction and comparison of spectral temperatures of $\Delta^0(1232)$'s in p+^{12}C and d+^{12}C interactions. Finally, the main results of the present work are summarized and concluded in Chapter No. 6.

This PhD work is the part of a series of papers [14–22] devoted to analysis of $\Delta(1232)$ production and its various properties in collisions of hadrons and nuclei with nuclei at relativistic energies. The material of this thesis is published in ISI indexed

impact factor international journals [18–22] and presented in various international physics conferences, listed at the end of this thesis.

Chapter 2
Experimental Procedures and Models

2.1 The Synchrophasotron and Accelerators complex of JINR

The Joint Institute for Nuclear Research (JINR) is situated in Dubna, 120 km north of Moscow, Russia. It is an international research centre for nuclear and particle physics, having a large number of staff members, scientists, and PhD scholars from its 18 member countries and other countries of the world. It was established by combining two research institutes, Institute for Nuclear Problems and the Electro-Physical Laboratory of the USSR Academy of Sciences, in Dubna in 1956. JINR has eight Laboratories and one University Centre (UC):

- Veskler and Baldin Laboratory of High Energies (VBLHE);
- Laboratory of Particle Physics (LPP);
- Dzhelepov Laboratory of Nuclear Problems (DLNP);
- Flerov Laboratory of Nuclear Reactions (FLNR);
- Frank Laboratory of Neutron Physics (FLNP);
- Bogolyubov Laboratory of Theoretical Physics (BLTP);
- Laboratory of Information Technologies (LIT);
- Laboratory of Radiation Biology (LRB).

The particle accelerator based upon synchrotron, Synchrophasotron, was established initially for interactions of protons, at the Joint Institute for Nuclear Research (JINR, Dubna, Russia) in 1957 under a leadership of the designer of synchrotron, V. I. Veksler. He discovered the principle of self phasing, which is used to operate the cyclic accelerators of high energies, at Lebedev Physical Institute (LPI), USSR Academy of Sciences, in Dubna in 1944. He supervised the construction and developing of the new accelerator, synchrophasotron, at LPI in 1949–1950. In order to investigate the field of high energy physics at synchrophasotron, the Electro-Physical Laboratory (EPL) of the USSR Academy of Sciences was established in 1953. This EPL was given the name of the Laboratory of High Energies (LHE) in March 1956, and it became a part of the Joint Institute for Nuclear Research. V. I. Veksler was appointed as the first Director of JINR. The synchrophasotron started operations in

April 1957 and produced protons with energies up to 10 GeV. It was the greatest energy, and the synchrophasotron was the largest colliding machine in the world at that time [42].

Figure 2.1: The synchrophasotron accelerator, LHE, JINR, Dubna

Veksler, along with his colleagues Makarov and Chuvilo, started the program of research at the synchrophasotron. The investigation of the elastic scattering processes at minimum and maximum transfers of momenta and multiple particle productions in hadron–nucleon collisions were the initial aims of this program. Various discoveries were made in many experiments under this program, like anti Σ^- hyperon, decay of φ^0 meson into e^-e^+ pair, and many other processes were discovered [42].

The third Director of LHE, A.M. Baldin, suggested starting research in a new field, relativistic nuclear physics (RNP), in order to reveal the quark structure of nuclei. This program was initiated at the Laboratory of High Energies to investigate the cumulative production of particles during relativistic nuclear collisions. The well developed synchrophasotron made it possible to accelerate the deuterons up to several GeV per nucleon and use them in the physical research in 1971. The synchrophasotron had been working until 1993, and at the same time the construction of a superconducting accelerator of relativistic nuclei, the Nuclotron, was also in progress. In 1993, the Nuclotron was made operational to continue the research in the field of

relativistic nuclear physics. Study of the strongly interacting matter under high temperatures or high baryonic densities, or both of them, is among the main aims of the modern high energy physics. It is believed that the extreme conditions of temperatures and densities should have been at the initial stages of evolutions of the Universe and may also be present in neutron stars nowadays, and that these conditions could be created in the laboratory in central collisions of heavy ions at ultra relativistic energies. This motivated the centers of high energy physics to construct the new heavy ion accelerators, or to increase the energies of existing accelerators [42].

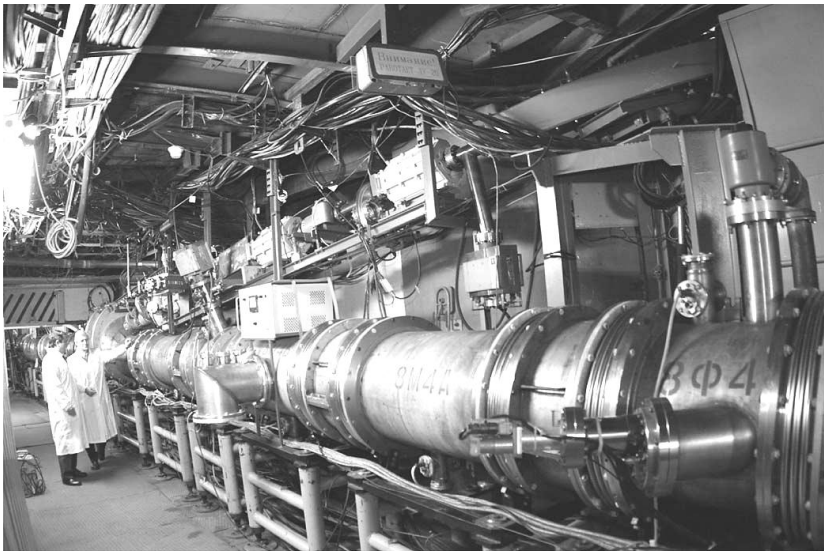

Figure 2.2: The Nuclotron accelerator at LHE, JINR, Dubna

According to a modern theory, the strongly interacting matter can undergo a phase transition by increasing either temperature or density of a nuclear matter, or both of them. Every heavy ion accelerator is designed to investigate some special part of a phase diagram of a strongly interacting matter. This part of the phase diagram is determined by the temperature and baryonic density of a matter, which can be attained in collisions of the nuclei, which depend on the energies and atomic numbers of colliding nuclei. The temperatures and baryonic densities obtained during the collisions of nuclei having atomic numbers ~200 at the highest energies ~5 GeV/nucleon achievable at that time [42] should be adequate to reach the region of a mixed phase, as

was estimated in the model at the Bogolyubov Laboratory of Theoretical Physics of JINR.

The first accelerator which provided the opportunity to obtain the beams of high energy particles was the synchrophasotron at JINR. Views of the synchrophasotron and Nuclotron accelerators are given in Figs. 2.1 and 2.2 respectively. For many years, the accelerators were used to accelerate the singly charged particles, protons, and electrons. Then it was suggested that the heavy ions of greater charges, instead of singly charged particles, should be used to accelerate in the accelerators to get collisions of higher energies, because in this way if an accelerator accelerates a proton suppose up to 10 GeV, then it could accelerate a heavy ion up to a greater energy, for example, ^{4}He nuclei should be accelerated up to 20 GeV. Initially a beam of deuterons was accelerated up to 9 GeV (4.5 GeV per nucleon) at JINR synchrophasotron in 1970s. Deuteron was chosen initially as the simplest nucleus having only two nucleons inside. This opened the way to carry out experiments on relativistic nuclei.

Under a leadership of Stavinskii [43], a group of physicists found the nuclear cumulative effect in d + Cu collisions, where deuteron beam was incident on the copper target. When the summation or accumulation of many homogeneous effects increases or enhances another effect, then this phenomenon is called a cumulative effect. Due to the existence of this effect, it was pointed out that under special conditions the nucleons of the nuclei act differently from the free nucleons.

The accelerators complex at the Laboratory of High Energies is the main part of the Joint Institute for Nuclear Research. It was established to generate the proton, deuteron, polarized deuteron, and other nuclear beams. It could accelerate the light and heavier nuclei up to energies of 6 and 5 GeV per nucleon, respectively. The schematic diagram of the Laboratory of High Energies accelerator complex is presented in Fig. 2.3. It includes the synchrophasotron as well as the Nuclotron. Nuclotron was constructed from 1987 to 1992, and it became operational in March 1993. Fig. 2.4 shows the accelerator complex of the LHE, JINR. The Nuclotron is constructed in the building of the synchrophasotron, in a tunnel below the ground floor.

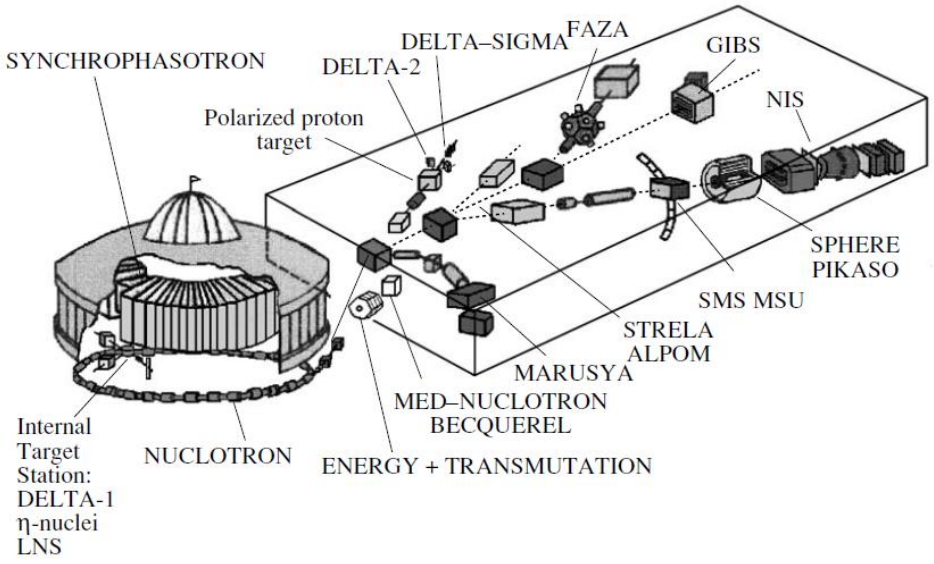

Figure 2.3: Schematic diagram of the accelerator complex of the LHE at JINR, Dubna

The Laboratory of High Energies consists of the followings:

- Synchrophasotron, now Superconducting Nuclotron accelerator;
- Linear accelerator;
- Electrons beam source of high charge state ions;
- Laser source of light ions;
- Source of polarized deuterons;
- Source of heavy ions;
- System of slow beam extraction;
- System of extracted beam channels;
- Internal target complex.

Table 2.1: The comparison of the main characteristics of Synchrophasotron and Nuclotron accelerators.

Parameter	Units	Synchrophasotron	Nuclotron
Energy (max)	*A* GeV	4.5	6
Extraction time (max)	s	0.5	10
Magnetic Field	T	1.5	2.1
Circumference	m	208	252
Chamber size	cm	120	12

The superconducting elements were cooled by two He liquefiers having capacity of 1.6 kW each. The main characteristics of both the accelerators are presented in Table 2.1. The presence of the extractions systems and a wide net of external beam lines were the main advantages of the LHE accelerator complex. The beams could be extracted from the synchrophasotron in two directions, MV-1 and MV-2, as observed from Fig. 2.4, leading towards two experimental halls, Experimental Hall 205 and Experimental Hall 1B, respectively. The beams could be extracted in a relatively long time interval of 0.5 s and forwarded to the experimental area in hall 205, through the MV-1, up to a maximum energy with 95% efficiency. While from MV-2 the beams could be extracted either fast ($t < 10^{-3}$ s) or slowly ($t = 0.35$ s). These beams would then be supplied to the physics setups in the experimental hall 1B. Both the extractions could operate at same time in the same cycle.

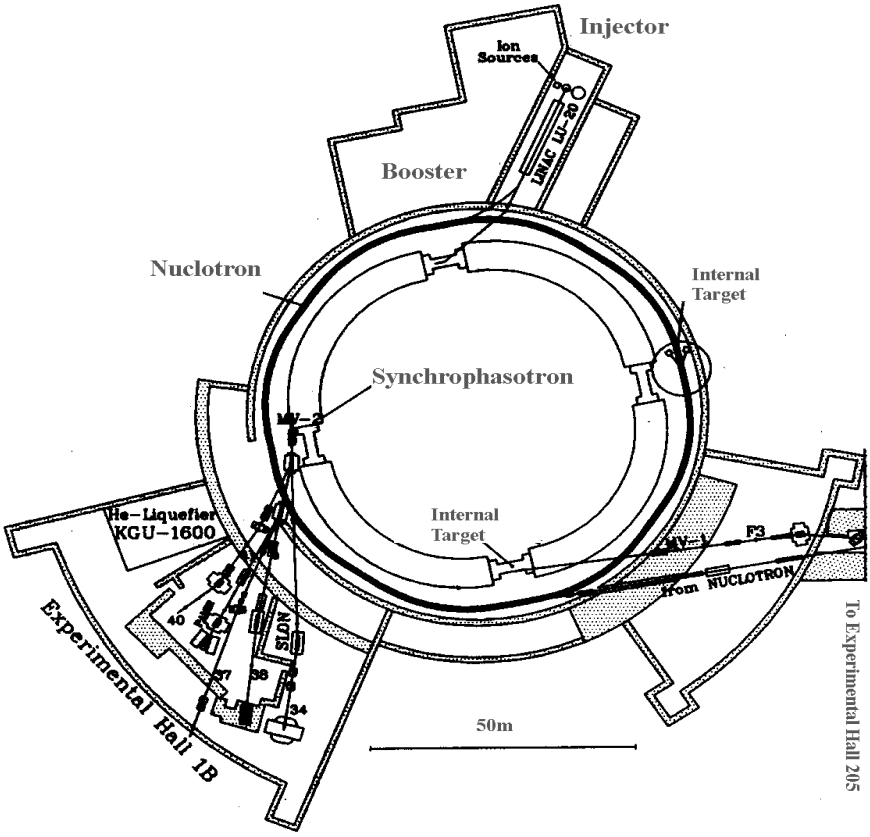

Figure 2.4: Accelerator Complex of the LHE, JINR, Dubna

In order to carry out the research, there are many arrangements at the Nuclotron. These are PIKASO, GIBS, FAZA, DELTA I and II, DISC, Leading

Particles, MARUSYA, SCAN, STRELA, Polarized Proton Target, and Medium Resolution Spectrometer (MRS), as shown in Fig. 2.3. More details are given in Ref. [44].

2.2 Bubble Chamber

The bubble chamber is a particle detector which was used to record the passages of charged particles through the gas in high energy experiments. Donald Glaser formulated first the work principle of a bubble chamber in 1952, and it remained in use up to forty years to study the complicated collisions of hadrons and nuclei with nuclei at various incident energies. It worked on a principle that when a charged particle passed through supper heated liquid, kept under high pressure about 5–20 atmospheres (1 atmospheres = 10^5 Pa), then gas bubbles were produced beside the track of the particle [45] which were photographed by cameras. It was working as follows [46]:

- The liquid was kept under the pressure of approximately 5 atm;
- The pressure was decreased to 2 atm. by a sudden pull of the piston to leave the gas to expand, just before the arrival of the bunch of particles from accelerator, which made the liquid superheated;
- As bunch of charged particles were passed through the liquid, the particles deposited energy to the system by ionization of atoms, and thus the liquid started boiling along the particle tracks and bubbles were produced;
- The collisions of various particles of the beam with the atomic nuclei also occurred, which were of great interest. In these collisions many charged particles were produced, which also continued the ionization processes of atoms of the liquid. Thus trails of bubbles were produced;
- The bubbles produced were allowed to increase in size up to 10 ms, and when their sizes of diameters became approximately equal to 1 mm, flash photographs were taken from many cameras in stereo which enabled the collisions to be reconstructed in three dimensions;

- Then the pressure was increased again, which cleared the bubbles and the bubble chamber became ready for the new bunch of particles;
- Each bunch contained maximum of ten particles.

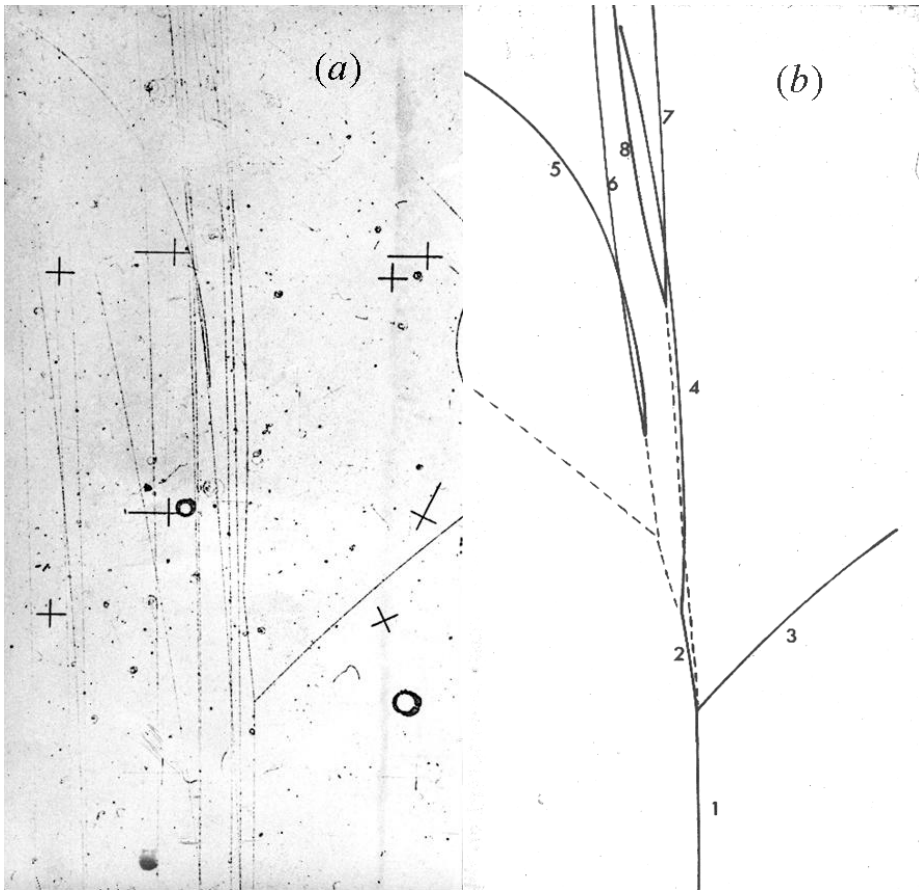

Figure 2.5: Typical photo of an event taken at 2 m bubble chamber at CERN (*a*), its clear image (*b*). The bubble chamber was filled with hydrogen (protons) in liquid form. The incident beam used was of negative kaons (K^-) having 8.2 GeV energy, incident from the bottom of the image. Line 1 is the incident particle, while lines 2-8 are secondary particles. Dotted lines are neutral particles [46].

All the above processes occurred in approximately one second, that's why the bubble chambers were used well for pulsed, cyclic accelerators, and beams from fixed targets having repetition rates of a similar order. Although the processes of taking pictures from bubble chambers were relatively slow, an experiment of many thousands events took many months to complete, the numbers of images were limited, and to

analyze these pictures was very intensive and time consuming task. But the images from bubble chambers were very liked, because they provided a direct way to see the nuclear collision events by naked eyes in a real world. However, the modern detectors allow detection of a several thousands of collision events in one second, and the pictures of interactions are reconstructed by computers, therefore the use of bubble chambers is practically stopped nowadays [46].

Usually the bubble chambers were filled with the simplest nuclei like hydrogen, deuterium, or heavy liquids like a mixture of neon-hydrogen, or propane (C_3H_8). The bubble chamber was put in a strong magnetic field of a strength $1.5 - 3.5$ T, produced by the electro-magnet of conventional or superconducting coils. The magnetic field was provided to measure the momenta of the secondary particles from the curvatures of their tracks via the relation

$$p = 0.3\rho B \qquad (2.1)$$

Where B is the magnetic field's strength in Tesla, p is the momentum of a particle in GeV/c, and ρ is the radius of a curvature of a particle track in meters.

The pictures of the tracks having bubbles around were taken on photographic films with the help of several cameras in three dimensions. The data obtained from the measurements of the images were converted into digital format, and different geometrical programs were used to reconstruct the tracks, and collision events in three dimensions. With the help of the bubble chambers, many particles were discovered which contributed significantly to a quark model, and made it possible to develop and establish this model.

Figure 2.5*a* shows a typical photo of a collision event taken in a bubble chamber, while Fig. 2.5*b* presents its clear reconstructed structure [46]. The crosses in the Fig. 2.5*a* are called fiducials (Latin word '*fiducia*' means truth), and these were marked on the walls or windows of the bubble chambers to calibrate well the images. The positions of these crosses were accurately known, and these were used to reconstruct the events in three dimensions. In order to analyze such pictures, one should know various relevant characteristics of tracks of particles and nuclei and their decay products [46]. For example:

- Interactions among beam particles and the protons of the target;
- To find various final state particles, and as many as possible, usually through analysis of their decays;
- Neutral particles mostly decay into positive particles and negative particles at the same time, and show characteristic letter V − shaped vertices;
- Charged particles mostly decay into other particles of the same charges, but of a lesser momenta, and at the same time at least one neutral particle is also produced;
- The abrupt changes in curvatures of particle tracks are called 'kinks', and these are either due to collisions with other particles or due to decay processes;
- Dark tracks are mostly due to protons;
- Spiral type tracks are due to electrons or positrons, since they are much lighter than all the other charged particles. They lose the energy very quickly via a process known as a bremsstrahlung.

The Sketches of different decay signatures occurred during interaction (collision) processes [46] are presented in Table 2.2. These are very helpful to identify secondary particles. Using these, one may become able to identify any particle. To get more and more information about the particle, one has to measure these tracks and then analyze them [46]. To analyze these tracks, it takes much time. More details about the measurements and methodical analysis in bubble chamber experiments can be found in Ref. [46].

Table 2.2: Sketches of different decay signatures.

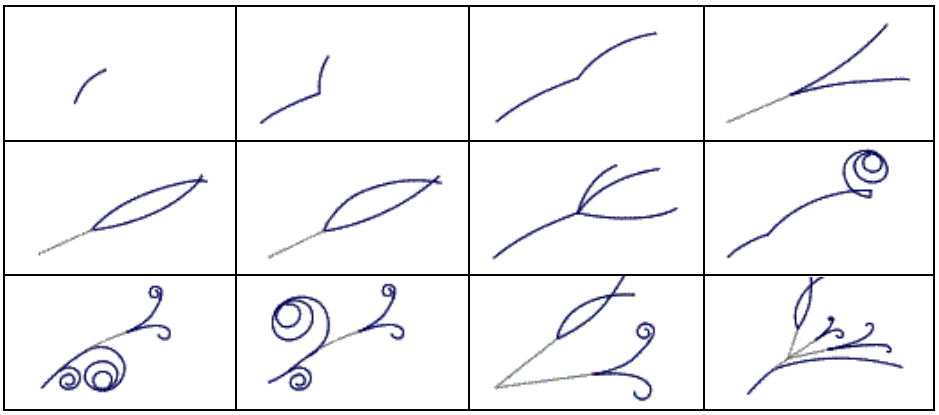

The 2 m (two meter) propane bubble chamber at JINR (Dubna, Russia) had a sensitive volume of (210 x 65 x 40) cm^3. About 500 liters of propane (C_3H_8) were kept in liquid state under a high pressure (~ 20 atm) in the chamber. It was operated at the temperature of about 58 °C. A constant magnetic field of 1.5 T (15 kG) was provided in a vertical direction. The piece of the upper magnetic pole was built as the construction part of the chamber. The piston to expand the liquid was constructed in the bottom of the chamber, thus the expansion of the propane was in downward direction. The chamber was illuminated through 26 holes. Each hole had its own lighting system. There were two photographic systems having three cameras each. Every part of the system was controlled from the remote control table, specially constructed for the chamber.

The experimental physics group under the supervision of Professor Wang Ganchang was busy in analysis of the photographs of thousands of nuclear interactions taken from the 2 m propane bubble chamber at JINR. He along with his group analyzed more than 40000 pictures and discovered the $\bar{\Sigma}^-$ hyperon. Later he along with his group and Professor V. I. Veksler were awarded the first JINR Prize.

2.3 Experiment

The experimental data collected by analyzing the stereo photographs from 2 m propane (C_3H_8) bubble chamber (PBC-500) of the Laboratory of High Energies (LHE) of Joint Institute for Nuclear Research (JINR, Dubna, Russia) placed in a magnetic field of strength 1.5 Tesla irradiated with beams of protons and deuterons accelerated to a momenta of 4.2 GeV/*c* per nucleon at Dubna synchrophasotron accelerator were analyzed in the present work. Collision events of protons and deuterons with propane (C_3H_8) were scanned, measured, reconstructed, and finally analyzed. The inelastic $p+^{12}C$ and $d+^{12}C$ collision events on carbon nuclei of the propane were extracted using the criteria based on the total charge of secondary particles, the total number of protons, the existence of protons bounced into backward hemisphere in the laboratory

system, and the number of π^- mesons produced, as described in detail in Refs. [31, 32, 47]. Interactions were assumed to occur on the ^{12}C target in the propane if at least one condition out of the followings ones was satisfied:

- $(n_+ - n_-) > (Z_{projectile} + 1)$;
- $n_{protons}(p_{lab} < 0.75\,\mathrm{GeV}/c) > 1$;
- $n_{protonsbackward} > 0$;
- $n_- > 1$ (for p+^{12}C interactions) and $n_- > 2$ (for d+^{12}C interactions);
- $n_{ch} = even$ (for p+^{12}C and d+^{12}C interactions).

Here n_+ denotes the number of positively charged particles, n_- represents the number of negatively charged particles, and n_{ch} represents the total number of the charged particles in a collision event. Detailed discussions of the presented criteria are given in Ref. [31]. Using the above criteria, about 70% of all the proton–carbon and deuteron–carbon interactions inelastic collision events were separated [31, 32]. This was estimated with the help of known cross sections [48–51] for p + p, p+^{12}C and d + p, and d +^{12}C collisions at a momentum of 4.2 A GeV/c and using the p:^{12}C ratio in a propane molecule [31, 33, 47, 52]. The remaining ~30% inelastic collision events of protons and deuterons with carbon nuclei were extracted statistically from p + p and d + p collisions on the quasi free protons of C_3H_8 molecules by introducing the relevant weights. These weights were obtained in such a way that the number of events produced on ^{12}C nuclei and hydrogens (protons of propane) corresponded to the number of events expected for the inelastic collisions based upon their cross sections [31, 33, 47, 52]. It is important to note that the numbers of such p + p and d + p collision events included into the data bases of p+^{12}C and d +^{12}C collisions were equal within statistical uncertainties to the numbers of p + n and d + n interaction events on the neutrons of ^{12}C, respectively. This is because the number of protons equals that of neutrons in carbon nucleus, and the cross sections of p + p and p + n interactions at 4.2 A GeV/c are close to each other. It should also be noticed that the number of p + p and d + p collision events on quasi free protons of ^{12}C nuclei is about 69% of the total number of p + p collisions events on protons from C_3H_8. It may also be estimated using

the simple fact that in a propane molecule, out of the total 26 protons, carbon nuclei contain 18 protons.

The particles emitted under large angles ($\approx 90^0$) to the photographic planes of the cameras were mostly lost due to their very short track lengths in a film, and therefore corrections were introduced to account for such losses. These corrections were estimated to be $\approx$ 3% for protons having momentum $p_{lab} > 300\ \mathrm{MeV}/c$, and about 15% for protons having momentum $p_{lab} < 300\ \mathrm{MeV}/c$ (so called slow protons) [31]. The protons and π^+ mesons up to a momentum of $p \approx 0.75\,\mathrm{GeV}/c$ could be separated visually based on their ionization in a chamber. However in the present experiment the protons and π^+ mesons could be separated with almost 100% efficiency up to a momentum of 0.5 GeV/*c*. Thus all the positively charged particles with momenta higher than 0.5 GeV/*c* were assigned weights to give the probability that a certain particle was a proton or a π^+ meson. Since the deuterons and target ^{12}C nuclei contain the same number of protons and neutrons, we assumed that equal numbers of π^+ and π^- mesons should be produced in d +^{12}C interactions. Hence, we can find the number of protons as [31]

$$n_{protons} = n^{+}_{z=1} - n_{\pi^+}, \text{ for } p_\mathrm{p} < 0.5 \text{ GeV}/c, \qquad (2.2)$$

$$n_{protons} = n^{+}_{z=1} - n_{\pi^-}, \text{ for } p_\mathrm{p} > 0.5 \text{ GeV}/c. \qquad (2.3)$$

Here the $n^{+}_{z=1}$ represents the number of all charged particles having Z = 1. However, since deuterons have also Z =1, they were also counted as protons in these estimates. But it was estimated that the admixture of deuterons among the singly charged positively particles is relatively small and doesn't exceed 10–15% [53–55]. All the particles having negative charges were identified as π^- mesons. It is essential to mention that π^- mesons make up the main fraction (> 95%) among the negatively charged particles produced in p+^{12}C and d +^{12}C collisions at a momentum of 4.2 *A* GeV/*c*. The admixture of fast electrons and strange particles among the negatively charged particles didn't exceed 5%. Protons and charged pions having momenta less than 150 MeV/*c* and 70 MeV/*c*, respectively, were not registered due to their short track lengths in the propane bubble chamber. The average uncertainty in measurement

of angles $\langle \Delta\theta \rangle$ of the secondary particles was about 0.8 degree, while the mean relative uncertainty in measuring the momenta of the particles, $\left\langle \frac{\Delta p}{p} \right\rangle$, from the curvatures of their tracks in a magnetic field was about 11% [31]. The inelastic cross sections were 265 ± 15 mb and 400 ± 20 mb for p+^{12}C and d+^{12}C inelastic collisions at 4.2 GeV/c per nucleon, respectively. The scanning of the stereo photographs of the p+^{12}C and d+^{12}C collision events were done to determine the experimental interaction cross sections [56]. The number of the incident beam tracks and the number of the collision events in the volume of a bubble chamber were counted and substituted in the following formula:

$$N = N_0\left[1 - \exp(-n\sigma x)\right].$$

Here N is the number of collision events in a propane chamber, N_0 is the number of the incident beam tracks, n is the number of nuclei in 1 cm^3 of the target, x is the propane layer thickness in the direction of the beam, and σ is the inelastic cross section. The density of the propane was 0.43 g/cm^3 in the PBC [56].

2.4 Modified FRITIOF Model

For a comparison with the experimental data, hadron–hadron (h+h), hadron–nucleus (h+A), and nucleus–nucleus (A+A) collisions are modeled using various Monte Carlo programs, which generate the simulated collision events [33]. The FRITIOF model [33, 39, 52, 57–59] is also based on a Monte Carlo method and is used to simulate relativistic h+h, h+A, and A+A collisions. FRITIOF model is based on a kinematics of two body inelastic collisions. If we are dealing with h+h collisions, then it can be described as $a + b \rightarrow a'$+b', where a and b are incident and target hadrons, and a' and b' are the excited hadrons after a collision. These a' and b' hadrons have masses greater than those of initial colliding hadrons, that is $m_{a'} > m_a$ and $m_{b'} > m_b$. The laws of conservation of energy and momentum in the center of mass frame of interacting hadrons can be described as under:

$$E_a + E_b = E_{a'} + E_{b'} = \sqrt{s_{ab}}\,, \qquad (2.4)$$

$$p_{al} + p_{bl} = p_{a'l} + p_{b'l} = 0, \qquad (2.5)$$

$$0 = \vec{p}_{a't} + \vec{p}_{b't}\,, \qquad (2.6)$$

where E_a, E_b and p_{al}, p_{bl} are the energies and longitudinal momenta of initial interacting hadrons *a* and *b*, and $E_{a'}$, $E_{b'}$ and $p_{a'l}$ $p_{b'l}$ are the energies and longitudinal momenta of final state excited hadrons *a*' and *b*', respectively, $\sqrt{s_{ab}}$ is the total center-of-mass energy of the colliding system, and $\vec{p}_{a't}$, $\vec{p}_{b't}$ are transverse momenta of final state excited hadrons. The initial interacting hadrons have zero transverse momenta, because it is assumed that both the colliding hadrons are moving towards each other in the same line in the center-of-mass frame. Addition and subtraction of relations (2.4) and (2.5) give:

$$P_a^+ + P_b^+ = P_{a'}^+ + P_{b'}^+\,, \qquad (2.7)$$

$$P_a^- + P_b^- = P_{a'}^- + P_{b'}^-\,. \qquad (2.8)$$

Here $P^+ = E + p_l$ and $P^- = E - p_l$.

The probability distributions of $P_{b'}^+$ and $P_{a'}^-$ used in the FRITIOF model are the following:

$$dW \sim \frac{dP_{b'}^+}{P_{b'}^+} \qquad (2.9)$$

$$dW \sim \frac{dP_{a'}^-}{P_{a'}^-} \qquad (2.10)$$

The permissible ranges in which $P_{a'}^-$ and $P_{b'}^+$ can lie are:

$$\left[P_a^-, P_b^-\right],\ \left[P_b^+, P_a^+\right]. \qquad (2.11)$$

In cases of *h*+*A* and *A*+*A* collisions, it is supposed that the excited nucleons of the initial collisions can make interactions with each other and with the other nucleons of nuclei, and, as a result of these consecutive interactions, the masses of the interacting nucleons become greater. If the projectile hadron *a* initially interacts with any nucleon of the colliding nuclei, then their reaction can be expressed as

$a + N_1 \rightarrow a' + N_1'$, here a and a' denote the incident and finally excited hadron, and N_1 and N_1' denote the initial and final nucleon. Now if this excited hadron a' makes another interaction with any other intra-nuclear nucleon, then their collision can be schematically written as $a' + N_2 \rightarrow a'' + N_2'$, where a' is the initially excited hadron, a'' is the doubly excited hadron, and N_2 and N_2' are the initial and final (excited) states of a second nucleon. As a result of successive collisions, the mass of the hadron a increases gradually. The same equations (2.4)−(2.6) are used for h+A interactions, but the relation (2.11) is replaced by

$$\left[P_{a'}^{-}, P_{N_2}^{-}\right], \quad \left[P_{N_2}^{+}, P_{a'}^{+}\right]. \qquad (2.12)$$

The analogous approach is used to simulate nucleus–nucleus (A+A) collisions.

The distribution in the transverse momentum exchange between the interacting (colliding) nucleons in the model is used as

$$dW = b^2 e^{-B p_t^2} p_t \, dp_t . \qquad (2.13)$$

The Modified FRITIOF model which is used for a comparison with the experimental data in a present work was obtained by introducing some modifications in the original FRITIOF model. The Glauber approximation [59] is used in the Modified FRITIOF model to obtain the time sequence of nucleon–nucleon collisions in case of h+A and A+A interactions. The properties of slow particles produced during the disintegration of nuclei are not described in the original model because of neglecting the cascade processes caused by secondary particles. To remove this discrepancy, the Reggeon model of nuclear breakup [59] was incorporated into the Modified FRITIOF model. In the model, the breakup of a nucleus is considered in two steps. In the first step, the number of inelastically interacting nucleons, called as hit nucleons, is determined with the use of the Glauber approach [60]. In the second step, the nucleons which are not taking part in the interactions are considered. If the distance between a non-interacting nucleon and a hit nucleon is r, then the probability of involvement of this non-interacting nucleon in a Reggeon cascade is

$$W = C_{nd} \, e^{-r^2 / r_{nd}^2} . \qquad (2.14)$$

Then this nucleon can involve another spectator nucleon, which can involve another one, and so on. In the model, all the interacting and hit nucleons leave the nucleus. The values of parameters C_{nd} and r_{nd} were taken as 1 and 1.2 fm, respectively, to describe correctly the multiplicities of protons participating in the collisions of protons and nuclei with ^{12}C nuclei. The excitation energies of the residual nuclei were calculated using the approach given in Ref. [61]. The simulations of the relaxations of excited nuclei were done using the evaporation model [62, 63]. The Glauber cross sections were used to make the absolute normalizations of the spectra in the model. In order to determine these cross sections [60], one should specify some characteristics of N+N interactions. These are the total cross section (σ_{NN}^{total}), the slopes of differential cross section for elastic scattering (B_{NN}), and, ρ_{NN}, the ratio of the real to the imaginary part of the amplitude of the elastic scattering at zero momentum transfer given by

$$\rho_{NN} = \frac{\mathrm{Re}\, f_{NN}(0)}{\mathrm{Im}\, f_{NN}(0)}. \qquad (2.15)$$

Here f_{NN} denotes the elastic scattering amplitude. The amplitude $f_{NN}(b)$ of elastic N+N scattering in terms of impact parameter representation was parameterized in the form standard for Glauber approximation:

$$f_{NN}(b) = \frac{\sigma_{NN}^{total}(1 - i\rho_{NN})}{4\pi B_{NN}} e^{-b^2/2B_{NN}}. \qquad (2.16)$$

The values of the parameters used were the same as given in Ref. [48]:

σ_{NN}^{total} = 42 mb, B_{NN} = 7.8 (GeV/c)$^{-2}$, and ρ_{NN} = – 0.23.

The single particle densities of nuclei heavier than helium nucleus were taken as

$$\rho(r) = \frac{const}{1 + e^{\left(\frac{r - R_A}{c}\right)}}. \qquad (2.17)$$

Here $R_A = 1.07A^{1/3}$ fm, and c = 0.545 fm.

2.5 Quark-Gluon-String Model

The Quark-Gluon-String Model (QGSM) [36] is a microscopic model which uses the Regge and strings phenomenology of particle production. Formation of quark gluon plasma is not assumed in this model. Strings are produced in *h*+*h*, *h*+*A*, and *A*+*A* interactions, and they decay later to form the secondary hadrons. The particles produced from a decay of strings in QGSM can also be scattered. The strings can also interact with each other forming di-quarks [64].

We know that the decay of baryon resonances is the predominant process for pion production in relativistic *h*+*A* and *A*+*A* interactions [18–21, 65]. Therefore the models describing the baryon resonances decay can be used to analyze the production of pions in these interactions. The QGSM [36] accounts for production and decay of baryon resonances. The QGSM was extrapolated to the region of intermediate energies ($\sqrt{s_{nn}} \leq 4$ GeV). This model is valid to analyze the interactions of *p* and *d* with carbon nuclei at momentum 4.2 GeV/*c* per nucleon, because this momentum corresponds to nucleon–nucleon center of mass energy $\sqrt{s_{nn}} = 3.14$ GeV. The QGSM can be helpful to understand and interpret the characteristics of hadrons produced in relativistic *h*+*A* and *A*+*A* collisions, and its degree of validity can also be checked through comparison with the experimental data.

The nuclear collisions were taken as a superposition of the independent collisions of the projectile and target nuclei nucleons, stable hadrons, and short lived resonances. In this model, the resonant reactions like $\pi + N \to \Delta$, absorption of pions by *N*+*N* quasi deuteron pairs, and also $\pi + \pi \to \rho$ reactions were incorporated. The formation time of hadrons was also accounted for in this model. The strings have very small masses at intermediate energies, and at $\sqrt{s_{nn}} = 3.14$ GeV they fragment through two particle decay channel in about 90% cases. The coordinates of the nucleons are obtained using the realistic densities of a nuclear matter. The spheres of the nuclei are supposed to be fully occupied by the nucleons provided that the nucleons should be located at a distance more than 0.8 fm from each other. The momenta (*p*) of nucleons

are distributed in the range from "0" to a maximum Fermi momentum of a nucleon, p_F, determined for a given nucleus by its nuclear density.

In QGSM the collision events are generated in three steps:

- The configurations of the interacting nucleons are defined;
- Quark gluon strings are produced;
- The produced strings fragment into hadrons, which we observe.

The topological quark diagrams used for the principal N+N and π+N interactions are presented in Fig. 2.6. Figure 2.6*a* shows the binary process, which is proportional to $1/p_{\text{lab}}$, and makes the main contribution in QGSM. This binary process corresponds to a rearrangement of quarks without direct particle emission during string fragmentation (decay). It mostly results in resonance production (like in reaction $p + p \to N + \Delta^{++}$). And the resonances produced are the main source of pions. The angular dependence of the binary process (Fig. 2.6*a*) is given by

$$\frac{d\sigma}{dt} \cong e^{-bt} \text{ , where } b(s) = 2.5 + 0.7 \ln(s/2).$$

Here t is the four-momentum transfer.

The "undeveloped" cylindrical diagrams (Fig. 2.6*b*) and diffractive processes (Figs. 2.6*c* and 2.6*d*) contribute comparably to the inelastic cross section, and their contributions decrease as p_{lab} decreases.

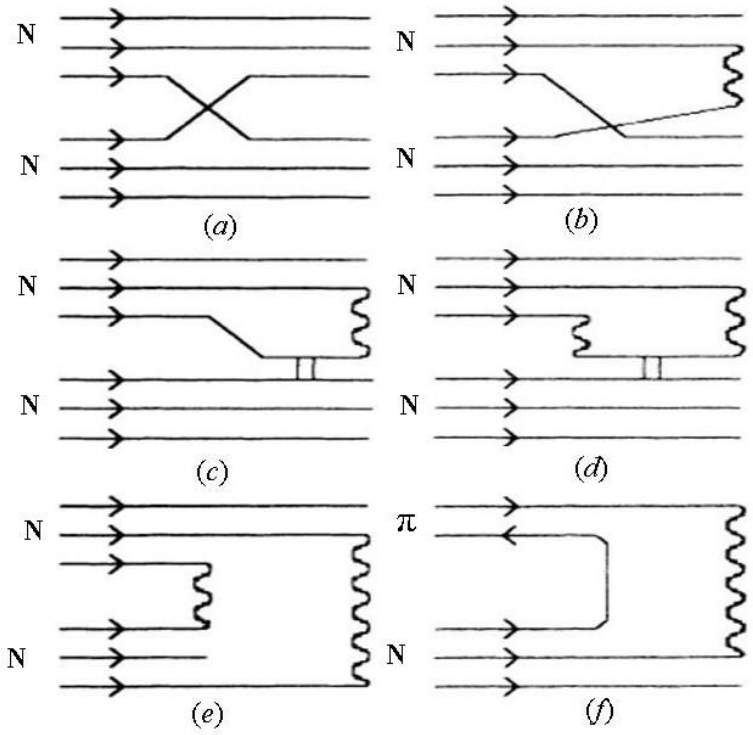

Figure 2.6: Topological quark diagrams for main processes taken in QGSM: (*a*) binary, (*b*) "undeveloped" cylindrical, (*c*) and (*d*) diffractive, (*e*) cylindrical, and (*f*) planar. The solid lines show quarks and the wavy curves represent strings.

The transverse momenta of pions created as a result of quark-gluon string fragmentation are the product of two factors:

- String motion on the whole due to the transverse motion of constituent quarks;
- Production of $q\bar{q}$ pairs from a string fragmentation (breakup).

Transverse motion of quarks inside the hadrons was parameterized by the Gaussian distribution having variance $\sigma^2 \cong 0.3$ (GeV/c)^2. The transverse momenta k_T of created $q\bar{q}$ pairs in the center-of-mass system of a string were described by the dependence given by

$$W(k_T) = \frac{3b}{\pi \left(1 + bk_T^2\right)^4}. \qquad (2.18)$$

Here b = 0.34 (GeV/c)$^{-2}$. For interactions of hadrons, the experimental cross sections were used. The predictions of additive quark model and isotopic invariance were used in the model to define the meson–meson cross sections and other necessary parameters not available in the experimental data. The cross sections of resonance interactions

were assumed to be equal to the cross sections of interaction of stable particles having the same quark contents. The decays of excited recoil nuclear fragments and a coupling of nucleons inside the nuclei were not taken into account in QGSM.

2.6 Dubna Cascade Model

The intra-nuclear cascade model, referred as Dubna Cascade Model (DCM) [66], designed and developed in Dubna is among the initial microscopic models describing the mechanisms of high energy nuclear interactions. It uses the Monte Carlo solutions of the Boltzmann type relativistic kinetic equations with the interaction terms, in which the cascade–cascade collisions are included. Only nucleons, pions, and delta resonances were considered for incident energies less than 1 GeV. Suitable representations of dynamics of pions and baryons for production of particles and processes of absorption are also included in the DCM [67].

The DCM describes the nucleon–nucleon interactions while assuming a constant mean field. Due to the constant mean field, the particles continue their motion in straight lines till the collisions take place with the other particles, or with a potential wall. The incident particle interacts with a nucleon of a target nucleus, and then a new particle can be produced. The incident particle gives momentum to the collided particle, and, as a result, it starts moving inside the nucleus. This particle which starts moving due to a collision is called the cascade particle. It can now make collisions (interactions) with the other nucleons of the nucleus or re-scatter elastically by the nucleons, and the new particles can also be produced. No interactions are assumed among the moving (cascade) particles, according to the DCM. When all the cascade particles get out of the nucleus or are absorbed inside it, then the process comes to an end. The Monte Carlo technique is used to simulate the cascade collisions in this model. The calculations for cascades can be done better at the energies greater than 1 GeV/nucleon as compared to the energies below 1 GeV/nucleon, since at higher energies the importance of nuclear potentials becomes smaller, and that of interaction terms increases.

Local particle densities $\rho(\vec{r},t)$ are used to formulate the DCM mathematically:

$$\rho(\vec{r},t) = \int d\vec{p}\; f(\vec{r},\vec{p},t). \qquad (2.19)$$

Here the average of $f(\vec{r},\vec{p},t)$ is taken over a small cell of radius *r* at a time *t* in DCM. The volume of the colliding nuclei is divided into a number of cells with step lengths of Δz= 0.3 to 0.5 fm along the axis of collision *z*, and cylindrical ring of radius Δr = 0.5 fm.

The propagations of particles within the intra-nuclear cascades are extracted by the relativistic Boltzmann equations including the mixtures of gases of nucleons *I*, given by

$$p^{\mu}_{(I)}\,\partial_{\mu} f^{I}(x, p_{(I)}) = \sum_{I'} D_{coll}(f^{I}, f^{I'}). \qquad (2.20)$$

Here x^{μ} and p^{μ} are the four-space and four-momentum of a particle and D_{coll} is the interaction term. The mixtures of gases are used to distinguish the spectator and participant nucleons in a collision. From the study of fireball created in the collision, the separation of spectator nucleons from participant nucleons in both the incident beam and target nucleus is believed to be obtained. Therefore the interaction term D_{coll} is expanded into three equations for three different types of gases: (*a*) spectators from projectiles, (*b*) spectators from target nucleus, and (*c*) participant nucleons, as given in equations (2.21)–(2.23), respectively:

$$p^{\mu}_{(1)}\,\partial_{\mu} f^{1}(x, p_{(1)}) = -\, f^{1} \sum_{J=2,3} \int f^{J} Q_{1J}\, \sigma^{1J}_{tot}\, d\omega_{J}\,, \qquad (2.21)$$

$$p^{\mu}_{(2)}\,\partial_{\mu} f^{2}(x, p_{(2)}) = -\, f^{2} \sum_{J=1,3} \int f^{J} Q_{2J}\, \sigma^{2J}_{tot}\, d\omega_{J}\,, \qquad (2.22)$$

$$p^{\mu}_{(3)}\,\partial_{\mu} f^{3}(x, p_{(3)}) = -\, f^{3} \sum_{J=1,2} \int f^{J} Q_{3J}\, \sigma^{3J}_{tot}\, d\omega_{J} + \sum_{J=1,2} \int\int f^{3'} f^{J} Q_{3'J} \sum_{\nu=2}^{n_{3'J}} \frac{d\sigma^{3J}(\nu)}{d\omega_{3}}\, d\omega_{3'}\, d\omega_{J}$$
$$+ \int\int f^{1} f^{2} Q_{12} \sum_{\nu=2}^{n_{12}} \frac{d\sigma^{12}(\nu)}{d\omega_{3}}\, d\omega_{1}\, d\omega_{2}\,, \qquad (2.23)$$

where $Q_{IJ} = \sqrt{p_{\mu(I)}\, p^{\mu}_{(J)} - (c^{2} m_{I} m_{J})^{2}}$, and $d\omega = \frac{d^{3}p}{E}$ is the element of invariant momentum-space volume.

The differential cross sections $\frac{d\sigma(\nu)}{d\omega}$ and the total cross sections σ_{tot} are used to take into account the characteristics of *h*+*A* interactions. The total cross sections are used to make corrections due to Pauli Exclusion Principle. The interactions among the

same gas particles are excluded in order to obey the Pauli principle for the spectator nucleons (equations 2.21 and 2.22). The minus signs in the equations (2.21) and (2.22) represent the losses of particles to the area of participant nucleons. In equation (2.23), for the gases of participant nucleons, the first term is a loss term; the second and third terms are for the spectator nucleons casually gained by the gas of participants. The dynamical effects of the field are ignored in the model.

In Dubna Cascade model, it is assumed for incident particles of small masses that the particles in a cascade stop interactions after a particular cascade time. In the case of incident particles of the greater masses, the particles continue their interactions even after that specific cascade time. The interactions of particles in the final sates are treated as a coalescence of the nucleons into composites having the probability of formation represented by a density of particles in a momentum space.

The densities of particles in a momentum space for different values of impact parameter *b* can be obtained using the individual particle distribution function as given in equation (2.24).

$$\rho(\vec{p},t;b) = \int d\vec{r}\ f(\vec{r},\vec{p},t;b) \qquad (2.24)$$

Chapter 3
Reconstruction of Mass Distributions of $\Delta^0(1232)$ Resonances

3.1 Momentum distributions and mean multiplicities of protons and pions

Protons having momenta $p_{lab} > 300$ MeV/c in p+^{12}C and d+^{12}C collisions at 4.2 GeV/c per nucleon were called participant protons [31, 33, 47, 52]. Protons having momentum $p_{\rm lab} > 3$ GeV/c and emission angle relative to the direction of incident beam $\theta_{\rm lab} < 3$ degrees in d+^{12}C interactions were classified as projectile spectator protons [31, 33, 47, 52]. We termed the protons with $p_{lab} < 300$ MeV/c "evaporated" or target spectator protons. The momentum distributions of protons generated from p+^{12}C and d+^{12}C collisions are presented in Figs. 3.1*a* and 3.2*a*, respectively.

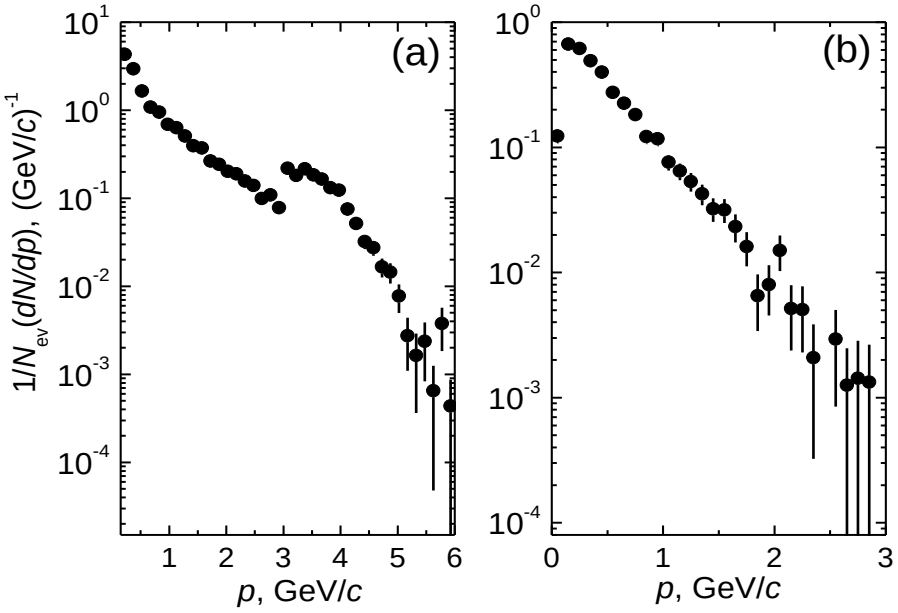

Figure 3.1: Momentum distributions of protons (*a*) and π^- mesons (*b*) obtained in p+^{12}C interactions at 4.2 GeV/*c*. The distributions are normalized by the total number of events.

The mean multiplicities of protons (per event) having momentum $p_{lab} > 150$ MeV/c and $p_{lab} > 300$ MeV/c in p+^{12}C interactions at 4.2 GeV/*c* were 2.44 ± 0.11 and 1.83 ± 0.10, respectively, on statistics of 2886 inelastic events in Ref. [31]. The mean multiplicity per event of participant protons was found to be 1.95 ± 0.08 in d+^{12}C collisions at 4.2 *A* GeV/*c* on statistics of 5404 inelastic events in Ref.

[31]. After incorporating all the corrections discussed in the previous chapter of this thesis, we determined the mean multiplicities of protons having momenta $p_{lab} > 150$ MeV/c and $p_{lab} > 300$ MeV/c to be 2.47 ± 0.05 and 1.83 ± 0.04 in p+^{12}C interactions on statistics of 6736 inelastic events in the present work. The mean multiplicity per event of participant protons was found to be 1.94 ± 0.06 in d+^{12}C collisions on statistics of 7071 inelastic events in the present analysis. All the events of p+^{12}C and d+^{12}C inelastic interactions were measured with 4π acceptance with the detection and identification of almost all the charged products of collisions.

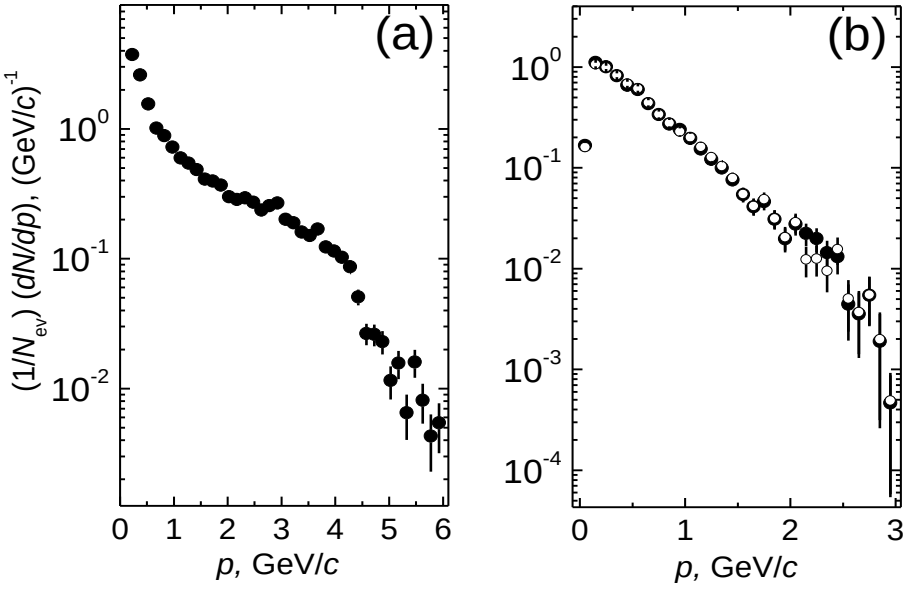

Figure 3.2: Momentum distributions of protons (*a*), π^- (●) and π^+ (○) mesons (*b*), obtained in d+^{12}C interactions at 4.2 GeV/c per nucleon. The distributions are normalized by the total number of events.

The mean multiplicities of participant protons in p+^{12}C and d+^{12}C collisions at 4.2 GeV/c per nucleon obtained using Dubna Cascade Model (DCM) [34, 68] were 1.79±0.01 and 1.97 ± 0.01 [31]; the same obtained using FRITIOF model [35, 41, 61, 68, 69] were 1.99±0.02 and 2.05 ± 0.03 [33], respectively; and the mean multiplicities of participant protons calculated using Quark-Gluon-String Model (QGSM) [36] were 1.77 ± 0.03 and 1.86 ± 0.02 [70], respectively. It is worth mentioning that there is a wide peak in the proton momentum spectrum in the region $\sim 3-4$ GeV/c as shown

in Fig. 3.1*a* . This is ascribed [18, 19] to the quasi elastic scatterings of incident protons on the ^{12}C target nucleons, demonstrated also earlier in Ref. [31].

The distributions for momenta of pions obtained in p+^{12}C and d+^{12}C interactions at 4.2 GeV/*c* per nucleon are presented in Figs. 3.1*b* and 3.2*b*, respectively. The momentum distribution of π^- mesons produced in p+^{12}C interactions is illustrated in Fig. 3.1*b*. The mean multiplicity of π^- mesons (per event) in p+^{12}C collisions was 0.36 ± 0.01, which agreed within uncertainties with the mean multiplicity of π^- mesons, 0.33 ± 0.02, calculated in an early work [32] on statistics of 1834 inelastic events. The momentum distributions of π^- and π^+ mesons produced in d+^{12}C interactions at 4.2 GeV/*c* per nucleon are presented in Fig. 3.2*b*. The mean multiplicities of π^- and π^+ mesons in d+^{12}C interactions practically coincided with each other. It was expected, because d+^{12}C interacting system is a symmetric one containing the equal number of protons and neutrons. The mean multiplicities per event of π^- and π^+ mesons produced in d+^{12}C collisions at 4.2 GeV/*c* per nucleon proved to be 0.66±0.01 in the present work. The mean multiplicity per event of π^- mesons in d+^{12}C interactions at 4.2 GeV/*c* per nucleon was measured to be 0.62 ± 0.03 in an early work [32] on statistics of 2171 inelastic events.

Table 3.1: The experimental mean multiplicities of participant protons and π^- mesons in p+^{12}C and d+^{12}C collisions at 4.2 GeV/*c* per nucleon, along with those calculated using various models [31–33, 70, 71].

Collision type	***p*+^{12}C**		***d*+^{12}C**	
Particle type	Protons	π^- mesons	Protons	π^- mesons
Experiment	1.83 ± 0.04	0.36 ± 0.01	1.94 ± 0.06	0.66 ± 0.01
DCM	1.79 ± 0.01	0.42 ± 0.01	1.97 ± 0.01	0.68 ± 0.02
FRITIOF	1.99 ± 0.02	0.41 ± 0.01	2.05 ± 0.03	0.70 ± 0.01
QGSM	1.77 ± 0.03	0.35 ± 0.01	1.86 ± 0.02	0.63 ± 0.01

The mean multiplicities of π^- mesons produced in p+^{12}C and d+^{12}C interactions calculated using Dubna Cascade Model (DCM) were found to be 0.42 ± 0.01 and 0.68 ± 0.02 [32], respectively; the same using FRITIOF model were 0.41±0.01 [69] and 0.70 ± 0.01 [33], respectively. The mean multiplicities of negative pions extracted

using Quark-Gluon-String Model (QGSM) were 0.35 ± 0.01 and 0.63 ± 0.01 [71] in p+^{12}C and d+^{12}C collisions, respectively. The experimental mean multiplicities of participant protons and π^- mesons in p+^{12}C and d+^{12}C collisions at 4.2 GeV/c per nucleon along with those calculated using Dubna Cascade Model (DCM), FRITIOF model, and Quark-Gluon-String Model (QGSM) are presented in Table 3.1.

3.2 The Method

The experimentally measured momenta of protons and π^- mesons were used to calculate the invariant mass M of the $p\pi^-$ system given by

$$M^2 = (E_p + E_\pi)^2 - (\vec{p}_p + \vec{p}_\pi)^2 \ . \qquad (3.1)$$

Here E_p, E_π are the energies, and $\vec{p}_p$, $\vec{p}_\pi$ are the momenta of the protons and π^- mesons, respectively. The experimental and background invariant mass spectra for $p\pi^-$ pairs in p+^{12}C and d+^{12}C collisions are given in Figs. 3.3*a* and 3.3*b*, respectively.

To construct the experimental invariant mass distribution of $p\pi^-$ pairs in p+^{12}C and d+^{12}C interactions, the protons and π^- mesons from every single event were combined. To obtain the background invariant mass distributions of $p\pi^-$ pairs, a method of event mixing (Monte Carlo Technique) was used. According to this method, the invariant mass of $p\pi^-$ pairs was calculated for protons and negative pions chosen randomly from different events, namely a combined proton was picked from one event and a corresponding pion from another one. Only the events having the same multiplicity of protons and pions were combined to preserve the experimental event topology in the background distribution. As obvious from Figs. 3.3*a* and 3.3*b*, the experimental invariant mass distributions of $p\pi^-$ pairs do not reveal resonance-like structure close to $M = 1232$ MeV/c^2, expected for $\Delta^0(1232)$'s in both p+^{12}C and d+^{12}C collisions. The maxima of experimental distributions in both the collisions, as seen from Figs. 3.3*a* and 3.3*b*, are shifted to the region $M < 1200$ MeV/c^2. A large combinatorial background from uncorrelated $p\pi^-$ pairs is the main cause of such shift of these spectra and that a resonance-like structure, expected at

around $M = 1232$ MeV$/c^2$, is suppressed. The same behavior of invariant mass distributions of proton pion pairs was also observed earlier in ^{16}O+p collisions [15] at 3.25 A GeV/c, ^{12}C +^{12}C [13], ^{4}He+^{12}C [17], and ^{12}C +^{181}Ta [16] collisions at 4.2 A GeV/c, and in π^-+ ^{12}C collisions at 40 GeV/c [14]. The method of analyzing an angle between the proton and pion was used to reduce as much as possible the large combinatorial background and reconstruct successfully the mass distributions of $\Delta^0(1232)$'s in Refs. [13–19, 72].

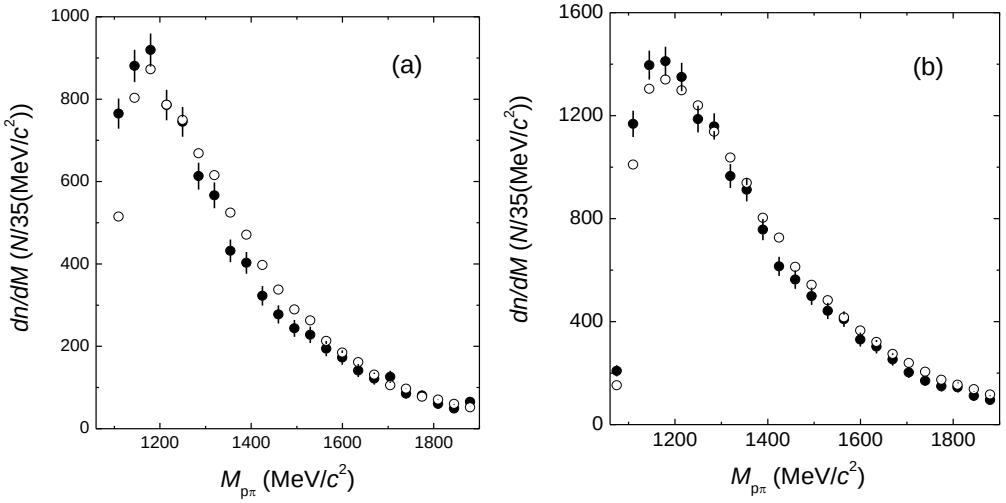

Figure 3.3: Experimental (●) and background (○) invariant mass distributions of $p\pi^-$ pairs in p+^{12}C (*a*) and d+^{12}C (*b*) collisions at 4.2 GeV/c per nucleon.

The angle α in the lab frame between the proton and pion emitted as a result of Δ resonance decay in flight is given by [13–20]

$$\cos\alpha = \frac{1}{p_p p_\pi}\left(E_p E_\pi - \frac{M_\Delta^2 - M_\pi^2 - M_p^2}{2}\right), \qquad (3.2)$$

where p_p, $E_p = \sqrt{M_p^2 + p_p^2}$ are the momentum and energy of proton, and p_π, $E_\pi = \sqrt{M_\pi^2 + p_\pi^2}$ are the momentum and energy of π^- meson, respectively, and $M_\Delta = 1232$ MeV/c^2 is the mass of free nucleon $\Delta^0(1232)$. We compared this value

with the cosine of the angle β between the emitted proton and pion, measured experimentally:

$$\cos\beta = \frac{\vec{p}_p \cdot \vec{p}_\pi}{p_p p_\pi} \ . \qquad (3.3)$$

The following criterion was used to construct the experimental spectra of invariant masses, $\frac{dn^{\exp}}{dM}$ for $p\pi^-$ pairs from p+^{12}C and d+^{12}C interactions. We kept only those combinations which satisfied the inequality

$$|\cos\beta - \cos\alpha| < \varepsilon. \qquad (3.4)$$

Here ε is a cutoff parameter. Theoretically it lies between zero and two. If the measurements of momenta of protons and pions are done with a good precision, then the upper limit of this interval should be low. In addition, it was required that all the events lie in the region allowed by kinematics of *NN* collisions determined by Byckling and Kajantie inequality [73]. These criteria were to exclude the physically uncorrelated $p\pi^-$ pairs [13–17].

It is necessary to add that in experiment the fraction of peripheral interaction events with impact parameter range $b > 2.6$ *fm* (greater than r.m.s. radius of ^{12}C ≈ 2.46 *fm* [74]) in p+^{12}C collisions was estimated to be (73±3)%, which is compatible with the corresponding value, 66%, of the fraction of peripheral p+^{12}C collision events calculated with the help of the modified FRITIOF model in Ref. [69].

The background invariant mass distributions, $\frac{dn^b}{dM}$, were constructed by the method of event mixing using the same criterion given in expression (3.4), as used for experimental distribution, and calculating the invariant mass of proton-negative pion pairs. It was also required that all the events should lie in the region allowed by kinematics of *NN* collisions, as was used for construction of experimental distribution. It is important to note that for each experimental spectrum with the certain value of cutoff parameter ε, the corresponding background distribution was constructed using the same value of ε. For the $p\pi^-$ pairs measured in a certain event, the corresponding background pair was selected from events with the same multiplicities of protons and

pions. It is essential to mention that condition of equal multiplicities for both the experimental and background distributions makes sure that the correlations caused by the dynamics of reaction and rescattering of pions in spectator matter are correctly subtracted from the experimental spectrum [2, 75, 76]. The number of mixed combinations for each background spectrum was five times greater than in experimental distribution. Then the number of background $p\pi^-$ combinations was normalized to that of $p\pi^-$ pairs in the experimental spectrum. As a result of above procedures, we got the sets of experimental and background invariant mass spectra from correlated and uncorrelated proton–negative pion pairs, respectively, in p+^{12}C and d+^{12}C collisions, constructed for different values of the cutoff parameter ε. Then, for each ε value, we analyzed the distribution of differences, $D(M)$, between experimental and background invariant mass spectra:

$$D(M) = \frac{dn^{\exp}}{dM} - a\frac{dn^{b}}{dM}, \qquad (3.5)$$

where a is the normalization factor varying between 0 and 1.

Considering the $D(M)$ distributions as a pure Δ^0 signal in p+^{12}C and d+^{12}C collisions at 4.2 GeV/c per nucleon, we fitted these $D(M)$ spectra in the region of invariant masses 1092–1407 MeV/c^2 by a relativistic Breit-Wigner function [77]

$$b(M) = C\frac{\Gamma M M_{\Delta}}{(M^2 - M_{\Delta}^2)^2 + \Gamma^2 M_{\Delta}^2}. \qquad (3.6)$$

Here M_{Δ} is the mass, Γ is the width of Δ resonance, and C is the fitting constant. The data set $D(M)$ was obtained for various values of cutoff parameter ε and parameter a. Then we fitted the data set $D(M)$ by a relativistic Breit-Wigner function $b(M)$ and the value of $\chi^2(a)$ was obtained for every fit. Here $\chi^2 = \sum_{i=1}^{n}\left(\frac{(y_{\exp}(i) - y_{\mathrm{mod}}(i))^2}{y_{\mathrm{mod}}(i)}\right)$, where $y_{\exp}(i)$ and $y_{\mathrm{mod}}(i)$ (i=1,n) are the experimental measurements and the respective model (fit) values. The value of ε varied from 0.01 to 1.00 using a step of 0.01, and a changed from 0.00 to 1.00 using the same step 0.01 for each ε value during above described fitting procedures. The best value of the parameter a for each ε value was obtained from the minimum of $\chi^2(a)$ function. In this way, the best background

distribution $\frac{a\,dn^b}{dM}$ at the best value of a, was obtained for each experimental distribution $\frac{dn^{\exp}}{dM}$ (for each ε value).

By analyzing the experimental and background spectra at different values of ε, we noticed that at ε < 0.10 the distributions $D(M)$ were narrow with the widths $\Gamma < 40$ MeV$/c^2$ and $\Gamma < 45$ MeV$/c^2$ for p+^{12}C and d+^{12}C collisions at 4.2 GeV/c per nucleon, respectively, while the masses obtained were M_Δ ~1232 MeV/c^2 for both collision types. This is because of the small statistics of the experimental spectra near the $\Delta^0(1232)$ resonance peak and dominance of the effect of the selected mass M_Δ in equation (3.2) for cutoff parameter values ε < 0.10. The experimental and background invariant mass spectra of $p\pi^-$ pairs in p+^{12}C and d+^{12}C collisions at cutoff parameter value ε = 0.05 are given in Figs. 3.4*a* and 3.5*a*, respectively, as an example.

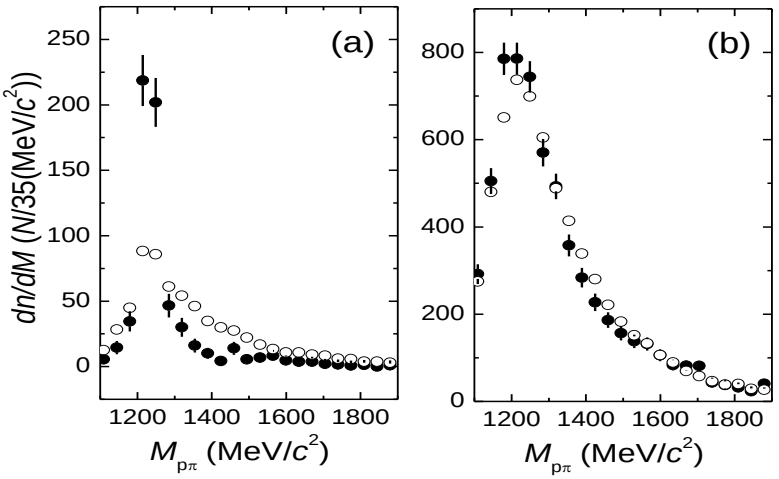

Figure 3.4: Experimental (●) and background (○) invariant mass spectra of $p\pi^-$ pairs in p+^{12}C collisions at 4.2 GeV/c obtained using the cutoff parameters ε = 0.05 (*a*) and ε = 0.90 (*b*).

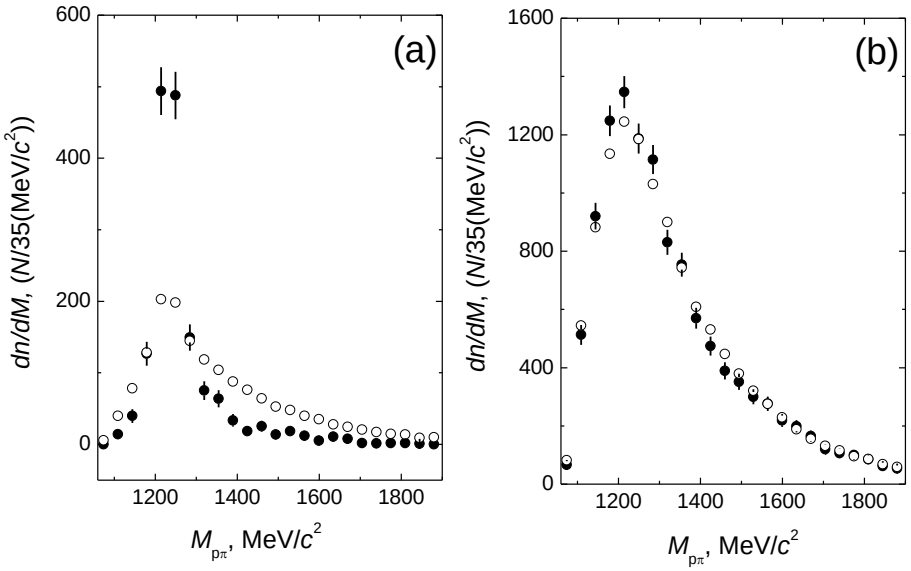

Figure 3.5: Experimental (●) and background (○) invariant mass spectra of $p\pi^-$ pairs in d+^{12}C interactions at 4.2 GeV/c per nucleon obtained using the cutoff parameters ε = 0.05 (*a*), and ε = 0.90 (*b*).

At the values ε >0.85 (ε >0.80), the experimental distributions $\frac{dn^{\exp}}{dM}$ in p+^{12}C (d+^{12}C) collisions start to become similar to the experimental spectra given in Fig. 3.3*a* (Fig. 3.3*b*). At such relatively high values of cutoff parameter ε, the resonance-like structure is masked by a large combinatorial background due to uncorrelated $p\pi^-$ pairs. The experimental and background invariant mass distributions of $p\pi^-$ pairs for cutoff parameter value ε =0.90 in p+^{12}C (d+^{12}C) collisions are shown in Fig. 3.4*b* (Fig. 3.5*b*), as an example. For both p+^{12}C and d+^{12}C collisions, with a further increase in the value of ε, the peak of the experimental spectrum shifts to the region M < 1200 MeV/c^2 and its width becomes larger approaching more the shape of the experimental spectra given in Figs. 3.3*a* and 3.3*b*, obtained without applying criterion given in relation (3.4).

3.3 Dependence of obtained parameters on cutoff parameter ε

The dependences of the best values of parameters a and of the corresponding values of mass (M) and width (Γ) on the cutoff parameter ε in p+^{12}C and d+^{12}C

collisions are presented in Figs. 3.6 and 3.7, respectively. Figures 3.6*a* and 3.7*a* show that in region $\varepsilon < 0.4$ the parameter *a*, characterizing the background contribution, increases, with an increase of ε. It is necessary to note that with an increase in parameter ε in region $\varepsilon < 0.4$ the total number of combinations in experimental spectra increases with an increase of the number of correlated and uncorrelated $p\pi^-$ pairs. In region $\varepsilon < 0.2$ ($\varepsilon < 0.15$), as it is obvious from Figs. 3.6*b* (3.7*b*) and 3.6*c* (3.7*c*), the distributions $D(M)$ are too narrow with the obtained widths $\Gamma < 40\ \mathrm{MeV}/c^2$ ($\Gamma < 60\ \mathrm{MeV}/c^2$) and masses $M_\Delta \sim 1232\ \mathrm{MeV}/c^2$ for p+^{12}C (d+^{12}C) collisions. This is, as discussed before, because of the relative smallness of the experimental statistics around the $\Delta^0(1232)$ peak and dominance of the effect of the selected mass M_Δ in equation (3.2) for cutoff parameter values $\varepsilon < 0.2$ ($\varepsilon < 0.15$) in p+^{12}C (d+^{12}C) collisions.

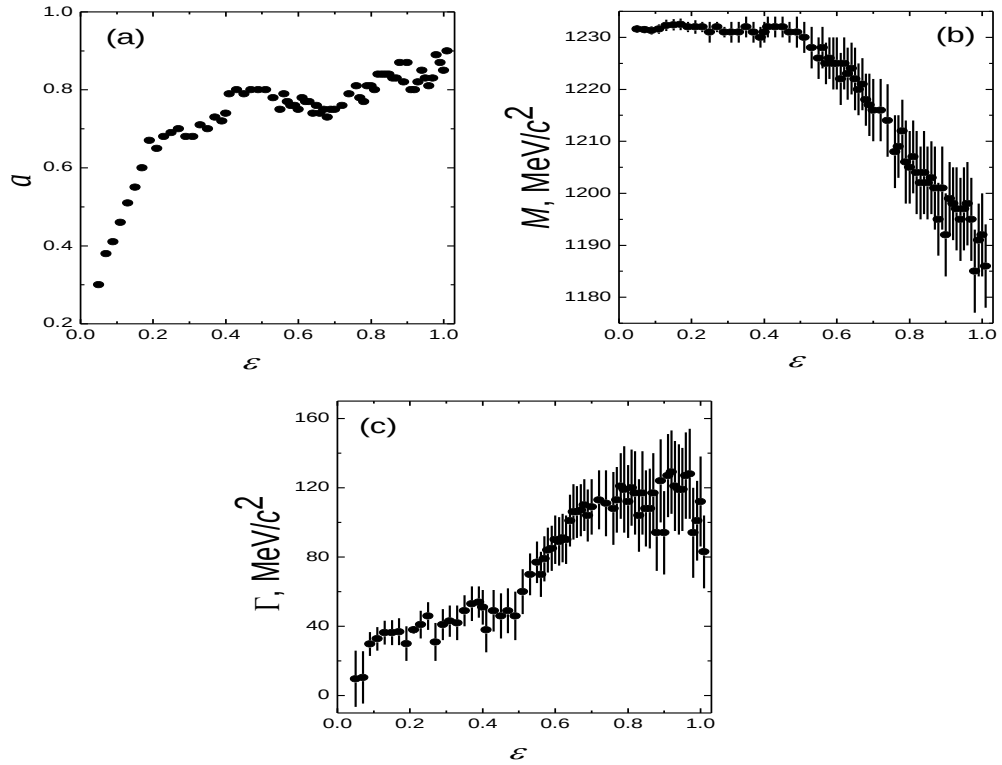

Figure 3.6: Dependence of the values obtained for the parameters *a* (*a*), *M* (*b*), Γ (*c*) on cutoff parameter ε in p+^{12}C collisions at 4.2 GeV/*c*.

Figure 3.6*a* (3.7*a*) demonstrates that there is almost a "plateau" in region $\varepsilon \approx$ 0.4–0.7 for p+^{12}C (d+^{12}C) collisions, in which the values of parameter a remain nearly constant within small fluctuations of this parameter. The maximal spread of parameter a in region $\varepsilon \approx 0.4$–0.7 is $| a_{max}–a_{min} | = 0.07$ ($| a_{max}–a_{min} | = 0.08$) in p+^{12}C (d+^{12}C) collisions at 4.2 GeV/c per nucleon.

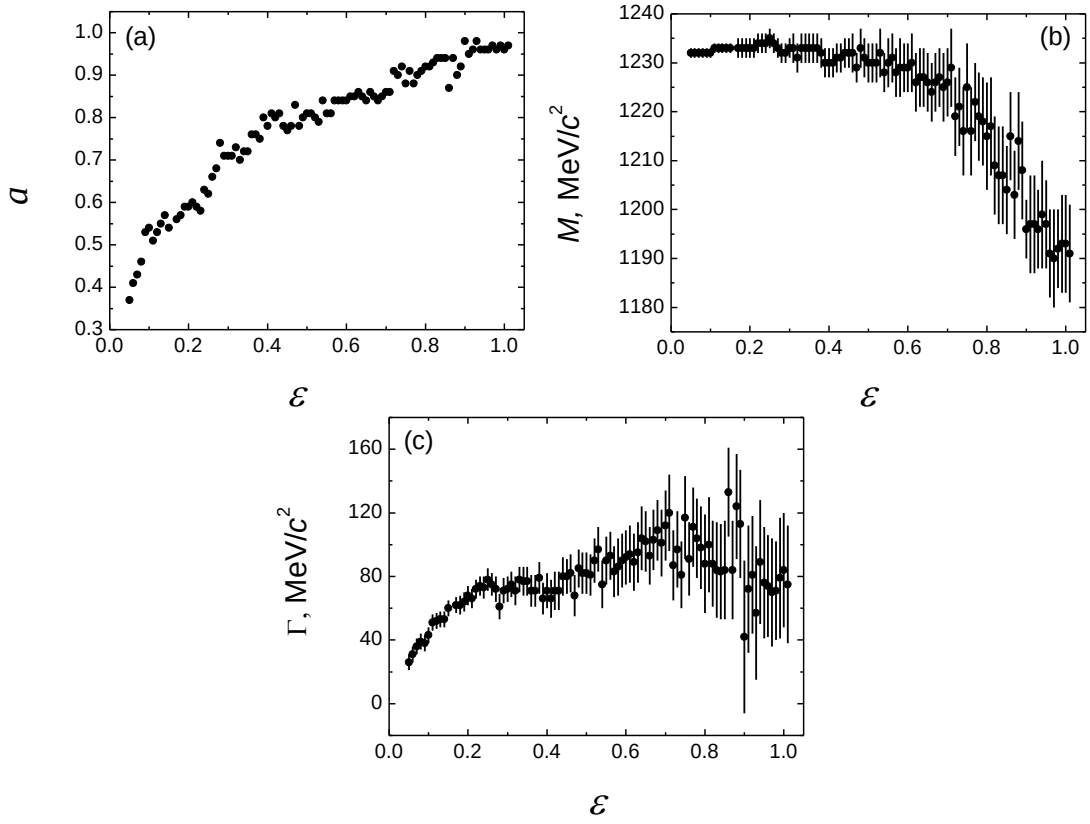

Figure 3.7: Dependence of the values obtained for the parameters a (*a*), M (*b*), Γ (*c*) on cutoff parameter ε in d+^{12}C collisions at 4.2 GeV/c per nucleon.

As the value of ε increases further, as obvious from Fig. 3.6*a* (Fig. 3.7*a*), the value of a on the whole increases showing large oscillations and unstable behavior for p+^{12}C (d+^{12}C) collisions. The value of this parameter becomes $a \sim 0.9$ ($a = 0.96$) at $\varepsilon =$ 1.0 in p+^{12}C (d+^{12}C) collisions. As observed from Figs. 3.6*b* (3.7*b*) and 3.6*c* (3.7*c*), there is a large decrease in a resonance mass M_Δ and the values of width Γ show very unstable behavior with large oscillations with an increase in parameter ε in region $\varepsilon >$

0.7. It is seen from Figs. 3.6*b* (3.7*b*) and 3.6*c* (3.7*c*) that the obtained parameters M_{Δ} and Γ have large fitting errors in region $\varepsilon > 0.7$. This can be explained by that the contribution of the combinatorial background from uncorrelated $p\pi^-$ pairs increases with almost no further contributions from correlated $p\pi^-$ pairs to the experimental distributions in region $\varepsilon > 0.7$ as the parameter ε increases. Consequently, the experimental distributions $\frac{dn^{\exp}}{dM}$ become similar to the experimental spectra given in Figs. 3.3*a* and 3.3*b* for p+^{12}C and d+^{12}C collisions, respectively, in region $\varepsilon > 0.85$, where the large combinatorial background from uncorrelated $p\pi^-$ pairs suppresses nearly completely the resonance-like structure.

3.4 Mass distributions of $\Delta^0(1232)$ resonances

The mass spectra of $\Delta^0(1232)$'s in p+^{12}C and d+^{12}C interactions at 4.2 *A* GeV/*c* were obtained selecting the best values of the cutoff parameter ε and the corresponding best values of parameter *a*. These best values of the parameters were obtained analyzing the behavior of the $\chi^2(\varepsilon,a)$ function. The minimum of $\chi^2(\varepsilon,a)$ function resulted in the following best values: $\varepsilon(\Delta^0) = 0.61 \pm 0.18$ and $a(\Delta^0) = 0.78\,^{+0.03}_{-0.05}$ for p+^{12}C collisions, and $\varepsilon(\Delta^0) = 0.52 \pm 0.16$ and $a(\Delta^0) = 0.80\,^{+0.06}_{-0.03}$ for d+^{12}C collisions.

It is important to mention that the obtained best values of the cutoff parameter ε lie within the "plateau" region ($\varepsilon \sim 0.4$–0.7), where the values of *a* remain nearly constant within uncertainties. The average experimental error in measuring the momentum, $\langle \Delta p/p \rangle \approx 11\%$, was used to estimate the uncertainty in cutoff parameter ε, $\Delta\varepsilon/\varepsilon \approx 30\%$, in p+^{12}C and d+^{12}C collisions at 4.2 GeV/*c* per nucleon. In what follows further, all the systematic uncertainties in the extracted parameters and kinematical characteristics of $\Delta^0(1232)$'s were estimated using the above deduced uncertainty in ε ($\Delta\varepsilon/\varepsilon \approx 30\%$).

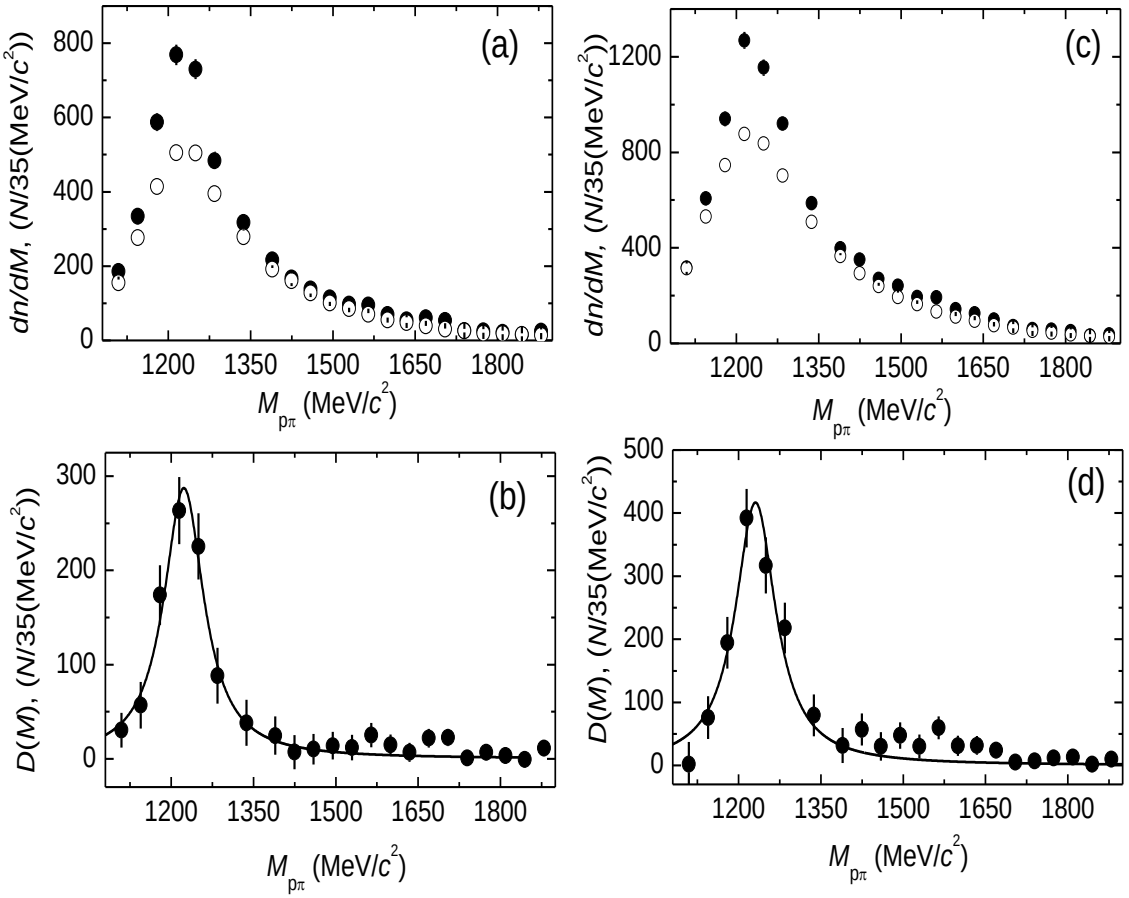

Figure 3.8: Experimental invariant mass spectra (●) and the best background spectra (○) for $p\pi^-$ pairs in p+^{12}C (*a*) and d+^{12}C (*c*) collisions at 4.2 GeV/*c* per nucleon reconstructed using the best values of ε and *a*. The difference (●) between the experimental and the best background invariant-mass spectra in p+^{12}C (*b*) and d+^{12}C (*d*) collisions for $p\pi^-$ pairs produced at the best values of ε and *a* along with the corresponding Breit-Wigner fits (solid lines).

In p+^{12}C collisions, the systematic error in *a* was estimated as the maximum deviation on the positive and negative sides from the best value $a(\Delta^0) = 0.78$ within the ε interval from $0.43\ (0.61-\Delta\varepsilon)$ to $0.79\ (0.61+\Delta\varepsilon)$. While for d+^{12}C collisions, the systematic error in *a* was determined analogously using the interval of ε between $0.36\ (0.52-\Delta\varepsilon)$ and $0.68\ (0.52+\Delta\varepsilon)$. The experimental invariant mass spectra $\frac{dn^{\exp}}{dM}$ and the best background invariant mass spectra $a\frac{dn^{b}}{dM}$ for $p\pi^-$ pairs at best values of ε and *a* are presented in Figs. 3.8*a* and 3.8*c* for p+^{12}C and d+^{12}C collisions,

respectively. The difference distributions, $D(M)$, obtained using the above selected best values of parameters ε and a, together with the corresponding fits with relativistic Breit-Wigner function, for p+^{12}C and d+^{12}C collisions are presented in Figs. 3.8*b* and 3.8*d*, respectively. The masses M_{Δ} and widths Γ of the $\Delta^0(1232)$'s produced in p+^{12}C and d+^{12}C interactions were extracted from fitting the difference distributions, $D(M)$, to relativistic Breit-Wigner function, $b(M)$, given in relation (3.6). Figs. 3.8*a* and 3.8*c* show statistically significant resonance-like structures, expected for $\Delta^0(1232)$'s, in the experimental invariant mass spectra of $p\pi^-$ pairs at the best values of parameter ε in p+^{12}C and d+^{12}C collisions, respectively. The slight excess of the experimental distribution over the background spectrum in region $M_{p\pi} > 1400$ MeV/c^2, as seen from Figs. 3.8*a* and 3.8*c*, is due to the contribution from higher lying resonances, the nearest of which is the $N^*(1440)$ resonance. It should be mentioned that the criterion given in relation (3.4) suppresses the contribution from higher lying resonances which tends to disappear as $\varepsilon \rightarrow 0$ [14].

Table 3.2: Parameters of mass distributions of $\Delta^0(1232)$ produced in p+^{12}C and d+^{12}C collisions at 4.2 *A* GeV/*c*, obtained from fitting by the relativistic Breit-Wigner function.

Collision Type	***C***	***M* (MeV/c^2)**	**Γ (MeV/c^2)**	***χ²/n.d.f***
p*+^{12}C, 4.2 GeV/*c	25575 ± 2695	$1222 \pm 5\ ^{+10}_{-14}$	$89 \pm 14\ ^{+32}_{-43}$	0.21
d*+^{12}C, 4.2 *A* GeV/*c	37407 ± 3714	$1230 \pm 4\ ^{+3}_{-6}$	$90 \pm 14\ ^{+19}_{-24}$	0.81

The parameters of $\Delta^0(1232)$'s, produced in p+^{12}C and d+^{12}C collisions, extracted from fitting their mass distributions by the function $b(M)$ in relation (3.6), are given in Table 3.2. As observed from $\chi^2/n.d.f.$ values in Table 3.2, the mass distributions of $\Delta^0(1232)$'s are fitted quite well by the relativistic Breit-Wigner function.

3.5 Fractions of negative pions coming from $\Delta^0(1232)$ decay

The fractions $R(\Delta^0/\pi^-)$ of negative pions originating from decays of $\Delta^0(1232)$'s (relative to the total number of π^-) in p+^{12}C and d+^{12}C interactions were obtained using the following relation applied to the above extracted best experimental and background invariant mass distributions:

$$R(\Delta^0/\pi^-) = \frac{\int_{M_p+M_\pi}^{M_x} \left(\frac{dn^{\exp t}}{dM} - a\frac{dn^b}{dM} \right) dM}{N_{in} n(\pi^-)}, \qquad (3.7)$$

where M_p+ $M_\pi \approx 1079$ MeV/c^2 – the sum of masses of proton and pion, $M_x \approx 1400$ MeV/c^2 ($M_x \approx 1410$ MeV/c^2) in case of p+^{12}C collisions (d+^{12}C collisions) – the lower and upper limits of integration; $n(\pi^-) = 0.36 \pm 0.01$ ($n(\pi^-) = 0.66 \pm 0.01$) – the mean multiplicity per event of negative pions, and $N_{in} = 6736$ ($N_{in} = 7071$) is the total number of inelastic collision events for p+^{12}C collisions (d+^{12}C collisions). The value of numerator in equation (3.7) is the total excess of the experimental distribution over the background spectrum, which is the number of produced $\Delta^0(1232)$'s denoted as $N_{\Delta^0 \to p\pi^-}$. We obtained $N_{\Delta^0 \to p\pi^-} = 939 \pm 31(\text{stat.})^{+237}_{-159}(\text{syst.})$ and $1390 \pm 37(\text{stat.})^{+269}_{-336}(\text{syst.})$ for p+^{12}C and d+^{12}C collisions at 4.2 A GeV/c, respectively. The systematic errors on these $N_{\Delta^0 \to p\pi^-}$ extracted for p+^{12}C and d+^{12}C collisions were deduced based on the corresponding uncertainties in parameter a.

Further the $\Delta^0(1232)$ parameters extracted in the present work for p+^{12}C and d+^{12}C collisions at 4.2 GeV/c per nucleon are compared with the corresponding parameters of $\Delta^0(1232)$'s estimated using the similar method in relativistic hadron–nucleus collisions. The masses and widths of $\Delta^0(1232)$'s , and the fractions $R(\Delta^0/\pi^-)$ of π^- mesons originating from $\Delta^0(1232)$ decay, extracted in the present work for p+^{12}C and d+^{12}C collisions at 4.2 A GeV/c in comparison with those estimated in π^-+^{12}C collisions [14] at 40 GeV/c and ^{16}O+p interactions [15] at 3.25 GeV/c per nucleon are listed in Table 3.3. The masses and widths of $\Delta^0(1232)$'s for the above collisions

coincide within uncertainties with each other, as can be seen from Table 3.3. The values of the estimated widths of $\Delta^0(1232)$'s shown in Table 3.3 are close to each other and agree with the average width, ~ 90 ± 10 MeV/c^2, extracted for $\Delta^0(1232)$'s produced in the relativistic C+C [13], ^{4}He+C [17], C+^{181}Ta [16], π^-+^{12}C [14], and ^{16}O+p [78] collisions. In Ref. [79], the theoretical calculations revealed a shift of a $\Delta(1232)$ mass by about –10 MeV/c^2 towards lower values relative to the mass of free nucleon $\Delta(1232)$. Despite the relatively large uncertainties, the average shifts of the absolute values of masses of $\Delta^0(1232)$, produced on ^{12}C and ^{16}O nuclei from the mass of free nucleon $\Delta^0(1232)$, as seen from Table 3.3, agree with the above result calculated theoretically in Ref. [79] and cited in Ref. [2].

Table 3.3: The masses and widths of $\Delta^0(1232)$, and fractions $R(\Delta^0/\pi^-)$ of π^- mesons originating from decay of $\Delta^0(1232)$ resonances, obtained in p+^{12}C and d+^{12}C collisions at 4.2 GeV/c per nucleon, in π^-+^{12}C collisions at 40 GeV/c, and in ^{16}O+p collisions at 3.25 GeV/c per nucleon.

Reaction, p_0	M **(MeV/c^2)**	Γ **(MeV/c^2)**	$R(\Delta^0/\pi^-)$ **(%)**
p+^{12}**C, 4.2 GeV/c**	$1222 \pm 5^{+10}_{-14}$	$89 \pm 14^{+32}_{-43}$	$39 \pm 3^{+10}_{-7}$
d+^{12}**C, 4.2 A GeV/c**	$1230 \pm 4^{+3}_{-6}$	$90 \pm 14^{+19}_{-24}$	$30 \pm 2^{+6}_{-7}$
π^- +^{12}**C, 40 GeV/c**	1226 ± 3	87 ± 7	6 ± 1
^{16}**O+p, 3.25 A GeV/c**	1224 ± 4	96 ± 10	41 ± 4

We encounter more complex situation in case of collisions of nuclei with nuclei at relativistic energies, particularly for heavy ion collisions. This is because the characteristics of $\Delta^0(1232)$'s can modify significantly in the high density hadronic matter created in relativistic nuclear collisions [1, 3, 80]. Shift of the mass of hadrons in a nuclear medium can be either positive or negative, and this mass shift depends on the value of hadron density [1]. For example, the masses of $\Delta^0(1232)$'s were shifted by approximately 60 MeV/c^2 and 80 MeV/c^2 towards lower masses in near central Nickel–Nickel and Gold–Gold interactions [1, 80] at energies between 1 to 2 GeV per nucleon. The deduced widths were approximately 50 MeV/c^2 in both collision types. The shift in the mass of $\Delta(1232)$ produced in the collisions of nuclei with nuclei was

shown to be approximately proportional to the number of participant nucleons [1, 3, 81]. The absolute value of mass shift decreased as the number of participants decreased with an increase in impact parameter *b*. We deal with ^{12}C, which is a light nucleus, and the results are averaged over all possible values of impact parameter *b* [13–15, 17–19]. The majority of the *p*+^{12}C and *d*+^{12}C collision events, which we analyzed in the present work, are the peripheral interaction events. Now if we assume that the high densities of the hadron matter, produced in near central relativistic heavy ion collisions, are the main cause of the significant decrease in the mass and width of $\Delta(1232)$, then the small modification of these parameters of $\Delta(1232)$'s observed in the present analysis is because of the predominantly peripheral nature of analyzed proton–carbon and deuteron–carbon collision events, in which the density of hadron matter is approximately equal to the density of normal nuclear matter [15].

As seen in Table 3.3, about $(39\pm3^{+10}_{-7})$% and $(30 \pm 2^{+6}_{-7})$% of π^- mesons are estimated to come from $\Delta^0(1232)$ decay in *p*+^{12}C and *d*+^{12}C collisions, respectively. Both values are compatible with each other. The fractions of π^- mesons originating from $\Delta^0(1232)$ decays were estimated to be (41 ± 4)% in ^{16}O+*p* collisions [15] at 3.25 *A* GeV/*c*, and only (6 ± 1)% of negative pions produced in π^-+^{12}C interactions at 40 GeV/*c* [14] came from decays of $\Delta^0(1232)$'s. It was the expected result [14], because at such high energies as 40 GeV, the probability of production of other heavier resonances as well as of ρ^0-, ω^0- and f^0-mesons increases significantly in comparison with incident energies in a range of a few GeV per nucleon [82, 83]. The authors of Ref. [83] estimated that about 30% of charged pions came from decay of ρ^0-, ω^0- and f^0-mesons in π^-+^{12}C interactions at 40 GeV/*c*. In Fig. 3.9, the fractions of π^- mesons originating from decays of $\Delta^0(1232)$'s in *p*+^{12}C and *d*+^{12}C collisions at 4.2 GeV/*c* per nucleon are compared with the corresponding fractions obtained for various colliding nuclei at different energies.

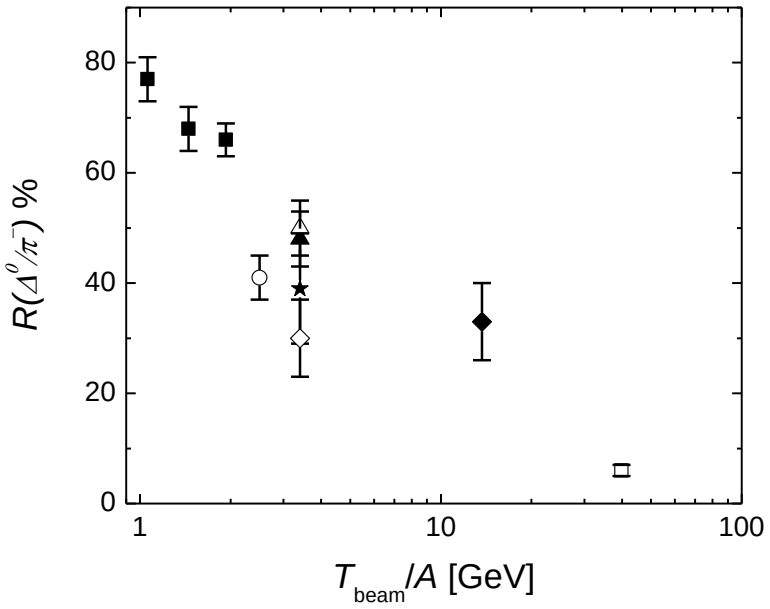

Figure 3.9: Dependence of fraction of π^- mesons originating from decay of $\Delta^0(1232)$ resonances on the incident kinetic energy per nucleon: (★) − for p+^{12}C collisions at 4.2 GeV/c ($T_{beam} \approx 3.4$ GeV) and (◊) − for d+^{12}C collisions at 4.2 GeV/c per nucleon ($T_{beam} \approx 3.4$ GeV per nucleon) in the present work; (○) − for ^{16}O+p collisions at 3.25 A GeV/c ($T_p \approx 2.5$ GeV in the oxygen nucleus rest frame); (■) − for central Ni+Ni collisions [76] at 1.06, 1.45, and 1.93 GeV per nucleon; (♦) – for central ^{28}Si+Pb collisions [84] at p_{lab} = 14.6 GeV per nucleon ($T_{beam} \approx$ 13.7 GeV per nucleon); (▲) and (Δ) – for ^{4}He+^{12}C and ^{12}C+^{12}C collisions, respectively, at 4.2 GeV/c per nucleon ($T_{beam} \approx 3.4$ GeV per nucleon); (□) – for π^-+^{12}C collisions at 40 GeV/c ($T_{beam} \approx 39.9$ GeV).

As observed from Fig. 3.9, the fraction of negative pions coming out of $\Delta^0(1232)$ decays shows decreasing behavior with an increase of incident kinetic energy per nucleon. The values of $R(\Delta^0/\pi^-)$ obtained for p+^{12}C and d+^{12}C collisions at 4.2 GeV/c per nucleon, as can be seen from Fig. 3.9, overlap within the error bars with the corresponding results for ^{4}He+^{12}C and ^{12}C+^{12}C collisions at the same incident energy per nucleon. On the whole, our results for $R(\Delta^0/\pi^-)$ are in line with those obtained for different sets of colliding nuclei at various incident energies.

3.6 Relative numbers of nucleons excited to $\Delta^0(1232)$ at freeze-out conditions

The relative numbers of nucleons excited to $\Delta^0(1232)$ at freeze-out conditions, $n(\Delta)/n(\text{nucleon}+\Delta)$, are estimated using the results given in the previous sections. Freeze-out can be defined as the stage when the average distance between the constituent hadrons of expanding "fireball", created in relativistic nuclear collisions, becomes larger than the strong interaction range. Hadron abundances will remain fixed after the freeze-out stage. The abundance of $\Delta^0(1232)$'s , $n(\Delta)$, can be calculated via the expression [80]

$$n(\Delta) = n(\pi^-)\, f_{isobar} \frac{\pi^-_{\Delta}}{\pi^-_{all}}, \qquad (3.8)$$

where $n(\pi^-)$ is the average number of π^- mesons per event (mean multiplicity), $\frac{\pi^-_{\Delta}}{\pi^-_{all}}$ is the fraction of π^- mesons originating from decays of $\Delta^0(1232)$'s , and f_{isobar} is the isobar model prediction [65] given by

$$f_{isobar} = \frac{n(\pi^- + \pi^0 + \pi^+)}{n(\pi^-)} = \frac{6(Z^2 + N^2 + NZ)}{5N^2 + NZ}, \qquad (3.9)$$

where N denotes the number of neutrons, and Z is the number of protons. The mean multiplicities of negative pions per event, $n(\pi^-)$, in p+^{12}C and d+^{12}C interactions at 4.2 GeV/c per nucleon are 0.36±0.01 and 0.66 ± 0.01, respectively. For p+^{12}C collisions $f_{isobar} \approx 3.43$, and for d+^{12}C collisions $f_{isobar} \approx 3.0$.

We assume

$$\frac{< n_p^{part} >}{< n_n^{part} >} = \frac{< n(\pi^+) >^{pC}}{< n(\pi^-) >^{pC}} = \frac{< n(\pi^+) >^{pN}}{< n(\pi^-) >^{pN}} = 1.7$$

from data on proton–nucleon interactions [49] for p+^{12}C collisions, and

$$\frac{< n_p^{part} >}{< n_n^{part} >} = 1$$

for d+^{12}C collisions [49] at 4.2 GeV/c per nucleon, which is due to the equal number of protons and neutrons in the colliding d+^{12}C system. Here $< n_n^{part} >$ denote the mean

multiplicities per event of participant neutrons in p+^{12}C and d+^{12}C collisions. Furthermore, we calculated n(nucleon+Δ) using the below given relations (3.10) and (3.11) for p+^{12}C and d+^{12}C collisions, respectively:

$$\begin{aligned} n(\text{nucleon}+\Delta) &= < n_p^{part} > + < n_n^{part} > + < n_\Delta > \\ &= 1.59 < n_p^{part} > + < n_\Delta > \end{aligned} \tag{3.10}$$

$$\begin{aligned} n(\text{nucleon}+\Delta) &= < n_p^{part} > + < n_n^{part} > + < n_\Delta > \\ &= 2 < n_p^{part} > + < n_\Delta > \end{aligned} \tag{3.11}$$

with $< n_p^{part} >$ = 1.83 ± 0.04 and 1.94 ± 0.06 and $< n_\Delta > = 0.14 \pm 0.01 \,^{+0.04}_{-0.03}$ and $0.20 \pm 0.02 \,^{+0.04}_{-0.07}$ being the mean multiplicities of participant protons and Δ^0(1232)'s in p+^{12}C and d+^{12}C collisions at 4.2 GeV/c per nucleon, respectively. Using the above results, the relative number of nucleons excited to Δ^0(1232) resonances at freeze-out was estimated to be $n(\Delta)/n(\text{nucleon}+\Delta) = (16 \pm 3 \,^{+4}_{-3})\%$ [19] and $(15 \pm 2 \,^{+3}_{-4})\%$ [20] in p+^{12}C and d+^{12}C collisions at 4.2 GeV/c per nucleon, respectively. Both the results proved to be in a good agreement coinciding with each other within uncertainties. In Fig. 3.10, the values of n(Δ)/n(nucleon+Δ) estimated in the present work for p+^{12}C and d+^{12}C collisions at 4.2 GeV/c per nucleon are compared with the corresponding results obtained in early works for various colliding nuclei at different incident energies. As seen from Fig. 3.10, the estimated relative numbers of nucleons excited to Δ^0(1232) at conditions of freeze-out in p+^{12}C and d+^{12}C collisions at 4.2 GeV/c per nucleon are consistent within the errors with the corresponding results presented in Refs. [13, 17, 19, 80, 84].

The dependence of the multiplicity of charged particles on Q value in p+^{12}C collisions at 4.2 GeV/c was studied in Ref. [69], where $Q = n_+ - n_- - n_p^{evap}$ with n_+ and n_- being the numbers of singly charged positive and negative particles in an event, respectively, and n_p^{evap} is the number of evaporated protons (p_{lab} < 300 MeV/c). Earlier it was noticed [69] that FRITIOF model underestimates the dependence of multiplicity of negative pions. For this reason, it was attempted to account for non-nucleon degrees of freedom in nuclei in the Modified FRITIOF model.

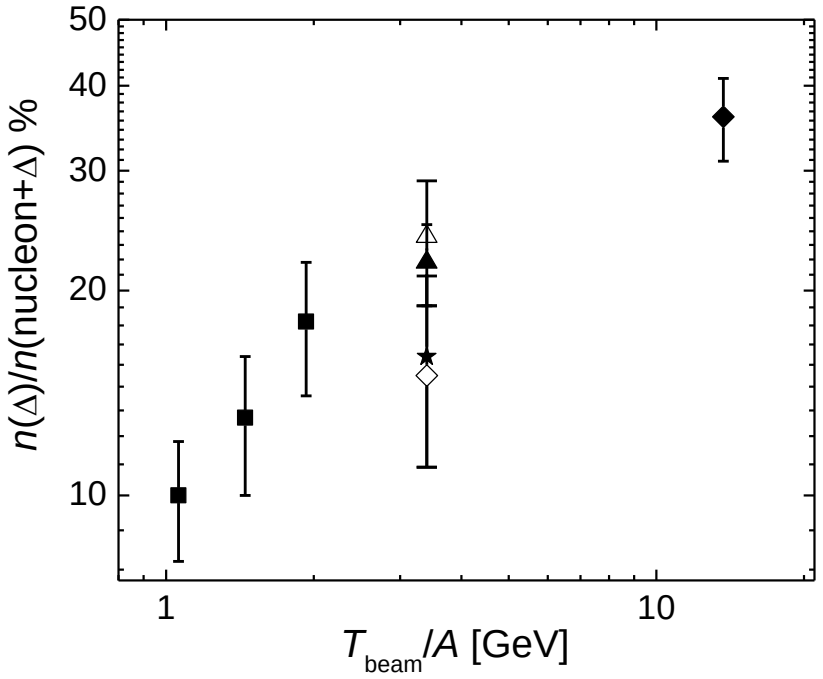

Figure 3.10: The relative numbers of nucleons excited to $\Delta^0(1232)$ resonances at conditions of freeze-out as a function of beam kinetic energy per nucleon: (★) − for p+^{12}C collisions and (◊) − for d+^{12}C collisions at 4.2 GeV/c per nucleon ($T_{beam} \approx 3.4$ GeV per nucleon) in the present work, (■) − for central Ni+Ni collisions obtained by FOPI collaboration; (♦) –for central ^{28}Si+Pb collisions at p_{lab} = 14.6 GeV/c per nucleon obtained by E814 experiment; (▲) and (Δ) – for ^{4}He+^{12}C and ^{12}C+^{12}C collisions, respectively, at 4.2 GeV/c per nucleon.

It was set in the Modified FRITIOF model [52, 69] that 20% of the total number of participant nucleons were excited to Δ^0 (Δ^+)'s. The Modified FRITIOF model taking into account the production of Δ resonances could describe quite well the experimental features of the secondary particles including the multiplicity dependence of negative pions. The relative numbers of nucleons excited to $\Delta^0(1232)$'s at freeze-out in p+^{12}C and d+^{12}C collisions, estimated in the present work, are compatible with the above assumption made in the Modified FRITIOF model.

Chapter 4
Comparison of Kinematical Spectra of $\Delta^0(1232)$ in $p+^{12}C$ and $d+^{12}C$ Collisions

4.1 Reconstruction of kinematical spectra of $\Delta^0(1232)$

The low transverse momentum (p_t) enhancement of pions in hadron–nucleus and nucleus–nucleus collisions at incident energies between 1 and 15 GeV per nucleon was shown to be due to the kinematics of Δ(1232) decay [84–86]. It was observed that the pions originating from decay of $\Delta^0(1232)$'s occupied mostly the low transverse momentum region of the spectrum [84–86]. We extracted the p_t spectra of negative pions from correlated $p\pi^-$ pairs which contributed to the $\Delta^0(1232)$ mass distributions presented in Fig. 3.8 for p+^{12}C and d+^{12}C collisions at 4.2 GeV/c per nucleon. The reconstructed transverse momentum distributions of π^- mesons originating from $\Delta^0(1232)$ decay along with the p_t spectra of all π^- produced in p+^{12}C and d+^{12}C collisions are shown in Figs. 4.1*a* and 4.1*b*, respectively.

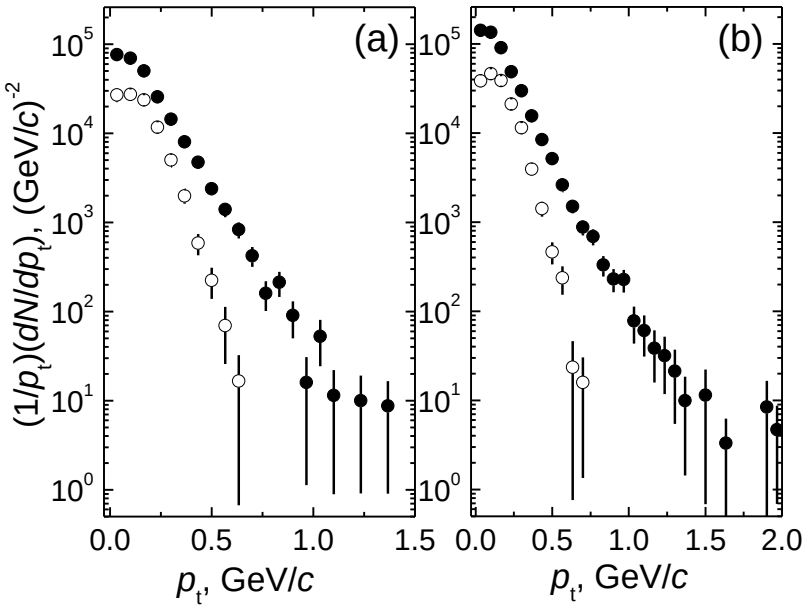

Figure 4.1: Transverse momentum distributions of all π^- mesons (●) and π^- originating from $\Delta^0(1232)$ decay (○) in p+^{12}C (*a*) and d+^{12}C (*b*) collisions at 4.2 GeV/c per nucleon.

The above figures show that π^- mesons coming from $\Delta^0(1232)$ decay occupy mainly the region of low transverse momentum (p_t < 0.6 GeV/c) of the p_t spectra, and this confirms that negative pions originating from $\Delta^0(1232)$ decay are responsible for the low transverse momentum enhancement of π^- spectra in p+^{12}C and d+^{12}C interactions at 4.2 GeV/c per nucleon.

4.1.1 Momentum, Transverse Momentum, Kinetic Energy, and Emission Angle distributions of $\Delta^0(1232)$ resonances

To estimate the mean kinematical characteristics of $\Delta^0(1232)$'s in p+^{12}C and d+^{12}C collisions at 4.2 A GeV/c per nucleon, we reconstructed the emission angle, transverse momentum, momentum, and kinetic energy spectra of $\Delta^0(1232)$'s in laboratory frame. For reconstructing such spectra, we used all $p\pi^-$ pairs which contributed to the experimental invariant mass spectra in Fig. 3.8, obtained using the best values of cutoff parameter ε. The momenta, transverse momenta, kinetic energies, and emission angles of $\Delta^0(1232)$ resonances were calculated using the relations (4.1)–(4.4), respectively, given below:

$$p_\Delta = \left| \vec{p}_p + \vec{p}_\pi \right|, \tag{4.1}$$

$$p_{\Delta t} = \left| \vec{p}_{pt} + \vec{p}_{\pi t} \right|, \tag{4.2}$$

$$T_\Delta = \sqrt{p_\Delta^2 + M_\Delta^2} - M_\Delta, \tag{4.3}$$

$$\theta_\Delta = \cos^{-1}\left(\frac{p_\Delta^L}{p_\Delta} \right), \tag{4.4}$$

where $\vec{p}_p$ and $\vec{p}_\pi$ – the proton and pion momenta, $\vec{p}_{pt}$ and $\vec{p}_{\pi t}$ – the proton and pion transverse momentum, M_Δ denote the invariant mass of $p\pi^-$ pair, and p_Δ and p_Δ^L are the total momentum and longitudinal momentum of $\Delta^0(1232)$, respectively. To take into account the contribution of background to the experimental invariant mass spectra presented in Fig. 3.8*a* and 3.8*c*, the estimated kinematical characteristics of $\Delta^0(1232)$'s

for every $p\pi^-$ pair were taken with a corresponding weight factor, w, calculated at $M = M_{p\pi}$ using the experimental and background invariant mass spectra of $p\pi^-$ pairs obtained at the best values of parameters ε and a:

$$w = \left(\frac{\frac{dn^{\exp}}{dM} - a\frac{dn^{b}}{dM}}{\frac{dn^{\exp}}{dM}} \right)_{M=M_{p\pi}} \qquad (4.5)$$

To estimate the systematic errors of obtained kinematical characteristics of $\Delta^0(1232)$'s in p+^{12}C and d+^{12}C collisions we proceeded as follows. For p+^{12}C collisions (d+^{12}C collisions), we took systematic uncertainties as the deviations between the kinematical characteristics of $\Delta^0(1232)$'s at the best value ε = 0.61 (ε = 0.52) and those obtained at ε = 0.43 (ε = 0.41) and ε = 0.68 (ε = 0.68), where we obtained the minimum and maximum width of $\Delta^0(1232)$'s, respectively, in the uncertainty interval 0.43–0.79 (0.36–0.68) of parameter ε. The reconstructed momentum, transverse momentum, kinetic energy, and emission angle distributions of $\Delta^0(1232)$ produced in p+^{12}C collisions (d+^{12}C collisions) for the above mentioned three different values of parameter ε are given in Fig. 4.2 (Fig. 4.3). As observed from Fig. 4.2 (Fig. 4.3), all the reconstructed kinematical spectra overlapped with each other within uncertainties for three different values of cutoff parameter ε.

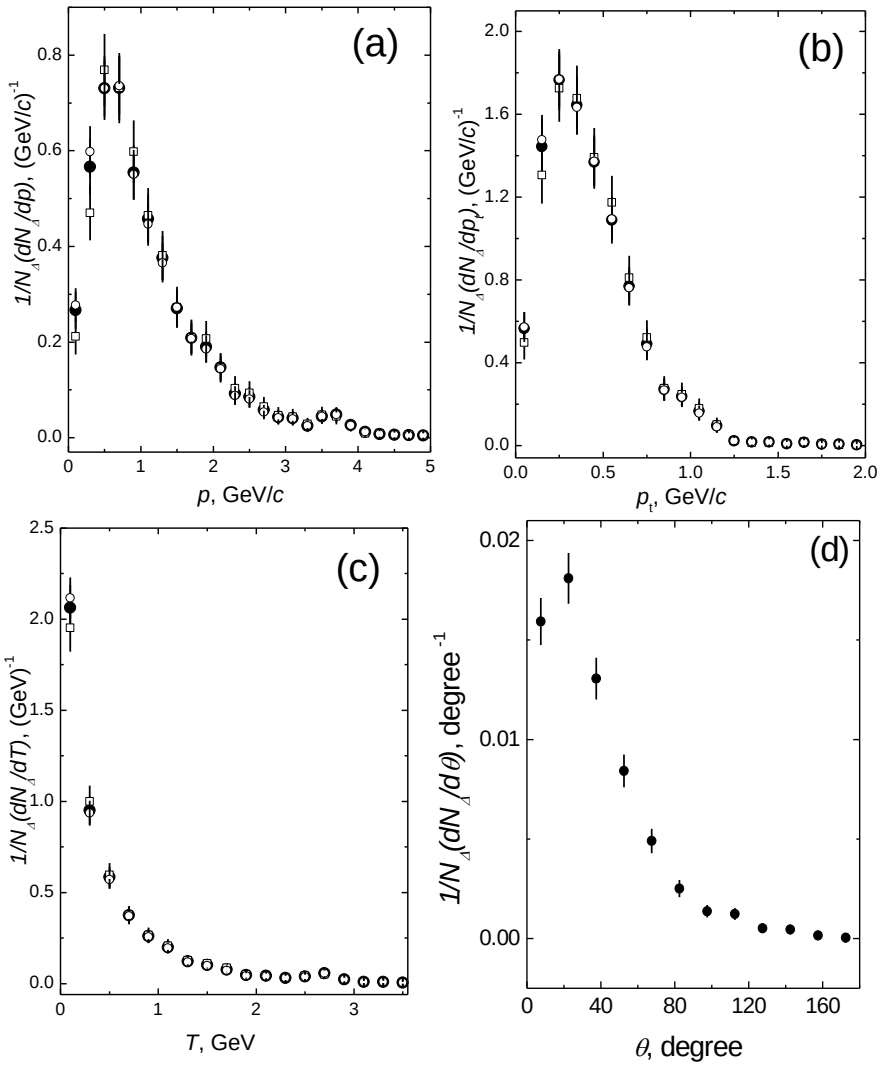

Figure 4.2: Reconstructed momentum (*a*), transverse momentum (*b*), and kinetic energy (*c*), distributions of $\Delta^0(1232)$ resonances in $p+^{12}C$ collisions at 4.2 GeV/*c* in the laboratory frame (normalized to the total number of $\Delta^0(1232)$) obtained for the values of ε=0.43 (□), ε=0.61 (●), and ε=0.68 (○). Reconstructed emission angle (*d*) distribution of $\Delta^0(1232)$ in $p+^{12}C$ collisions at 4.2 GeV/*c* in the laboratory frame obtained for the value of ε=0.61 (normalized to the total number of $\Delta^0(1232)$).

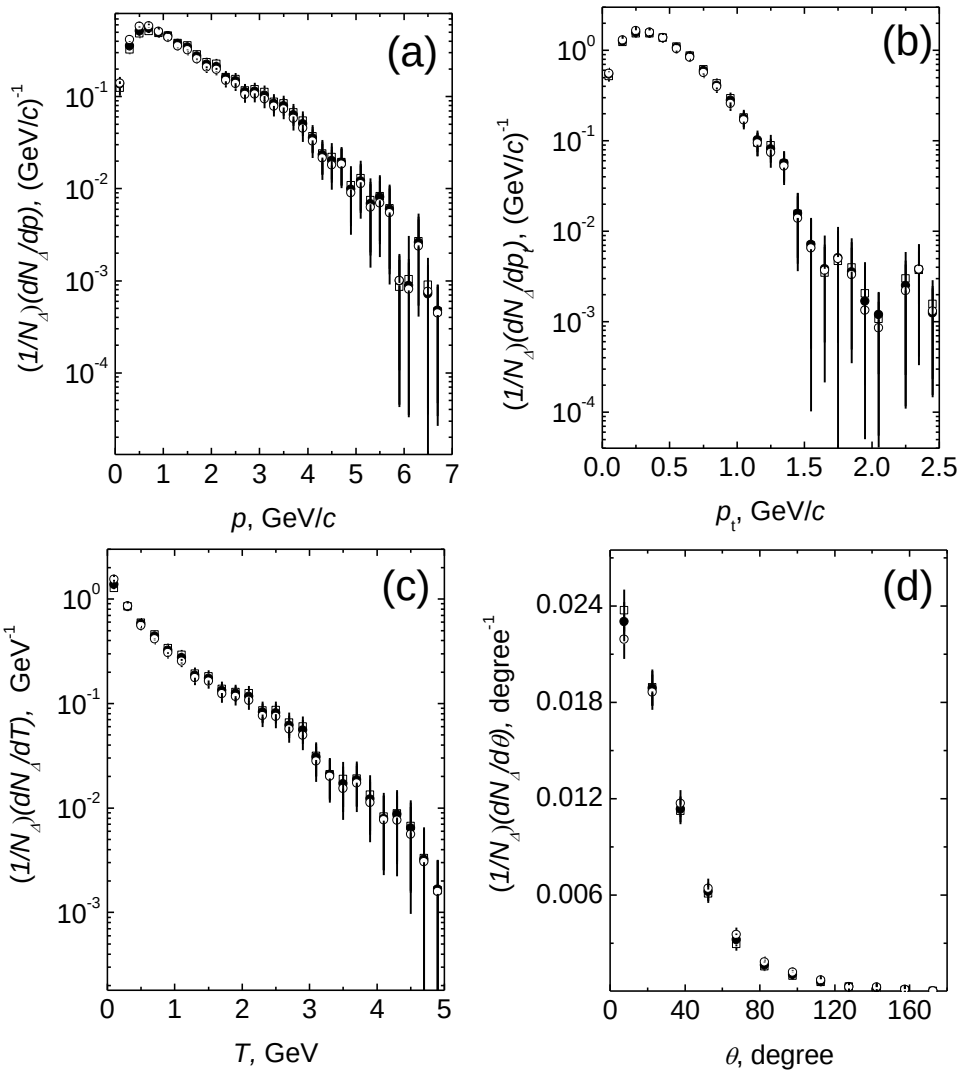

Figure 4.3: Reconstructed momentum (*a*), transverse momentum (*b*), kinetic energy (*c*), and emission angle (*d*) distributions of $\Delta^0(1232)$ in d+^{12}C collisions at 4.2 GeV/*c* per nucleon in the laboratory frame (normalized to the total number of $\Delta^0(1232)$) obtained for the values of ε = 0.41 (□), ε = 0.52 (●), and ε = 0.68 (○).

The comparison of the total momentum, transverse momentum, kinetic energy, and emission angle spectra of $\Delta^0(1232)$'s produced in p+^{12}C and d+^{12}C collisions is presented in Figs. 4.4*a* – 4.4*d*, respectively.

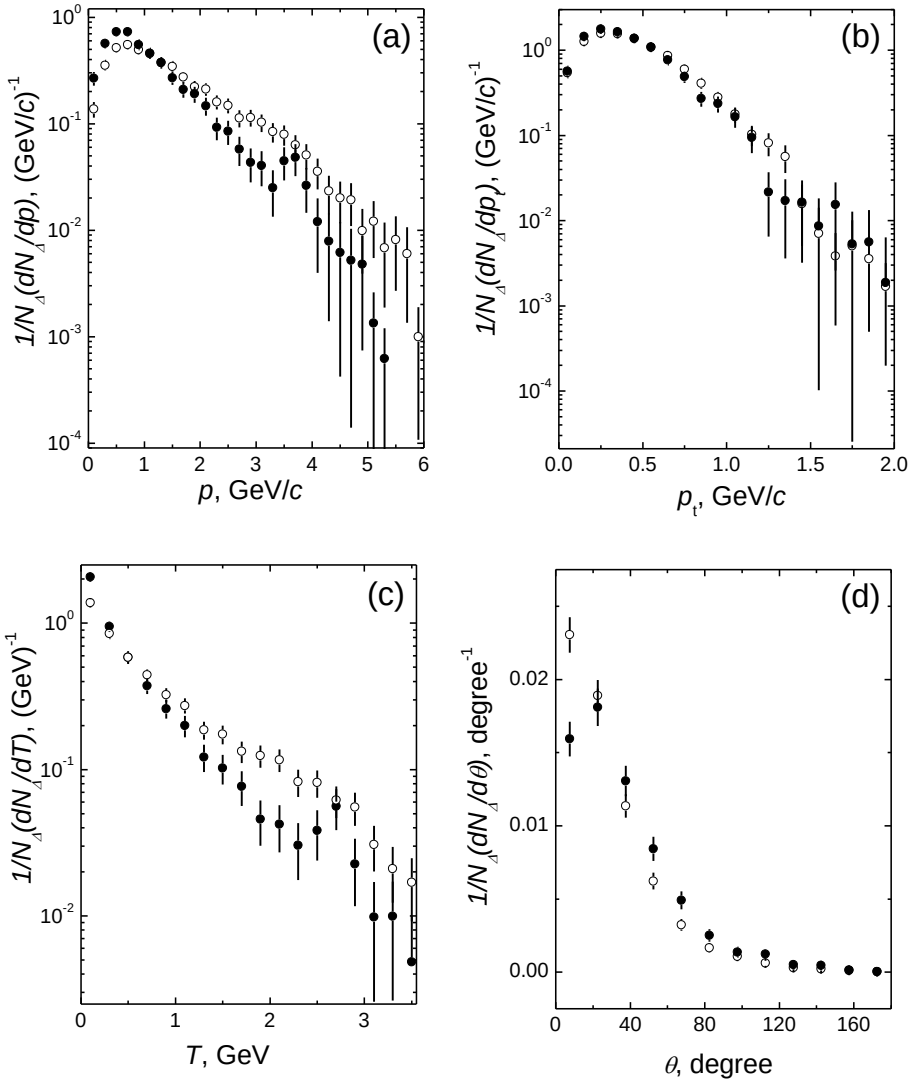

Figure 4.4: Reconstructed momentum (*a*), transverse momentum (*b*), kinetic energy (*c*), and emission angle (*d*) distributions of $\Delta^0(1232)$ in p+^{12}C (●) and d+^{12}C (○) collisions at 4.2 GeV/*c* per nucleon in the laboratory frame (normalized to the total number of $\Delta^0(1232)$).

The momentum spectrum of $\Delta^0(1232)$'s in d+^{12}C collisions presented in Fig. 4.4*a* shows a noticeable "shoulder" like structure in region p > 2.25 GeV/*c*. This structure is manifested as a significant excess of momentum distribution of $\Delta^0(1232)$'s in d+^{12}C interactions over the corresponding distribution of $\Delta^0(1232)$'s in p+^{12}C interactions in this part of the spectrum. The $\Delta^0(1232)$ resonances originating from neutrons of incident deuterons could probably be a reason for appearance of a

"shoulder" like structure in region p > 2.25 GeV/c. Similarly, the kinetic energy distribution of $\Delta^0(1232)$'s in d+^{12}C collisions has significant excess over the corresponding distribution of $\Delta^0(1232)$ in p+^{12}C collisions in region T > 1.75 GeV, as shown in Fig. 4.4*c*. As obvious from Fig. 4.4*d*, the maximum peak of emission angle spectrum of $\Delta^0(1232)$'s for p+^{12}C interactions is situated at a significantly higher value of emission angle than the corresponding peak of emission angle spectrum of $\Delta^0(1232)$'s for d+^{12}C collisions. The contribution from $\Delta^0(1232)$'s originated from neutrons of incident deuterons is the most probable reason for this observation. Indeed, the $\Delta^0(1232)$'s generated from neutrons of incident deuterons should move closer to and along the incident beam direction and be emitted at lower angles in the laboratory system in comparison with $\Delta^0(1232)$'s generated from target carbon nucleons.

Table 4.1: The mean values of momenta, kinetic energies, transverse momenta, emission angles, and rapidities of $\Delta^0(1232)$ resonances in p+^{12}C and d+^{12}C collisions at 4.2 GeV/c per nucleon in the laboratory frame [21].

Collision Type	p+^{12}C	d+^{12}C
$\langle p \rangle$, **MeV/*c***	$1103 \pm 27\ ^{+33}_{-15}$	$1483 \pm 29\ ^{+43}_{-63}$
$\langle T \rangle$, **MeV**	$523 \pm 20\ ^{+14}_{-9}$	$797 \pm 22\ ^{+30}_{-45}$
$\langle p_t \rangle$, **MeV/*c***	$422 \pm 9\ ^{+11}_{-3}$	$455 \pm 8\ ^{+5}_{-4}$
$\langle \theta \rangle$, **degree**	$36 \pm 1\ ^{-1}_{+1}$	$29 \pm 1\ ^{+2}_{-1}$
$\langle Y \rangle$	$0.59 \pm 0.02\ ^{+0.02}_{-0.01}$	$0.78 \pm 0.01\ ^{+0.02}_{-0.03}$

The mean values of momentum, transverse momentum, kinetic energy, emission angle, and rapidity of $\Delta^0(1232)$'s in p+^{12}C and d+^{12}C collisions are presented in Table 4.1. These mean values of kinematical characteristics of $\Delta^0(1232)$'s confirm the above findings. As observed from Table 4.1, the mean values of momentum and kinetic energy of $\Delta^0(1232)$'s in d+^{12}C collisions are significantly greater than those obtained in p+^{12}C interactions, whereas the mean emission angle of $\Delta^0(1232)$'s in d+^{12}C collisions is significantly lower than the corresponding value for $\Delta^0(1232)$'s in

p+^{12}C collisions. The transverse momentum distributions of $\Delta^0(1232)$'s and their mean values in p+^{12}C and d+^{12}C collisions at 4.2 GeV/c per nucleon, as seen from Fig. 4.4*b* and Table 4.1, almost do not differ and practically coincide with each other within uncertainties.

4.2 Rapidity distributions of $\Delta^0(1232)$ resonances

The reconstructed rapidity distributions of $\Delta^0(1232)$'s obtained for the cutoff parameter values ε = 0.43, 0.61, and 0.68 in p+^{12}C collisions and for the values of ε = 0.41, 0.52, 0.68 in d+^{12}C collisions at 4.2 GeV/c per nucleon are presented in Figs. 4.5*a* and 4.5*b*, respectively. The rapidities of $\Delta^0(1232)$'s were calculated using the relation (4.6):

$$Y = \frac{1}{2}\ln\left(\frac{E_\Delta + p_\Delta^L}{E_\Delta - p_\Delta^L}\right), \qquad (4.6)$$

where E_Δ and p_Δ^L are the total energy and longitudinal momentum of $\Delta^0(1232)$, respectively. As visible from Fig. 4.5*a*, the rapidity spectrum of $\Delta^0(1232)$'s in p+^{12}C interactions has a peak between c.m. rapidity (y ~ 0.28) of p+^{12}C collisions and nucleon–nucleon c.m. rapidity ($y_{\text{c.m.}}$ = 1.1) at 4.2 GeV/c. On the other hand, Fig. 4.5*b* shows that the reconstructed rapidity spectrum of $\Delta^0(1232)$'s in d+^{12}C interactions at 4.2 GeV/c per nucleon has a peak located near to c.m. rapidity (y ~ 0.45) of d+^{12}C collisions at 4.2 A GeV/c. The peaks of reconstructed rapidity distributions of $\Delta^0(1232)$'s in p+^{12}C and d+^{12}C collisions are located at a significantly lower rapidity values as compared to nucleon–nucleon c.m. rapidity at 4.2 GeV/c ($y_{\text{c.m.}}$ = 1.1 for 4.2 A GeV/c). If $\Delta^0(1232)$'s were produced in first chance nucleon–nucleon collisions, then the rapidity spectrum of $\Delta^0(1232)$'s would have a peak at nucleon–nucleon c.m. rapidity $y_{\text{c.m.}}$= 1.1. But in p+^{12}C and d+^{12}C collisions the peaks of the rapidity spectra of $\Delta^0(1232)$'s are located near the region of target carbon fragmentation. This shows that $\Delta^0(1232)$ resonances are mainly produced in secondary interactions on nucleons of

carbon nuclei as well as in peripheral interactions of incident protons and deuterons with target carbon nuclei.

The average numbers of participant protons per event $< n_p^{part} >$=1.83±0.04 and 1.94 ± 0.06 in p+^{12}C and d+^{12}C interactions at 4.2 GeV/c per nucleon, respectively, are significantly greater than the average number of participant protons per event in proton–nucleon collisions, $< n_p^{part} >_{pN}$, which is the average of the mean multiplicities of protons participating in $p + p$ and $p + n$ interactions [49]:

$$< n_p^{part} >_{pN} = \frac{< n_p^{part} >_{pp} + < n_p^{part} >_{pn}}{2} = 1.15. \qquad (4.7)$$

This indicates that secondary interactions have significant contribution to the mean multiplicities per event of participant protons even for such light nucleus as ^{12}C [31]. It is obvious that without secondary interactions (collisions) in carbon nuclei the mean multiplicities of participant protons in p+^{12}C collisions would coincide with the mean multiplicities of participant protons in proton–nucleon collisions. The rapidity spectrum of Δ^0(1232)'s in d+^{12}C interactions, as observed from Fig. 4.5*b*, has a noticeable "shoulder" type enhancement in region $y \sim 1.2 - 1.9$, which is likely due to Δ^0(1232) resonances generated from nucleons of incident deuterons.

For comparison of the rapidity spectra of Δ^0(1232)'s with those of protons in p+^{12}C and d+^{12}C interactions at 4.2 GeV/c per nucleon, we also included the rapidity spectra of protons in Figs. 4.5*a* and 4.5*b*. The rapidity spectra of protons have a noticeable peak at around $y \approx 0.2$, which is due to the slow target protons having momenta $p_{\text{lab}} < 300$ MeV/c, as shown early in Ref. [31]. Figure 4.5*a* also exhibits an enhancement of a significantly smaller height in region $y \approx 1.8 - 2.1$, which is due to the incident protons scattered quasi elastically on ^{12}C nucleons [31]. The similar enhancement was also visible in momentum spectrum of protons given in Fig. 3.1*a*. The rapidity distribution of protons in d+^{12}C collisions, as seen from Fig. 4.5*b*, has a large "shoulder" like structure of a relatively small height in region $y \sim 1.2$–2.1. This is most probably due to the protons originating from nucleons of incident deuterons [31].

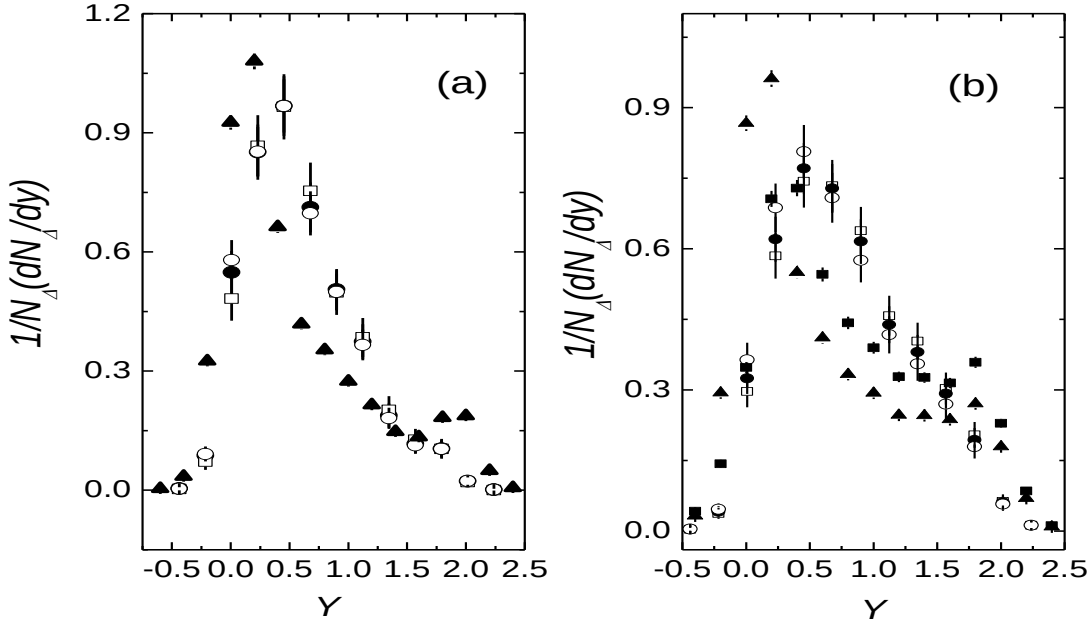

Figure 4.5: Reconstructed rapidity spectra of $\Delta^0(1232)$ resonances obtained for the values of ε=0.43 (□), ε=0.61 (●), and ε=0.68 (○) in p+^{12}C (*a*) collisions and for the values of ε = 0.41 (□), ε = 0.52 (●), and ε = 0.68 (○) in d+^{12}C (*b*) collisions at 4.2 GeV/*c* per nucleon in the laboratory frame (normalized to the total number of respective $\Delta^0(1232)$). Rapidity spectra of all protons (▲) in p+^{12}C collisions at 4.2 GeV/*c*, and of all protons (▲) and participant protons (■) in d+^{12}C collisions at 4.2 GeV/*c* per nucleon (normalized to the total number of respective protons).

The shapes of rapidity distributions of protons in Figs. 4.5*a* and 4.5*b* showed that the secondary interactions in ^{12}C nuclei and the mostly peripheral nature of the analyzed collisions are the main source of protons in p+^{12}C and d+^{12}C collisions, as was also observed for $\Delta^0(1232)$'s. However, a significant fraction of protons, as in case of $\Delta^0(1232)$'s, is generated from nucleons of incident deuterons in d+^{12}C collisions at 4.2 *A* GeV/*c*. It should be noted that the rapidity distributions of protons in p+^{12}C and d+^{12}C interactions at 4.2 *A* GeV/*c* were described quite satisfactorily by the Dubna Cascade Model in Ref. [31], Modified FRITIOF model in Refs. [4, 12, 33], and QGSM in Ref. [70].

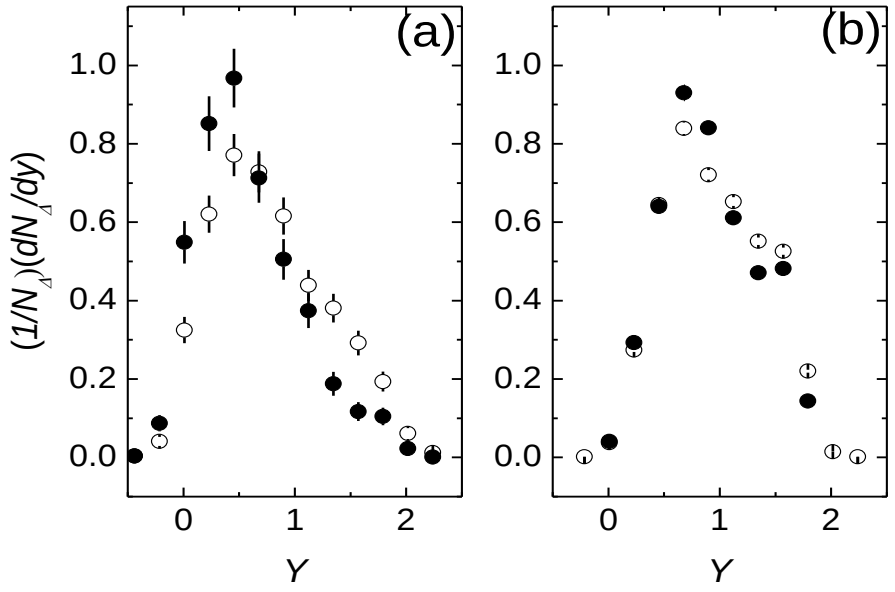

Figure 4.6: Reconstructed rapidity distributions of $\Delta^0(1232)$ resonances in p+^{12}C (●) and d+^{12}C (○) collisions at 4.2 GeV/c per nucleon in the laboratory frame in experiment (*a*) and obtained using Modified FRITIOF model (*b*) (normalized to the total number of respective $\Delta^0(1232)$).

The reconstructed rapidity distributions of $\Delta^0(1232)$'s in p+^{12}C and d+^{12}C collisions at 4.2 GeV/c per nucleon are shown in Fig. 4.6*a* for a comparison. As observed from Fig. 4.6*a*, the rapidity spectrum of $\Delta^0(1232)$'s produced in d+^{12}C collisions has a statistically significant enhancement over the rapidity spectrum of $\Delta^0(1232)$'s for p+^{12}C collisions in region y ~1.2–1.9. Such enhancement, although of a lesser magnitude as compared to experiment, is also visible in Fig. 4.6*b*, which contains a comparison of the corresponding rapidity spectra of $\Delta^0(1232)$'s calculated using Modified FRITIOF model with allowance for $\Delta(1232)$ production [4]. Nearly all the $\Delta^0(1232)$'s in p+^{12}C interactions at 4.2 GeV/c, as shown in Ref. [18], originated from nucleons of target ^{12}C nuclei.

Table 4.2: The mean values of momenta, kinetic energies, transverse momenta, emission angles, and rapidities of $\Delta^0(1232)$ resonances in p+^{12}C and d+^{12}C collisions at 4.2 GeV/c per nucleon in the laboratory frame extracted for the values of ε = 0.61, ε = 0.43, and ε = 0.68 in p+^{12}C collisions and for the values of ε = 0.52, ε = 0.41, and ε = 0.68 in d+^{12}C collisions along with the respective values of $N_{\Delta^0(1232)\to p\pi^-}$.

Collision	p+^{12}C			d+^{12}C		
ε	0.61	0.43	0.68	0.52	0.41	0.68
$\langle p \rangle$, **MeV/c**	$1103\pm27\,^{+33}_{-15}$	1136±30	1088±24	$1483\pm29\,^{+43}_{-63}$	1526±30	1420±29
$\langle T \rangle$, **MeV**	$523\pm20\,^{+14}_{-9}$	537±22	514±18	$797\pm22\,^{+30}_{-45}$	827± 24	752 ± 23
$\langle p_t \rangle$, **MeV/c**	$422\pm9\,^{+11}_{-3}$	433±9	419± 8	$455\pm8\,^{+5}_{-4}$	460 ± 8	446 ± 8
$\langle \theta \rangle$ **(degree)**	$36\pm1\,^{-1}_{+1}$	37±1	35± 1	$29\pm1\,^{+2}_{-1}$	28 ± 1	31 ± 1
$\langle Y \rangle$	$0.59\pm0.02\,^{+0.02}_{-0.01}$	0.61±0.02	0.58±0.01	$0.78\pm0.01\,^{+0.02}_{-0.03}$	0.80±0.01	0.75±0.01
$N_{\Delta^0(1232)\to p\pi^-}$	$939\pm31\,^{+237}_{-159}$	780±28	1176±34	$1390\pm37\,^{+269}_{-336}$	1054±32	1659±41

As seen from Fig. 4.6*a*, the rapidity spectrum of $\Delta^0(1232)$'s in p+^{12}C collisions has a main peak at y~ 0.45 (at around target ^{12}C fragmentation region), which is significantly higher than the corresponding main peak in case of $\Delta^0(1232)$'s produced in d+^{12}C collisions. The mean value of rapidity of $\Delta^0(1232)$'s was estimated to be 0.59 ± 0.02 $^{+0.02}_{-0.01}$ and 0.78 ± 0.01 $^{+0.02}_{-0.03}$ in p+^{12}C [18, 19] and d+^{12}C [20] collisions, respectively. Thus the mean rapidity of $\Delta^0(1232)$'s in d+^{12}C collisions proved to be noticeably greater than the corresponding mean rapidity of $\Delta^0(1232)$'s produced in p+^{12}C collisions. The difference between p+^{12}C and d+^{12}C colliding systems is in one extra neutron in incident deuteron. In the light of above observations, we may conclude that in d+^{12}C collisions at 4.2 GeV/c per nucleon a majority of $\Delta^0(1232)$'s is generated from nucleons of target ^{12}C nuclei, while still a significant number of $\Delta^0(1232)$'s are originated from neutrons of incident deuterons, as is expressed by a "shoulder" like structure in rapidity spectrum of $\Delta^0(1232)$'s in region y ~ 1.2–1.9 in Fig. 4.6*a*.

The mean values of momenta, kinetic energies, transverse momenta, emission angles, and rapidities of $\Delta^0(1232)$'s extracted for three different values of cutoff

parameter ε in p+^{12}C and d+^{12}C collisions are presented in Table 4.2. Table 4.2 contains also the corresponding values of $N_{\Delta^0(1232)\to p\pi^-}$ for p+^{12}C and d+^{12}C collisions.

Table 4.3: Comparison of the mean values of momenta, transverse momenta, and rapidities of protons originating from decay of $\Delta^0(1232)$ resonances with the corresponding mean values for participant protons in experiment [33] and calculated using three different models for p+^{12}C and d+^{12}C collisions at 4.2 GeV/c per nucleon.

Parameters	$\langle p \rangle$, **MeV/*c***		$\langle p_t \rangle$, **MeV/*c***		$\langle Y \rangle$	
Collision Type	***p*+^{12}C**	***d*+^{12}C**	***p*+^{12}C**	***d*+^{12}C**	***p*+^{12}C**	***d*+^{12}C**
Protons from Δ^0(1232)	$878\pm24^{+18}_{-11}$	$1163\pm26^{+30}_{-44}$	$365\pm8^{+6}_{-3}$	$386\pm7^{+3}_{-6}$	0.58±0.01 ± 0.01	0.76±0.01 ± 0.03
Protons (experiment)	1292 ± 7	1289 ± 8	443 ±2	437 ±2	0.77±0.01	0.77±0.01
Protons (DCM)	1294 ± 6	1370 ± 5	459 ±3	468 ±2	0.75±0.01	0.77±0.01
Protons (FRITIOF)	1170 ± 3	1250 ± 2	420 ±1	440 ±1	0.72±0.01	0.75±0.01
Protons (QGSM)	1372 ± 7	1376 ± 8	437 ±3	520 ±2	0.74±0.01	0.75±0.01

The mean values of momenta, transverse momenta, and rapidities of protons and π^- mesons coming from $\Delta^0(1232)$ decay were extracted from the correlated $p\pi^-$ pairs which contributed to the mass spectra of $\Delta^0(1232)$'s in p+^{12}C [18, 19] and d+^{12}C [20] collisions at 4.2 GeV/c per nucleon, shown in Fig. 3.8. The mean momenta, transverse momenta, and rapidities of protons and π^- mesons coming from decay of $\Delta^0(1232)$'s were compared with the corresponding mean values for participant protons and π^- mesons, produced in p+^{12}C and d+^{12}C collisions, presented in Tables 4.3 and 4.4, respectively. For sake of comparison, the mean values of the kinematical characteristics of participant protons and π^- mesons produced in p+^{12}C and d+^{12}C collisions obtained in experiment [33] and the corresponding data extracted from Dubna Cascade Model, FRITIOF model, and QGSM [31–33, 70, 71] are also given in Tables 4.3 and 4.4.

The method used to estimate the systematic uncertainties in the calculated mean kinematical characteristics of protons and π^- mesons originating from decay of $\Delta^0(1232)$, presented in Tables 4.3 and 4.4, was similar to the approach used to calculate

the systematic errors in mean momenta, transverse momenta, emission angles, and rapidities of $\Delta^0(1232)$'s generated in p+^{12}C [18, 19] and d+^{12}C [20] collisions. The maximal variations in the mean values of the extracted parameters within the uncertainty range of the cutoff parameter ε, used to reconstruct the mass spectra of $\Delta^0(1232)$'s in Refs. [18–20], gave the systematic uncertainties for the corresponding mean kinematical characteristics of protons and negative pions originating from decay of $\Delta^0(1232)$'s.

Table 4.4: Comparison of the mean values of momenta, transverse momenta, and rapidities of π^- mesons coming from decay of $\Delta^0(1232)$ resonances with the corresponding mean values for all negative pions in experiment [33] and calculated using three different models [32, 33, 71] for p+^{12}C and d+^{12}C collisions at 4.2 GeV/c per nucleon.

Parameters	$\langle p \rangle$, **MeV/c**		$\langle p_t \rangle$, **MeV/c**		$\langle Y \rangle$	
Collision Type	**p+^{12}C**	**d+^{12}C**	**p+^{12}C**	**d+^{12}C**	**p+^{12}C**	**d+^{12}C**
π^- from $\Delta^0(1232)$	$361\pm8\,^{+15}_{-5}$	$444\pm8\,^{+10}_{-15}$	$193\pm3\,^{+7}_{-3}$	$205\pm3\,^{+3}_{-4}$	$0.75\pm0.02\,^{+0.02}_{-0.01}$	$0.95\pm0.02\,^{+0.02}_{-0.03}$
π^- (experiment)	504 ± 8	564 ± 7	244 ± 3	251± 3	0.84 ± 0.01	0.98 ± 0.01
π^- (DCM)	490	550	214	228	0.85	0.98
π^- (FRITIOF)	480 ± 3	540 ± 2	236 ± 1	240 ± 1	0.86 ± 0.01	0.97 ± 0.01
π^- (QGSM)	457 ± 4	507 ± 3	217 ± 2	223 ± 1	0.83 ± 0.01	0.93 ± 0.01

As seen from Table 4.2, the mean momentum and mean rapidity of $\Delta^0(1232)$'s are significantly larger in d+^{12}C interactions as compared to those of $\Delta^0(1232)$'s produced in p+^{12}C interactions, whereas their mean transverse momenta are compatible with each other. As shown above, this difference is due to contribution from the relatively fast $\Delta^0(1232)$'s originating from neutrons of projectile deuterons in d+^{12}C collisions. It is also seen from Table 4.3 that the protons coming from decay of $\Delta^0(1232)$'s have noticeably lower mean values of momentum and transverse momentum as compared to the corresponding mean values for participant protons in experiment and calculated using the relevant models.

Table 4.4 shows that the mean momentum and mean rapidity of π^- mesons originating from decays of $\Delta^0(1232)$'s in $d+^{12}C$ interactions are noticeably larger than the corresponding mean values for negative pions generated out of $\Delta^0(1232)$ decay in $p+^{12}C$ interactions, whereas their mean transverse momenta are compatible to each other. This difference is due to the contribution from the relatively fast $\Delta^0(1232)$'s generated from neutrons of incident deuterons in $d+^{12}C$ collisions, as was also discussed above for the protons coming from decay of $\Delta^0(1232)$. It is also seen from Table 4.4 that mean values of momenta and transverse momenta of π^- mesons originating from decays of $\Delta^0(1232)$'s are noticeably smaller than those for all negative pions produced in experiment [33] and the mean values calculated using the models.

Chapter 5
Temperatures of $\Delta^0(1232)$ Resonances

5.1 Spectra of Invariant Cross Sections of $\Delta^0(1232)$ in p+^{12}C and d+^{12}C collisions

The spectra of invariant cross sections $\frac{Ed^3\sigma}{d^3p}$ were reconstructed for $\Delta^0(1232)$'s in p+^{12}C and d+^{12}C collisions at 4.2 GeV/c per nucleon versus their kinetic energies T in the laboratory frame for the values of cutoff parameters ε = 0.61 (ε = 0.52), 0.43 (0.41), and 0.68 (0.68) for p+^{12}C (d+^{12}C) collisions. Figures 5.1*a* and 5.2*a* represent the invariant cross sections spectra of $\Delta^0(1232)$'s extracted at the best cutoff parameter values ε = 0.61 and ε = 0.52 in p+^{12}C and d+^{12}C collisions, respectively.

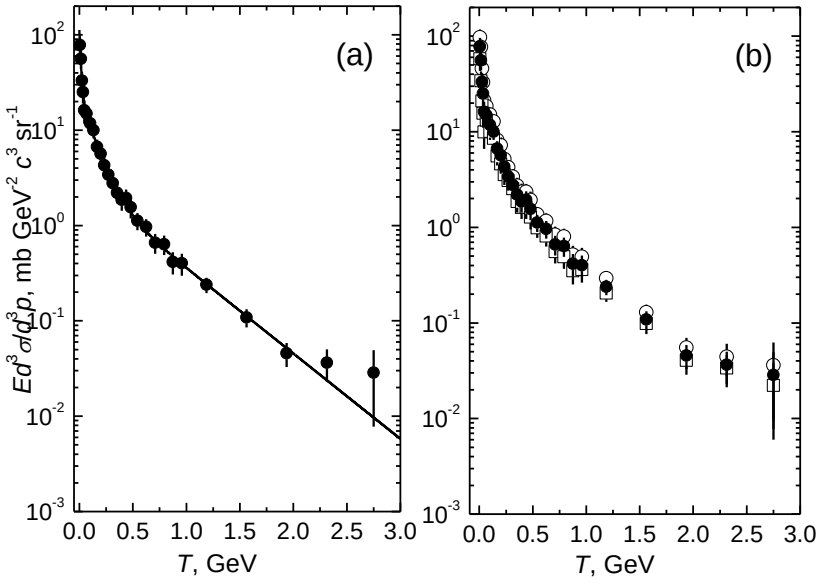

Figure 5.1: (*a*) Reconstructed invariant cross sections of $\Delta^0(1232)$ resonances in p+^{12}C collisions at 4.2 GeV/c as a function of their kinetic energy T in the laboratory frame for ε = 0.61 and fit (solid line) by the function in equation (5.2); (*b*) Reconstructed invariant cross sections of $\Delta^0(1232)$ resonances for the values of ε=0.43 (□), ε=0.61 (●), and ε=0.68 (○) in p+^{12}C collisions at 4.2 GeV/c.

In the present analysis, we considered only those $\Delta^0(1232)$'s which decayed through $\Delta^0 \to p + \pi^-$ channel. In order to reconstruct the total yield of $\Delta^0(1232)$ resonances, accounting also for $\Delta^0 \to n + \pi^0$ decay channel, the spectra given in Figs. 5.1 and 5.2 should be multiplied by a factor of three, since using Clebsh-Gordan

coefficients [1], one gets the following expression giving the probability of decay of $\Delta^0(1232)$'s into two different channels:

$$\Delta^0 \rightarrow \frac{2}{3}\cdot(n+\pi^0)+\frac{1}{3}\cdot(p+\pi^-).$$

As visible from Figs. 5.1*a* and 5.2*a*, the invariant cross sections of $\Delta^0(1232)$'s have three distinct regions characterized by differing slopes:

- $T < 0-50$ MeV,
- $T \sim 50-400$ MeV, and
- $T > 400$ MeV.

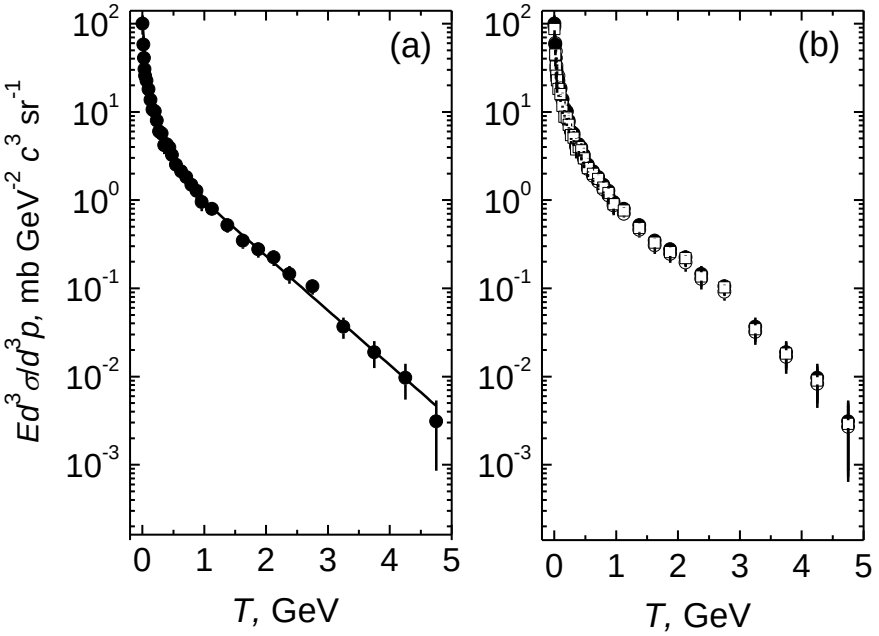

Figure 5.2: (*a*) Reconstructed invariant cross sections of $\Delta^0(1232)$ resonances in d+^{12}C collisions at 4.2 GeV/*c* per nucleon as a function of their kinetic energy T in the laboratory frame for ε = 0.52 and fit (solid line) by the function in equation (5.2); (*b*) Reconstructed invariant cross sections of $\Delta^0(1232)$ resonances for the values of ε=0.41 (□), ε=0.52 (●), and ε =0.68 (○) in d+^{12}C collisions at 4.2 GeV/*c* per nucleon.

The spectra of invariant cross sections extracted for three different cutoff parameter values show the identical behavior overlapping with each other within the uncertainties in p+^{12}C and d+^{12}C collisions, as can be observed from Figs. 5.1*b* and

5.2*b*, respectively. As can be seen from Figs. 5.1 and 5.2, the region $T \sim 0–50$ MeV of invariant cross sections of $\Delta^0(1232)$'s produced in p+^{12}C [18, 19] and d+^{12}C [20] collisions at 4.2 GeV/c per nucleon is characterized by steep slopes. The similar behavior was observed earlier in region $T \sim 0–30$ MeV of the spectrum of invariant cross sections of $\Delta^0(1232)$ produced in ^{16}O+p collisions at 3.25 A GeV/c [15].

5.2 Estimation of the freeze-out temperatures of $\Delta^0(1232)$ from analysis of reconstructed invariant transverse mass spectra

The temperature of hadrons and the density of nuclear media created in high energy collisions of hadrons and nuclei with nuclei are two important parameters necessary to characterize the excited nuclear matter and determine its equation of state [87]. The freeze-out temperatures of particles can be estimated analyzing the slopes of the energy or transverse momentum spectra of particles [65]. More generally, the temperatures extracted from the spectra of the particles are called the spectral temperatures. The freeze-out temperature can generally be defined as the temperature at which strong interactions among the particles of the expanding "fireball" cease and they no longer remain a part of the "fireball" becoming free particles [26], or it is the temperature of a system at the point where thermal equilibrium ceases [65].

The predictions of the thermodynamic model [38] can be used to extract the temperature of $\Delta^0(1232)$'s. In particular, the energy spectra of $\Delta^0(1232)$'s in the c.m.s. of colliding nuclei can be considered using the temperature T_0 of a Maxwell-Boltzmann gas [88]. The freeze-out temperature of the particles can be estimated by fitting the exponential function to their scaled kinetic energy spectrum [87]:

$$\frac{d^3N}{dp^3} = \frac{d^2N}{p^2\,dpd\Omega} = \frac{d^2N}{p\,E\,dTd\Omega} = A_0 \exp\left(-\frac{T}{T_0}\right), \qquad (5.1)$$

where p and E are the momentum and total energy of a particle, respectively, T is its kinetic energy, T_0 is the freeze-out temperature, and A_0 is the fitting constant.

Table 5.1: The values of parameters obtained from fitting the spectra of reconstructed invariant cross sections of $\Delta^0(1232)$ in p+^{12}C collisions at 4.2 GeV/c by the function given in equation (5.2) for three different cutoff parameter ε values.

ε	**0.61**	**0.43**	**0.68**
A_1, (mb GeV^{-2} c^3 sr^{-1})	$88.78 \pm 30.82^{+20.90}_{-14.99}$	73.88 ± 36.45	109.68 ± 33.22
T_1, (GeV)	$0.013 \pm 0.005^{+0.001}_{-0.004}$	0.009 ± 0.004	0.014 ± 0.005
A_2, (mb GeV^{-2} c^3 sr^{-1})	$20.93 \pm 4.69^{+5.69}_{-4.42}$	16.51 ± 3.05	26.62 ± 6.17
$T_2 = T_0$, (GeV)	$0.116 \pm 0.020^{+0.010}_{-0.003}$	0.126 ± 0.020	0.113 ± 0.019
A_3, (mb GeV^{-2} c^3 sr^{-1})	$2.81 \pm 0.75^{+0.85}_{-0.74}$	2.07 ± 0.63	3.66 ± 0.91
T_3, (GeV)	$0.485 \pm 0.048^{+0.030}_{-0.012}$	0.515 ± 0.059	0.473 ± 0.043
χ^2/*n.d.f.*	0.25	0.28	0.31

The invariant cross section spectra of $\Delta^0(1232)$'s were fitted by the function given in relation (5.2) in regions T = 0–3 GeV and T = 0–5 GeV for p+^{12}C and d+^{12}C collisions, respectively:

$$f(T) = A_1 \exp\left(-\frac{T}{T_1}\right) + A_2 \exp\left(-\frac{T}{T_2}\right) + A_3 \exp\left(-\frac{T}{T_3}\right), \qquad (5.2)$$

where T_1, $T_2 = T_0$, and T_3 three different (inverse) slope parameters, and $T_2 = T_0$ shall be an estimate of the freeze-out temperature of $\Delta^0(1232)$.

Fitting the spectrum of invariant cross sections of $\Delta^0(1232)$'s produced in ^{16}O+p collisions at 3.25 A GeV/c by an exponential with a single temperature T_0 in region of comparatively small kinetic energies 30 – 400 MeV in the oxygen nucleus rest frame we estimated the spectral temperature of $\Delta^0(1232)$'s in Ref. [15]. This estimated temperature was in satisfactory agreement [15] with the values of freeze-out temperatures extracted using various methods for $\Delta^0(1232)$'s produced in collisions of different nuclei at various energies.

Table 5.2: The values of parameters obtained from fitting the spectra of reconstructed invariant cross sections of $\Delta^0(1232)$ in d+^{12}C collisions at 4.2 GeV/c per nucleon by the function given in equation (5.2) for three different cutoff parameter ε values.

ε	**0.52**	**0.41**	**0.68**
A_1, (mb GeV^{-2} c^3 sr^{-1})	101.18 ± 42.52	88.08 ± 41.53	78.79 ± 32.72
T_1, (GeV)	$0.013 \pm 0.005^{+0.004}_{-0.001}$	0.012 ± 0.005	0.017 ± 0.007
A_2, (mb GeV^{-2} c^3 sr^{-1})	25.96 ± 4.84	21.09 ± 4.07	28.80 ± 5.95
T_2=T_0, (GeV)	$0.147 \pm 0.021^{+0.003}_{-0.007}$	0.150 ± 0.023	0.140 ± 0.020
A_3, (mb GeV^{-2} c^3 sr^{-1})	4.00 ± 0.56	3.76 ± 0.55	3.58 ± 0.52
T_3, (GeV)	$0.703 \pm 0.034^{+0.001}_{-0.004}$	0.704 ± 0.035	0.699 ± 0.035
χ^2/*n.d.f.*	0.23	0.25	0.20

The values of parameters extracted from fitting the spectra of reconstructed invariant cross sections of $\Delta^0(1232)$'s in p+^{12}C and d+^{12}C collisions, given in Figs. 5.1*a* and 5.2*a*, by the function given in equation (5.2) for three different cutoff parameter ε values are presented in Tables 5.1 and 5.2, respectively.

As observed from Figs. 5.1*a* and 5.2*a* and the values of χ^2/*n.d.f.* in Tables 5.1 and 5.2, the spectra of invariant cross sections of $\Delta^0(1232)$'s in p+^{12}C and d+^{12}C collisions are fitted well by the function given in equation (5.2). We obtained the values of $T_1 = (13 \pm 5^{+1}_{-4})$ MeV and $(13 \pm 5^{+4}_{-1})$ MeV, $T_2 = T_0 = (116 \pm 20^{+10}_{-3})$ MeV and $(147 \pm 21^{+3}_{-7})$ MeV, and $T_3 = (485 \pm 48^{+30}_{-12})$ MeV and $(703 \pm 34^{+1}_{-4})$ MeV, for p+^{12}C and d+^{12}C collisions at 4.2 GeV/c per nucleon, respectively. Here the parameter T_1 is certainly related to region T~ 0–50 MeV, T_0 is related to region T~ 50–400 MeV and can be taken as a rough estimate of the freeze-out temperature of $\Delta^0(1232)$'s, while T_3 is most likely related to region T > 400 MeV of relatively high kinetic energies. In region T > 400 MeV characterized by relatively large T_3 values, the $\Delta^0(1232)$'s are most probably produced in relatively hard p+^{12}C and d+^{12}C scatterings, and therefore T_3 cannot serve as an estimate of freeze-out temperature. It is necessary to mention that the spectra of invariant cross sections of $\Delta^0(1232)$ in region $T \sim 0-50$ MeV have

slopes $T_1 = (13 \pm 5^{+1}_{-4})$ MeV and $(13 \pm 5^{+4}_{-1})$ MeV in p+^{12}C and d+^{12}C collisions, respectively, which are of the same order of magnitude with the temperatures ~5–8 MeV characterizing the nucleons coming from evaporation processes. The results for T_1 coincided for both collision types. The reason for this being is that the $\Delta^0(1232)$'s having small kinetic energies, 0–50 MeV, are most likely produced in peripheral interactions with the relatively small momentum transfers, comparable to Fermi momenta of nucleons in ^{12}C nucleus. Therefore we can assume that the production of $\Delta^0(1232)$ resonances on nucleons of ^{12}C nuclei in both p+^{12}C and d+^{12}C collisions occurs under practically identical conditions in peripheral interactions, regardless of the type of an incident particle (deuteron or proton), which could account for coincidence of the slopes of invariant cross sections of $\Delta^0(1232)$'s in p+^{12}C and d+^{12}C collisions in region $T \sim 0$–50 MeV.

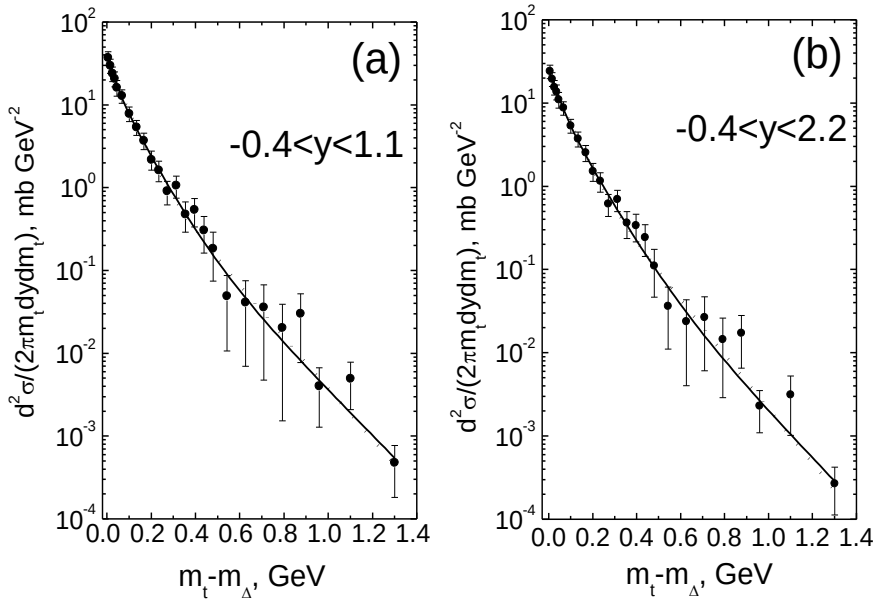

Figure 5.3: Reconstructed invariant cross sections $f(m_t)$ of $\Delta^0(1232)$ resonances as a function of their reduced transverse masses obtained at the best value of cutoff parameter $\varepsilon = 0.61$ in p+^{12}C collisions at 4.2 GeV/c and the corresponding fits by the sum of two (dotted line) and three (solid line) exponentials having two and three slope parameters (both fit curves are very close to each other) for rapidity intervals $-0.4 < y < 1.1$ (*a*) and $-0.4 < y < 2.2$ (*b*).

The rough estimate of the freeze-out temperature $T_0 = (116 \pm 20^{+10}_{-3})$ MeV ($T_0 = (147 \pm 21^{+3}_{-7})$ MeV) extracted for $\Delta^0(1232)$'s in mainly peripheral p+^{12}C (d+^{12}C collisions) collisions using approximation by function given in equation (5.2) seems to be overestimation. This could be because of an influence of the region of high kinetic energies with the relatively large values of parameter T_0 and because the spectra get boosted longitudinally due to impinging protons (deuterons). Moreover, the values of T_0 obtained for both p+^{12}C and d+^{12}C collisions have large fitting uncertainties which show the relative instability of T_0.

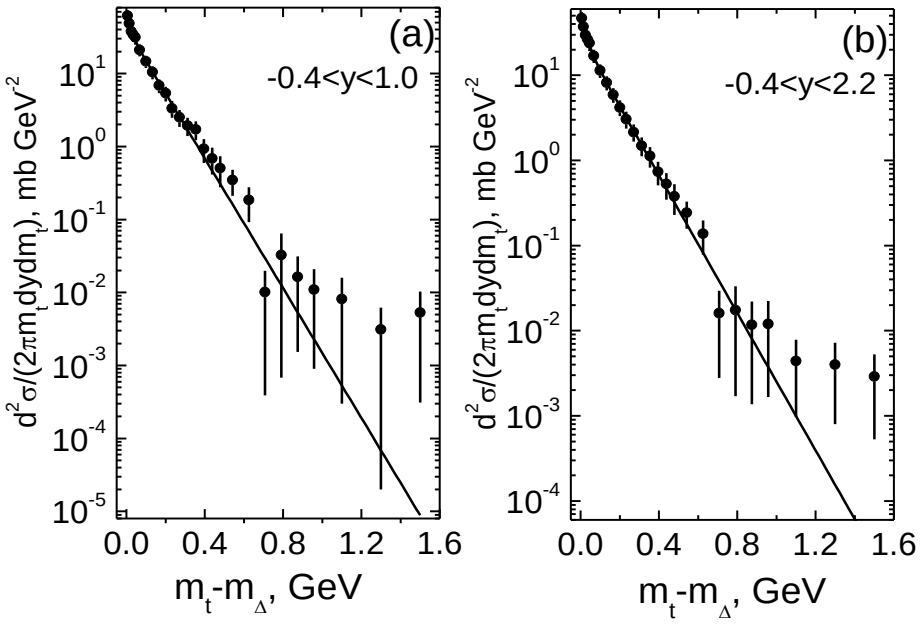

Figure 5.4: Reconstructed invariant cross sections $f(m_t)$ of $\Delta^0(1232)$ resonances as a function of their reduced transverse masses obtained at the best value of cutoff parameter $\varepsilon = 0.52$ in d+^{12}C collisions at 4.2 GeV/c per nucleon and corresponding fits (solid line) by the sum of two exponentials having two slope parameters for rapidity intervals $-0.4 < y < 1.0$ (*a*) and $-0.4 < y < 2.2$ (*b*).

To get the better estimate of freeze-out temperature T_0, which would be free from possible "longitudinal" effects, we reconstructed the spectra of invariant cross sections $f(m_t) = \dfrac{d^2\sigma}{2\pi m_t dy dm_t}$ of $\Delta^0(1232)$'s in p+^{12}C and d+^{12}C collisions as a function

of their reduced transverse mass $m_t - m_\Delta$, where $m_t = \sqrt{m_\Delta^2 + p_t^2}$ is the transverse mass of $\Delta^0(1232)$ resonance [18–20]. The main advantage of the reduced transverse mass is its Lorentz invariance with respect to longitudinal boost.

The invariant cross sections $f(m_t)$ of $\Delta^0(1232)$'s as functions of their reduced transverse masses reconstructed at the best values of ε for p+^{12}C (d+^{12}C) collisions along with the corresponding fits by the functions (given in below written equations (5.3) and (5.4)) with two or/and three slope parameters for two regions of rapidities $-0.4 < y < 1.1$ $(-0.4 < y < 1.0)$ and $-0.4 < y < 2.2$ $(-0.4 < y < 2.2)$ are shown in Figs. 5.3*a* (5.4*a*) and 5.3*b* (5.4*b*), respectively.

$$f(m_t) = A_1 \exp\left(\frac{-(m_t - m_\Delta)}{T_1}\right) + A_2 \exp\left(\frac{-(m_t - m_\Delta)}{T_2}\right). \quad (5.3)$$

$$f(m_t) = A_1 \exp\left(\frac{-(m_t - m_\Delta)}{T_1}\right) + A_2 \exp\left(\frac{-(m_t - m_\Delta)}{T_2}\right) + A_3 \exp\left(\frac{-(m_t - m_\Delta)}{T_3}\right). \quad (5.4)$$

Table 5.3: The values of parameters obtained from fitting the invariant cross sections of $\Delta^0(1232)$ resonances in p+^{12}C collisions at 4.2 GeV/c versus their reduced transverse masses at the best value of cutoff parameter ε = 0.61 by the sum of two and three exponentials given in equations (5.3) and (5.4) for rapidity intervals $-0.4 < y < 1.1$ and $-0.4 < y < 2.2$.

Fitting functions	**Parameters**	$-0.4 < y < 1.1$	$-0.4 < y < 2.2$
Sum of two exponentials (equation (5.3))	A_1, (mb GeV^{-2})	30.88±3.94	19.53±2.73
	T_1, (GeV)	0.062±0.009	0.062±0.011
	A_2, (mb GeV^{-2})	4.49±2.81	3.77±2.30
	T_2, (GeV)	0.141±0.016	0.134±0.014
	χ^2/n.d.f.	0.405	0.423
Sum of three exponentials (equation (5.4))	A_1, (mb GeV^{-2})	17.35±14.97	12.12±11.16
	T_1, (GeV)	0.028±0.031	0.036±0.034
	A_2, (mb GeV^{-2})	21.55±13.80	12.54±10.04
	T_2=T_0, (GeV)	0.082±0.032	0.090±0.041
	A_3, (mb GeV^{-2})	1.78±3.77	0.97±3.27
	T_3, (GeV)	0.161±0.048	0.160±0.071
	χ^2/n.d.f.	0.384	0.415

The parameters obtained from fitting the $f(m_t)$ spectra of $\Delta^0(1232)$'s in p+^{12}C and d+^{12}C collisions by functions in equations (5.3) or/and (5.4) are presented in Tables 5.3 and 5.4, respectively. As seen from Table 5.3, for p+^{12}C collisions, the

values of T_2 and T_3 extracted from fitting by sum of three exponentials (equation (5.4)) are significantly lower than the corresponding values of T_2 and T_3 given in Table 5.1. This confirms that the earlier extracted $T_2 = T_0 = (116 \pm 20^{+10}_{-3})$, using approximation by expression given in (5.2), was overestimation of freeze-out temperature. Analogously, as observed for d+^{12}C collisions in Table 5.4, the values of T_2 extracted from fitting by sum of two exponentials (equation (5.3)) are markedly lower than the corresponding values of T_2 given in Table 5.2.

Table 5.4: The values of parameters obtained from fitting the invariant cross sections of $\Delta^0(1232)$ resonances in d+^{12}C collisions at 4.2 A GeV/c versus their reduced transverse masses at the best value of cutoff parameter $\varepsilon = 0.52$ by the sum of two exponentials given in equation (5.3) for rapidity intervals $-0.4 < y < 1.0$ and $-0.4 < y < 2.2$.

Parameter	**Rapidity interval**	
	$-0.4 < y < 1.0$	$-0.4 < y < 2.2$
A_1, (mb GeV^{-2})	29.03 ± 16.85	23.36 ± 9.62
T_1, (GeV)	0.019 ± 0.015	0.027 ± 0.016
A_2, (mb GeV^{-2})	41.32 ± 6.13	27.64 ± 4.77
T_2, (GeV)	0.098 ± 0.005	0.108 ± 0.006
χ^2/*n.d.f.*	0.747	0.427

It is important to mention that the fitting of the $f(m_t)$ spectra of $\Delta^0(1232)$'s in d+^{12}C collisions, given in Fig. 5.4, by function with three exponentials given in equation (5.4) results in almost the same values of T_1 and T_2, as in case of fitting by function in equation (5.3), but with unsatisfactorily large value of χ^2/*n.d.f.* >>1 and with a parameter $T_3 \approx T_2$ (here T_2 refers to a parameter obtained from fitting by function in equation (5.3)).

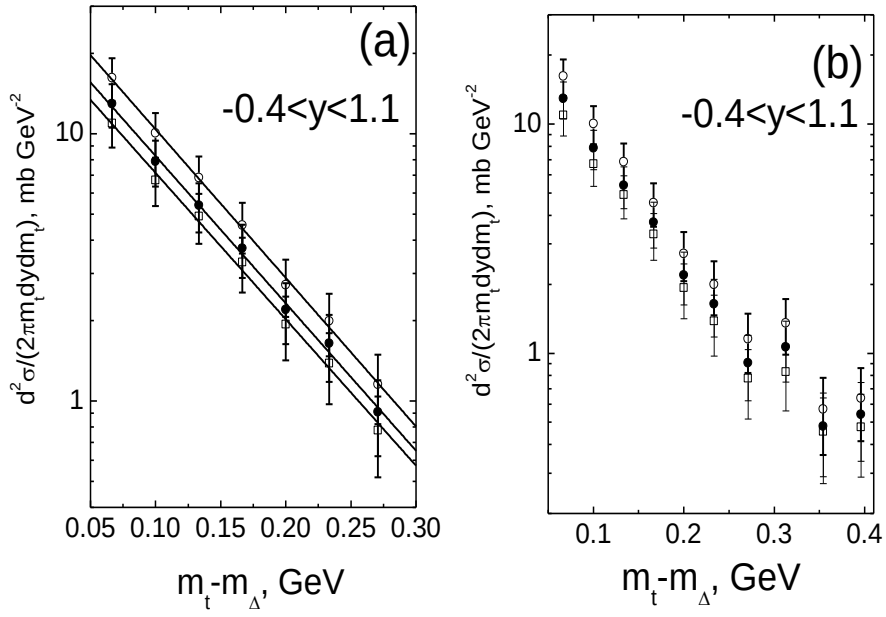

Figure 5.5: Reconstructed invariant cross sections $f(m_t)$ of $\Delta^0(1232)$ resonances in p+^{12}C collisions as a function of their reduced transverse masses for the values of ε = 0.43 (□), ε = 0.61 (●), and ε = 0.68 (○) in regions $m_t - m_\Delta$ = 50–300 MeV (*a*) and 50–400 MeV (*b*) and the respective fits (solid lines) in regions $m_t - m_\Delta$ = 50–300 MeV with one slope Boltzmann distribution function. The $f(m_t)$ spectra are extracted for rapidity interval $-0.4 < y < 1.1$.

In order to extract even better estimates of freeze-out temperature T_0, a single slope region of $f(m_t)$ spectra was searched in various regions within the interval $m_t - m_\Delta$ = 50–400 MeV in both p+^{12}C and d+^{12}C collisions. For p+^{12}C collisions, the $f(m_t)$ spectra of $\Delta^0(1232)$'s in regions $m_t - m_\Delta$ =50–300 MeV and 50–400 MeV, reconstructed for three different values of cutoff parameter ε, along with the corresponding fits with one slope Boltzmann distribution function, $A_0 \exp\left(\frac{-(m_t - m_\Delta)}{T_0}\right)$ are shown in Figs. 5.5*a* and 5.5*b*. The single slope region was searched from the $f(m_t)$ spectra of $\Delta^0(1232)$'s in p+^{12}C and d+^{12}C interactions reconstructed for rapidity ranges $-0.4 < y < 1.1$ and $-0.4 < y < 1.0$, respectively. These rapidity intervals were chosen because there $\Delta^0(1232)$ resonances came mostly from the target ^{12}C fragmentation region with almost no contribution to the $f(m_t)$ spectra from $\Delta^0(1232)$'s originating

from projectile nucleons. The $f(m_t)$ spectra of $\Delta^0(1232)$'s in p+^{12}C and d+^{12}C collisions reconstructed for rapidity range $-0.4 < y < 2.2$ were also analyzed, for sake of comparison.

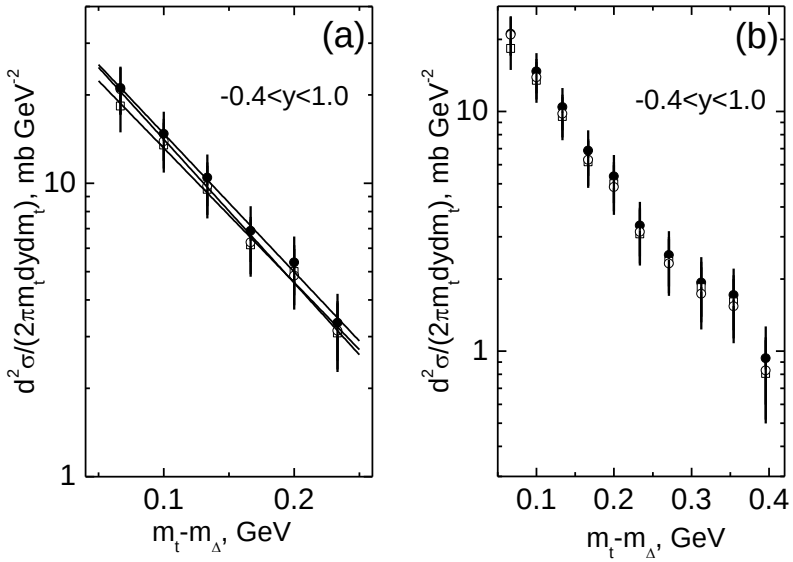

Figure 5.6: Reconstructed invariant cross sections $f(m_t)$ of $\Delta^0(1232)$ resonances in d+^{12}C collisions as a function of their reduced transverse masses for the values of $\varepsilon = 0.41$ (□), $\varepsilon = 0.52$ (●), and $\varepsilon = 0.68$ (○) in regions $m_t - m_\Delta$ =50–250 MeV (*a*) and 50–400 MeV (*b*) and the respective fits (solid lines) in region $m_t - m_\Delta$ =50–250 MeV with one slope Boltzmann distribution function. The $f(m_t)$ spectra are extracted for rapidity interval $-0.4 < y < 1.0$.

The $f(m_t)$ spectra of $\Delta^0(1232)$'s in d+^{12}C interactions in regions $m_t - m_\Delta$ = 50–250 and 50–400 MeV for three different values of cutoff parameter ε along with the corresponding fits with a single slope Boltzmann distribution function, $A_0 \exp\left(\frac{-(m_t - m_\Delta)}{T_0}\right)$, are shown in Figs. 5.6*a* and 5.6*b*. The corresponding parameters obtained from fitting the $f(m_t)$ spectra of $\Delta^0(1232)$'s in p+^{12}C collisions by a single slope Boltzmann distribution function for fitting ranges $m_t - m_\Delta$ =50–300, 50–400 MeV and $m_t - m_\Delta$ = 50–250, 100–300 MeV and rapidity intervals $-0.4 < y < 1.1$ and $-0.4 < y < 2.2$ are given in Tables 5.5 and 5.6.

Table 5.5: The obtained parameters of approximation of $f(m_t)$ spectra of $\Delta^0(1232)$ in p+^{12}C collisions (at three different values of cutoff parameter ε) with a single slope Boltzmann function for fitting ranges $m_t - m_\Delta$=50–300 and 50–400 MeV and rapidity intervals $-0.4 < y < 1.1$ and $-0.4 < y < 2.2$.

ε	Parameter	$-0.4 < y < 1.1$		$-0.4 < y < 2.2$	
		$m_t - m_\Delta$ = **50–300 MeV**	$m_t - m_\Delta$ = **50–400 MeV**	$m_t - m_\Delta$ = **50–300 MeV**	$m_t - m_\Delta$ = **50–400 MeV**
0.61	A_0, (mb GeV^{-2})	29.37±6.27	24.19±4.51	19.93±4.12	16.29±2.93
	T_0, (GeV)	**0.079±0.008±0.001**	0.089±0.008	**0.079±0.008**	0.090±0.008
	χ^2/*n.d.f.*	0.0515	0.5508	0.0661	0.5299
0.43	A_0, (mb GeV^{-2})	25.17±5.44	21.03±4.00	17.15±3.59	14.25±2.61
	T_0, (GeV)	**0.079±0.009**	0.089±0.008	**0.080±0.008**	0.090±0.008
	χ^2/*n.d.f.*	0.0644	0.4569	0.0884	0.4560
0.68	A_0, (mb GeV^{-2})	37.36±7.69	30.60±5.49	25.18±5.04	20.48±3.56
	T_0, (GeV)	**0.078±0.008**	0.088±0.007	**0.079±0.008**	0.089±0.007
	χ^2/*n.d.f.*	0.0331	0.6162	0.0485	0.5809

Table 5.6: The obtained parameters of approximation of $f(m_t)$ spectra as in Table 5.5 for fitting ranges $m_t - m_\Delta$ = 50–250 and 100–300 MeV at the best value of cutoff parameter ε = 0.61.

ε	Parameter	$-0.4 < y < 1.1$		$-0.4 < y < 2.2$	
		$m_t - m_\Delta$ = **50–250 MeV**	$m_t - m_\Delta$ = **100–300 MeV**	$m_t - m_\Delta$ = **50–250 MeV**	$m_t - m_\Delta$ = **100–300 MeV**
0.61	A_0, (mb GeV^{-2})	28.88±6.94	30.26±13.87	19.38±4.53	20.92±9.16
	T_0, (GeV)	**0.080±0.011**	**0.078±0.014**	**0.081±0.010**	**0.078±0.014**
	χ^2/*n.d.f.*	0.0587	0.0582	0.0666	0.0808

The corresponding parameters obtained from fitting the $f(m_t)$ spectra of $\Delta^0(1232)$'s in d+^{12}C interactions by a single slope Boltzmann distribution function for fitting ranges $m_t - m_\Delta$ = 50 – 250, 50 – 300 and $m_t - m_\Delta$ = 100 – 300, 50 – 400 MeV and rapidity interval $-0.4 < y < 1.0$ for three different values of cutoff parameter ε are given in Table 5.7.

The region of a single slope of $f(m_t)$ spectra of $\Delta^0(1232)$ resonances and the corresponding value of T_0 in p+^{12}C and d+^{12}C collisions at 4.2 GeV/c per nucleon were found from the minimum of χ^2/*n.d.f.* values. As can be observed from Tables 5.5 and 5.6, we obtained the minimum value of χ^2/*n.d.f.* for the fitting range 50–300 MeV and rapidity interval $-0.4 < y < 1.1$ for p+^{12}C collisions. The corresponding estimate for freeze-out temperature T_0 of $\Delta^0(1232)$'s in p+^{12}C interactions at 4.2 GeV/c was (79 ± 8 ± 1) MeV. This value, as seen from Table 5.5, was stable within ± 1 MeV for all the three cutoff parameter ε values.

Table 5.7: The obtained parameters of approximation of $f(m_t)$ spectra of $\Delta^0(1232)$ in d+^{12}C collisions with a single slope Boltzmann function for different fitting ranges of $m_t - m_\Delta$ and rapidity interval $-0.4 < y < 1.0$ for three different values of cutoff parameter ε.

ε	Parameter	$m_t - m_\Delta$ ranges (MeV)			
		50–250	**50–300**	**100–300**	**50–400**
0.52	A_0, (mb GeV^{-2})	43.59±9.94	42.53±8.70	42.02±12.15	36.78±6.26
	T_0, (GeV)	**0.092±0.013±0.003**	0.094±0.011	0.095±0.014	0.105±0.009
	χ^2/*n.d.f.*	0.041	0.045	0.055	0.258
0.68	A_0, (mb GeV^{-2})	43.54±10.15	42.04±8.80	39.91±11.79	36.12±6.29
	T_0, (GeV)	**0.089±0.012**	0.092±0.011	0.093±0.014	0.102±0.009
	χ^2/*n.d.f.*	0.036	0.051	0.048	0.262
0.41	A_0, (mb GeV^{-2})	37.80±8.72	36.89±7.64	37.58±11.11	32.62±5.58
	T_0, (GeV)	**0.095±0.014**	0.097±0.012	0.096±0.015	0.106±0.009
	χ^2/*n.d.f.*	0.067	0.069	0.079	0.230

Similarly, as observed from Table 5.7, we obtained the minimum value of χ^2/*n.d.f.* for the fitting range 50–250 MeV and rapidity interval $-0.4 < y < 1.0$ in case of d+^{12}C collisions. The corresponding estimate for freeze-out temperature T_0 of $\Delta^0(1232)$'s in d+^{12}C interactions at 4.2 GeV/c per nucleon was (92 ± 13 ± 3) MeV.

This value, as seen from Table 5.7, was stable within ± 3 MeV for all the three cutoff parameter ε values.

As can be seen from Figs. 5.5*b* and 5.6*b*, the $f(m_t)$ spectra of $\Delta^0(1232)$'s in region $m_t - m_\Delta > 300$ MeV start to deviate from a single slope behavior observed for range $m_t - m_\Delta < 300$ MeV. This is most probably due to onset of contribution from hard scattering processes with the relatively larger momentum transfers to the $f(m_t)$ spectra. The comparison of the values of $\chi^2/n.d.f.$ presented in Tables 5.5 and 5.7 also supports the above observations from Figs. 5.5*b* and 5.6*b*. Indeed, the value of $\chi^2/n.d.f.$ increases almost by ten times when the fitting range changes from $50-300$ MeV to $50-400$ MeV in case of p+^{12}C collisions, and $\chi^2/n.d.f.$ increases by about six times while changing the fitting range from 50–250 MeV to $50-400$ MeV in case of d+^{12}C collisions. The above estimated freeze-out temperatures T_0 = (79 ± 8 ± 1) MeV and (92 ± 13 ± 3) MeV of $\Delta^0(1232)$'s in p+^{12}C and d+^{12}C interactions at 4.2 GeV/c per nucleon, as seen from Tables 5.5 and 5.7, are characterized by sufficiently low $\chi^2/n.d.f.$ values, which are about five to six times smaller than the corresponding $\chi^2/n.d.f.$ values obtained for $T_2 = T_0$ given in Tables 5.1 and 5.2.

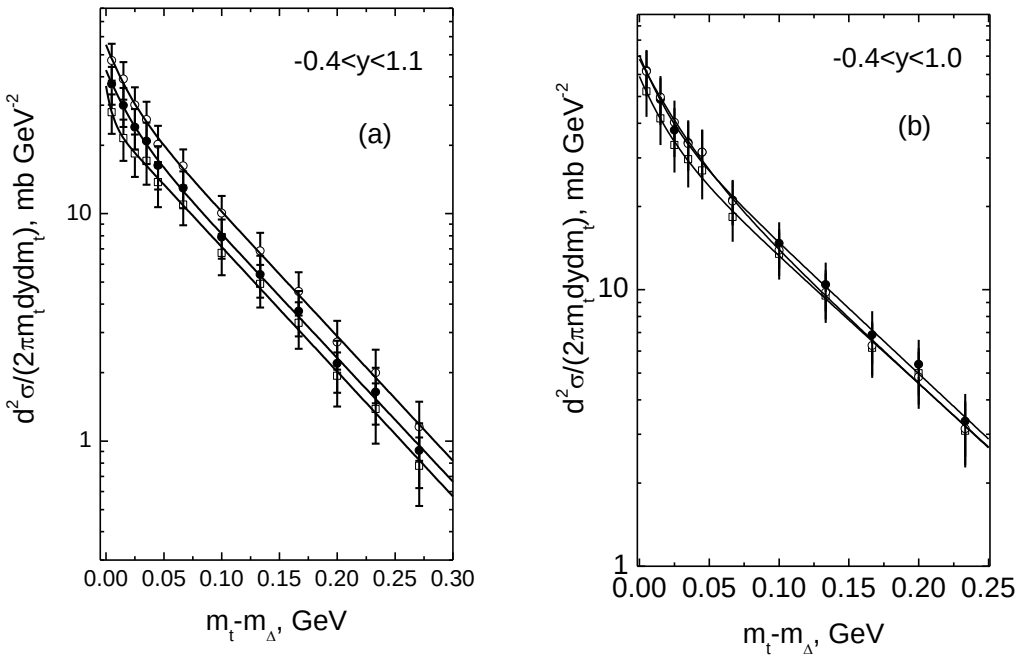

Figure 5.7: Reconstructed invariant cross sections $f(m_t)$ of $\Delta^0(1232)$ resonances obtained in p+^{12}C collisions (*a*) at 4.2 GeV/*c* for the values of cutoff parameter ε=0.43 (□), ε=0.61 (●), and ε=0.68 (○) and in d+^{12}C collisions (*b*) at 4.2 *A* GeV/*c* for the values of cutoff parameter ε = 0.43 (□), ε = 0.61 (●), and ε = 0.68 (○), and the corresponding fits by the sum of two exponentials with two slopes for fitting range 0–300 MeV (0–250 MeV) and rapidity interval $-0.4 < y < 1.1$ ($-0.4 < y < 1.0$) for p+^{12}C (d+^{12}C) collisions.

We also approximated the $f(m_t)$ spectra of $\Delta^0(1232)$'s in range $m_t - m_\Delta$ = 0–300 MeV (0–250 MeV) for rapidity interval $-0.4 < y < 1.1$ ($-0.4 < y < 1.0$) by the sum of two exponentials with two slopes given in equation (5.3) for three different cutoff parameter ε values in p+^{12}C (d+^{12}C) collisions. The corresponding $f(m_t)$ spectra and fitting curves for p+^{12}C and d+^{12}C collisions are shown in Figs. 5.7*a* and 5.7*b*, respectively, and the parameters obtained from fitting the corresponding spectra of invariant cross sections $f(m_t)$ are presented in Table 5.8. Table 5.8 shows that the values of $T_2 = T_0$ are in very good agreement with the above estimated freeze-out temperatures of $\Delta^0(1232)$ resonances (T_0 = (79±8±1) MeV and (92±13±3) MeV for p+^{12}C and d+^{12}C

collisions, respectively). The data presented in Table 5.8 also confirm the existence of a steep slope of $f(m_t)$ spectra in region $m_t - m_\Delta < 30 - 40$ MeV for p+^{12}C and d+^{12}C collisions. However, in this case, the $\Delta^0(1232)$'s with kinetic energies greater than 50 MeV and relatively low transverse momenta and moving along the beam direction can influence this region of low $m_t - m_\Delta$. Although the values of T_1 in Table 5.8 have large fitting errors, they agree within uncertainties with the corresponding values T_1 = (13 ± 5^{+1}_{-4}) MeV and (13 ± 5^{+4}_{-1}) MeV, given in Tables 5.1 and 5.2, extracted for a region of kinetic energies $T < 50$ MeV in p+^{12}C and d+^{12}C collisions, respectively.

Table 5.8: The parameters obtained from fitting the $f(m_t)$ spectra of $\Delta^0(1232)$ resonances by the sum of two exponentials with two slopes for fitting range $m_t - m_\Delta$ =0–300 MeV (0–250 MeV) and rapidity interval $-0.4 < y < 1.1$ ($-0.4 < y < 1.0$) in p+^{12}C (d+^{12}C) collisions.

Parameters	**p+^{12}C**			**d+^{12}C**		
	ε=0.61	**ε=0.43**	**ε=0.68**	**ε=0.52**	**ε=0.41**	**ε=0.68**
A_1, (mb GeV^{-2})	14.44±11.65	11.22±48.72	19.51±14.58	26.78±19.08	21.14±16.51	29.38±23.22
T_1, (GeV)	0.017±0.024	0.005±0.022	0.016±0.021	0.018±0.022	0.018±0.025	0.026±0.032
A_2, (mb GeV^{-2})	28.30±8.50	25.25±3.61	35.80±9.81	43.67±14.55	37.96±13.00	38.90±26.02
T_2, (GeV)	**0.080±0.011**	**0.079±0.007**	**0.079±0.010**	**0.092±0.017**	**0.095±0.019**	**0.093±0.030**
χ^2/n.d.f.	0.0426	0.0504	0.0440	0.061	0.062	0.037

The temperatures of reconstructed Δ(1232) resonances in central collisions of heavy ions in energy range from 1 to 2 GeV per nucleon [2] were found to be lower than the temperatures of protons. This was explained by that the reconstructed Δ(1232) resonances are originated from the relatively "colder" collision phase. On the other hand, in central heavy ion collisions the $\Delta^0(1232)$'s coming from the earlier "hotter" collision phase are more difficult to reconstruct due to the possible scattering of the decay pions in a dense nuclear matter before they leave the collision zone. However, in the present analysis the estimated apparent temperatures of $\Delta^0(1232)$'s, T_0 = (79 ± 8 ±1) MeV and (92 ± 13 ± 3) MeV, proved to be noticeably larger than the

corresponding temperatures of protons, T_p=(62 ± 2) MeV and (67 ± 2) MeV, estimated in Ref. [89] for p+^{12}C and d+^{12}C collisions at 4.2 GeV/c per nucleon, respectively. Moreover, the minimum kinetic energies of $\Delta^0(1232)$'s extracted in the present work were found to be sufficiently low: $(T_\Delta)_{\min} \approx 1.2$ MeV and $(T_\Delta)_{\min} \approx 1$ MeV in p+^{12}C and d+^{12}C collisions, respectively. The above facts suggest that the reconstruction of almost all $\Delta^0(1232) \to p\pi^-$ could be done quite efficiently in the present work.

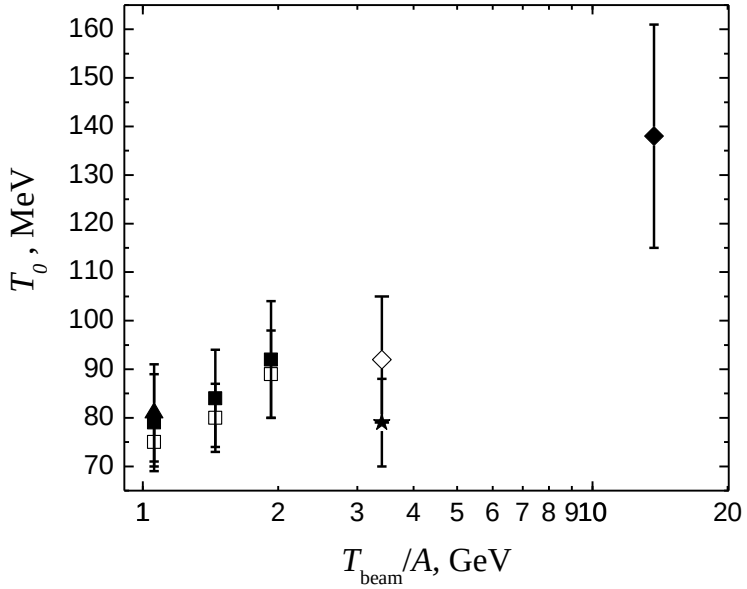

Figure 5.8: Dependence of T_0 on kinetic energy per nucleon of a beam: (★) and (◊) − T_0 estimated in the present analysis for p+^{12}C and d+^{12}C collisions at 4.2 GeV/c per nucleon ($T_{\text{beam}} \approx 3.4$ GeV per nucleon), respectively; T_0 deduced from the radial flow analysis (■) and using the hadro-chemical equilibrium model (□) for Δ resonances produced in central Ni+Ni collisions; (▲) – T_0 extracted from the radial flow analysis for Δ^0 resonances produced in central Au+Au interactions at 1.06 GeV per nucleon; (♦) – T_0 estimated for Δ resonances produced in central ^{28}Si+Pb interactions at p_{lab} = 14.6 GeV/c per nucleon.

The values of the freeze-out temperatures of $\Delta(1232)$'s, obtained for central collisions of Ni with Ni nuclei [80] at incident kinetic energies between 1 and 2 GeV per nucleon, were extracted using hadrochemical equilibrium model [90, 91] and the extracted fractions of nucleons, $n(\Delta)/n(\text{nucleon}+\Delta)$, excited to $\Delta(1232)$'s. The values of freeze-out temperatures of $\Delta(1232)$'s produced in central collisions of Ni with Ni nuclei at incident energies between 1 and 2 GeV per nucleon and central Au+Au

collisions at 1.06 GeV per nucleon, were estimated in Refs. [85, 92] using the radial flow analysis. Moreover, the pion enhancement at low transverse momenta was used to obtain the $\Delta(1232)$ abundance in central collisions of ^{28}Si nuclei with Aluminum and Lead nuclei [84] at momenta p_{lab} = 14.6 GeV/c per nucleon ($T_{\text{beam}} \approx$ 13.7 GeV per nucleon), and then the freeze-out temperatures of $\Delta(1232)$'s were estimated using the obtained $\Delta(1232)$ abundance. It was suggested [84] that in central ^{28}Si+Pb collisions at 14.6 GeV/c per nucleon a "fireball" is created with a large number of excited Δ resonances which freeze out at $T_0 = 138^{+23}_{-18}$ MeV. The freeze-out temperatures estimated in the present work along with the freeze-out temperatures of $\Delta(1232)$ resonances extracted for collisions of different nuclei at various beam energies per nucleon are presented in Fig. 5.8. As observed from Fig. 5.8, the freeze-out temperatures of $\Delta(1232)$ resonances extracted for central collisions of heavy ions generally increase with an increase of beam kinetic energy per nucleon. The freeze-out temperatures, T_0 = (79 ± 8 ±1) MeV and (92 ± 13 ± 3) MeV, estimated in the present analysis for $\Delta^0(1232)$'s generated in p+^{12}C and d+^{12}C interactions at 4.2 GeV/c per nucleon, respectively, agree with each other within the uncertainties. However, the freeze-out temperatures extracted in present analysis for both collision types do not obey the increasing behavior with an increase of beam energy which was observed in case of central heavy ion collisions. This is most likely because of the mainly peripheral nature of the analyzed collisions with ^{12}C nuclei and the relative smallness of the colliding p+^{12}C and d+^{12}C systems.

5.3 Extraction of the spectral temperatures of $\Delta^0(1232)$ within the framework of Hagedorn Thermodynamic Model

Analysis of the slopes of energy or/and transverse momentum spectra of the produced particles with the help of theoretical models is generally done to estimate the freeze-out temperatures of the particles [65, 87]. Since transverse momentum or transverse mass spectra are Lorentz invariant under longitudinal boosts, analysis of such spectra is preferred to estimate the temperatures of hadrons [37, 87, 93]. The temperatures estimated from kinematical spectra of hadrons using the theoretical expressions of thermodynamics, derived under assumption of thermal equilibrium of the source of hadrons, are also called as the spectral temperatures of hadrons [26]. The transverse momentum spectra of hadrons produced in relativistic nuclear collisions could be analyzed successfully in the framework of Hagedorn Thermodynamic Model [37, 38] in the earlier works [87, 93, 94] to extract the spectral temperatures of hadrons.

For sake of comparison with the experimental data, we simulated 50000 collision events using Modified FRITIOF model [39–41, 69] separately for p+^{12}C and d+^{12}C collisions at 4.2 GeV/c per nucleon. The parameters used for model simulations were the same as given in Ref. [40].

In the framework of Hagedorn Thermodynamic Model [37, 38] the normalized transverse momentum (p_t) distributions of hadrons can be described as

$$\frac{dN}{N\,p_t dp_t} = A\cdot(m_t T)^{1/2}\exp\left(-\frac{m_t}{T}\right), \qquad (5.5)$$

where N is either the total number of inelastic events or the total number of respective hadrons, which depends on the choice of normalization, $m_t = \sqrt{m^2 + p_t^2}$ is the transverse mass, T is the spectral temperature, and A is the fitting coefficient. We shall refer to the expression given in equation (5.5) as the one-temperature Hagedorn function in the present analysis. In case of two temperatures T_1 and T_2, this expression modifies as

$$\frac{dN}{N\,p_t dp_t} = A_1\cdot(m_t T_1)^{1/2}\exp\left(-\frac{m_t}{T_1}\right) + A_2\cdot(m_t T_2)^{1/2}\exp\left(-\frac{m_t}{T_2}\right). \qquad (5.6)$$

This expression in equation (5.6) is referred to as two-temperature Hagedorn function in the present work. The above expressions (5.5) and (5.6) were obtained assuming that $m_t >> T$ [87, 93].

We approximated the experimental p_t spectra of $\Delta^0(1232)$'s in p+^{12}C and d+^{12}C interactions as well as the corresponding transverse momentum spectra calculated using Modified FRITIOF model with the one-temperature as well as two-temperature Hagedorn function [22]. Fitting the experimental transverse momentum spectra of $\Delta^0(1232)$ resonances with the two-temperature Hagedorn function gave very unstable values for the parameters T_1 and T_2 as well as A_1 and A_2, which had very large fitting uncertainties in case of both p+^{12}C and d+^{12}C collisions. We observed that fitting the experimental p_t spectra of $\Delta^0(1232)$'s became stable with the sufficiently low fitting errors only when we assumed initially that $T_1 = T_2$. Similarly, in case of Modified FRITIOF model spectra, approximating the p_t spectra of $\Delta^0(1232)$'s with the two-temperature Hagedorn function resulted in nearly coinciding values of T_1 and T_2 for both collision types.

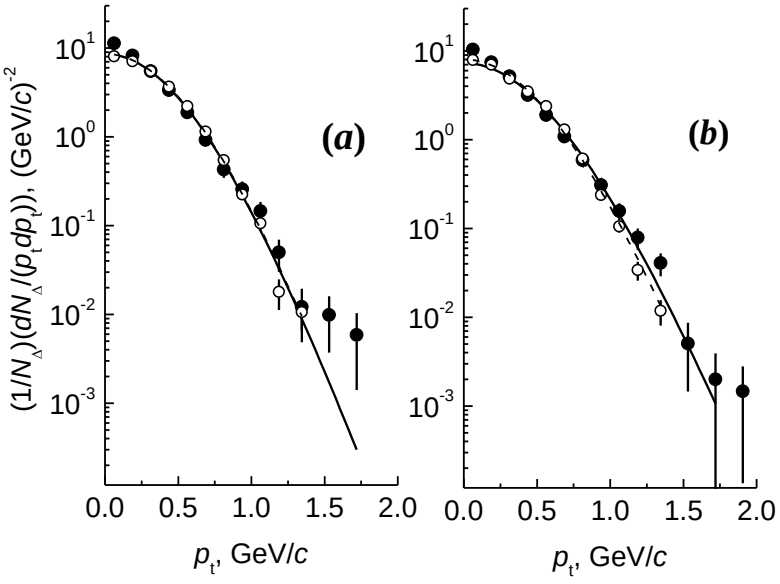

Figure 5.9: Transverse momentum spectra of $\Delta^0(1232)$ in p+^{12}C (*a*) and d+^{12}C (*b*) collisions at 4.2 GeV/*c* per nucleon in the experiment (●) and obtained using Modified FRITIOF model (○). The corresponding fits of experimental (solid curve) and model transverse momentum spectra (dashed curve) with one-temperature Hagedorn function. The spectra are normalized by the total number of $\Delta^0(1232)$ resonances.

This suggested that fitting with the one-temperature Hagedorn function was sufficient for both the experimental and model p_t spectra of $\Delta^0(1232)$'s in p+^{12}C and d+^{12}C interactions.

The experimental and model p_t spectra of $\Delta^0(1232)$'s in p+^{12}C and d+^{12}C collisions and the corresponding fits with one-temperature Hagedorn function are given in Figs. 5.9*a* and 5.9*b*, respectively. As observed from Figs. 5.9*a* and 5.9*b*, the experimental as well as model p_t spectra of $\Delta^0(1232)$ in p+^{12}C and d+^{12}C collisions are fitted quite well with the one-temperature Hagedorn function. The corresponding spectral temperatures of $\Delta^0(1232)$ resonances extracted from fitting their experimental and model p_t spectra with the one-temperature Hagedorn function are presented in Table 5.9.

The c.m. rapidity of nucleon–nucleon collisions at projectile per nucleon momentum of 4.2 GeV/*c* is $y_{\rm cm} \approx 1.1$, and a majority of $\Delta^0(1232)$'s in p+^{12}C and d+^{12}C collisions at 4.2 GeV/*c* per nucleon were shown [19, 20, 21] to originate from the target ^{12}C fragmentation region ($-0.4 \leq y \leq 1.0$). We reconstructed the p_t distributions of $\Delta^0(1232)$ resonances for the rapidity region $-0.4 \leq y \leq 1.0$ and for the total rapidity range $-0.4 \leq y \leq 2.2$ as well in order to examine the influence of $\Delta^0(1232)$'s produced in the projectile fragmentation region on the shape of the total transverse momentum spectra of $\Delta^0(1232)$'s in p+^{12}C and d+^{12}C collisions.

Table 5.9: Spectral temperatures of $\Delta^0(1232)$ resonances extracted from approximating their p_t spectra with one-temperature Hagedorn function in the experiment and Modified FRITIOF model.

Type		**$-0.4 \leq y \leq 1.0$**		**Total *y* interval**	
		***T*, MeV**	**χ^2/*n.d.f.***	***T*, MeV**	**χ^2/*n.d.f.***
p+^{12}C, 4.2 GeV/*c*	**Experiment**	82 ± 4	1.22	84 ± 3	1.19
	Modified Fritiof	88 ± 2	0.68	84 ± 1	0.96
d+^{12}C, 4.2 *A* GeV/*c*	**Experiment**	96 ± 4	1.29	97 ± 3	1.15
	Modified Fritiof	89 ± 2	1.37	90 ± 1	1.77

Table 5.9 shows that the spectral temperatures obtained from approximation of the experimental and model p_t spectra of $\Delta^0(1232)$ with the one-temperature Hagedorn function coincide within fitting uncertainties for both rapidity ranges. The spectral temperatures of $\Delta^0(1232)$'s in p+^{12}C and d+^{12}C collisions estimated from fitting their p_t spectra by the one-temperature Hagedorn function, as seen from Table 5.9, proved to be slightly greater than the corresponding temperatures T_0=(79 ± 8 ±1) MeV and (92 ± 13 ± 3) MeV for p+^{12}C and d+^{12}C collisions at 4.2 GeV/c per nucleon, respectively, extracted earlier [19, 20] from analysis of the invariant cross sections $f(m_t)$ spectra of $\Delta^0(1232)$ resonances. Nevertheless the spectral temperatures of $\Delta^0(1232)$'s extracted by using both the techniques agree with each other within uncertainties. Similarly, the spectral temperatures of $\Delta^0(1232)$'s extracted in the framework of Hagedorn thermodynamic model were significantly higher as compared to the temperatures of protons, (62 ± 2) MeV and (67 ± 2) MeV, estimated in Ref. [89] for p+^{12}C and d+^{12}C collisions at 4.2 GeV/c per nucleon, respectively. It is necessary to mention that the spectral temperatures estimated from Modified FRITIOF model p_t spectra, as seen from Table 5.9, are consistent within uncertainties with the corresponding temperatures extracted from the experimental p_t spectra of $\Delta^0(1232)$'s .

5.4 Comparison of spectral temperatures of $\Delta^0(1232)$ and negative pions in p+^{12}C and d+^{12}C collisions

It seems interesting to compare the extracted spectral temperatures of $\Delta^0(1232)$'s with the corresponding temperatures of negative pions produced in p+^{12}C and d+^{12}C collisions. Therefore we fitted the p_t spectra of negative pions produced in p+^{12}C and d+^{12}C interactions with one-temperature Hagedorn function as was done above in case of p_t spectra of $\Delta^0(1232)$'s . For sake of comparison, the corresponding p_t spectra of negative pions extracted using Modified FRITIOF model were also approximated with the one-temperature Hagedorn function. The experimental and model p_t distributions of π^- mesons in p+^{12}C and d+^{12}C collisions at 4.2 GeV/c per nucleon along with the corresponding fits with the one-temperature Hagedorn function

are shown in Figs. 5.10*a* and 5.10*b*, respectively. Both the experimental and model p_t spectra of negative pions, as can be observed from Figs. 5.10*a* and 5.10*b*, are approximated quite well by the one-temperature Hagedorn function. The corresponding spectral temperatures of negative pions extracted from approximation of their p_t spectra with the one-temperature Hagedorn function in the experiment and Modified FRITIOF model are given in Table 5.10. As observed from Tables 5.9 and 5.10, the spectral temperatures of $\Delta^0(1232)$'s and π^- mesons in d+^{12}C collisions coincided with each other within uncertainties in the experiment as well as in the model.

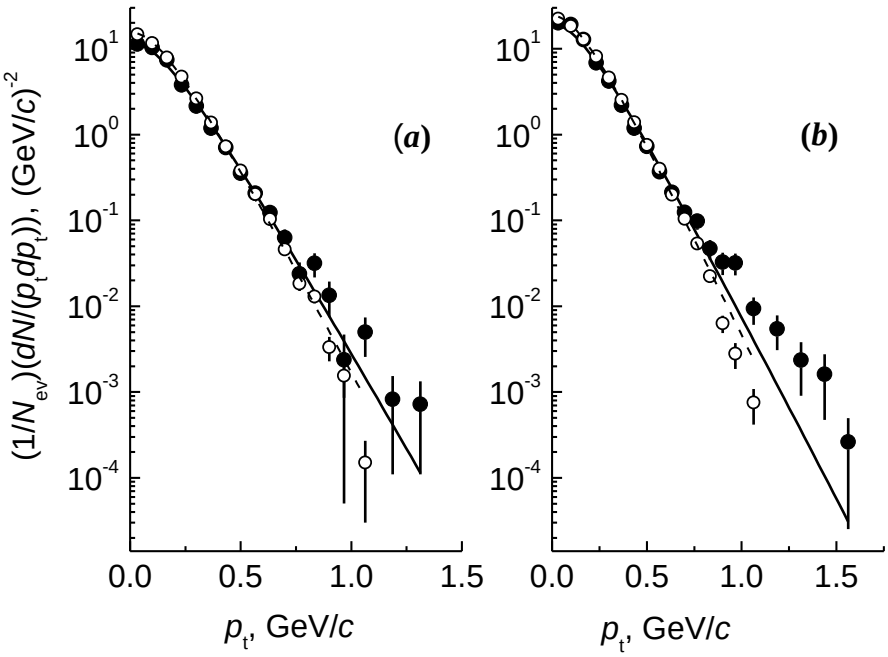

Figure 5.10: Transverse momentum spectra of π^- mesons produced in p+^{12}C (*a*) and d+^{12}C (*b*) interactions at 4.2 GeV/*c* per nucleon in the experiment (●) and obtained using Modified FRITIOF model (○) along with the corresponding fits of the experimental (solid curve) and model spectra (dashed curve) with one-temperature Hagedorn function. The spectra are normalized by the total number of events.

Table 5.10: Spectral temperatures of negative pions extracted from fitting their p_t distributions with one-temperature Hagedorn function in the experiment and Modified FRITIOF model.

Type		***T*, MeV**	χ^2**/*n.d.f.***
p+^{12}C, 4.2 GeV/c	**Experiment**	93 ± 2	0.77
	Modified Fritiof	86 ± 1	3.83
d+^{12}C, 4.2 A GeV/c	**Experiment**	98 ± 2	1.71
	Modified Fritiof	91 ± 1	6.02

The experimental spectral temperature of $\Delta^0(1232)$'s was found to be slightly lower than the corresponding temperature of negative pions in p+^{12}C collisions. Nevertheless, as observed from Tables 5.9 and 5.10, the spectral temperatures of $\Delta^0(1232)$'s and negative pions agree with each other within two standard errors in p+^{12}C collisions. It is necessary to note that the spectral temperatures of $\Delta^0(1232)$'s and π^- mesons extracted from model p_t spectra practically coincided with each other in both p+^{12}C and d+^{12}C collisions, as can be seen from Tables 5.9 and 5.10.

Chapter 6
Summary and Conclusions

We reconstructed the mass distributions of $\Delta^0(1232)$ resonances produced in p+^{12}C and d+^{12}C collisions at 4.2 GeV/c per nucleon using the angular criterion. The mass and width of $\Delta^0(1232)$'s were estimated to be ($1222 \pm 5^{+10}_{-14}$) MeV/c^2 (($1230 \pm 4^{+3}_{-6}$) MeV/c^2) and ($89 \pm 14^{+32}_{-43}$) MeV/c^2 (($90 \pm 14^{+19}_{-24}$) MeV/c^2), respectively, in p+^{12}C collisions (d+^{12}C collisions). The fractions of π^- mesons (relative to the total number of π^- mesons) originating from decay of $\Delta^0(1232)$'s were estimated to be ($39 \pm 3^{+10}_{-7}$)% and ($30 \pm 2^{+6}_{-7}$)% in p+^{12}C and d+^{12}C collisions, respectively, being in agreement within uncertainties with the corresponding fractions of π^- mesons extracted earlier for ^{4}He+^{12}C and ^{12}C +^{12}C collisions at the same incident momentum per nucleon. The relative numbers of nucleons excited to $\Delta^0(1232)$'s at freeze-out conditions were estimated to be ($16 \pm 3^{+4}_{-3}$)% and ($15 \pm 2^{+3}_{-4}$)% in p+^{12}C and d+^{12}C collisions, respectively.

We showed that the $\Delta^0(1232)$ decay kinematics was responsible for the low transverse momentum enhancement of p_t spectra of negative pions produced in p+^{12}C and d+^{12}C collisions at 4.2 GeV/c per nucleon, as was also observed earlier in Refs. [84, 86, 95] for different colliding nuclei at incident energy range between 1 and 15 GeV per nucleon.

The momentum, kinetic energy, transverse momentum, emission angle, and rapidity distributions of $\Delta^0(1232)$'s produced in p+^{12}C and d+^{12}C collisions were reconstructed and their mean values extracted. Comparison of reconstructed rapidity spectra of $\Delta^0(1232)$'s in p+^{12}C and d+^{12}C interactions revealed that in case of d+^{12}C collisions a major fraction of $\Delta^0(1232)$'s are generated from nucleons of target ^{12}C nuclei, while still a noticeable fraction of $\Delta^0(1232)$'s originate from neutrons of incident deuterons, as was reflected by a "shoulder" like structure in region $y \sim 1.2$–1.9 of rapidity spectrum of $\Delta^0(1232)$'s in d+^{12}C collisions. This statement was further verified from a comparative analysis of reconstructed emission angle, momentum, and

kinetic energy spectra of $\Delta^0(1232)$'s and their mean values in p+^{12}C and d+^{12}C collisions.

The reconstructed spectra of invariant cross sections of $\Delta^0(1232)$'s versus their kinetic energies had (inverse) slopes T_1 = (13±5 $^{+1}_{-4}$) MeV and (13 ± 5 $^{+1}_{-4}$) MeV in region T ~ 0–50 MeV for p+^{12}C and d+^{12}C collisions, respectively, which were of the order of temperatures 5–8 MeV, typical for nucleons coming from evaporation processes.

The freeze-out temperatures of $\Delta^0(1232)$'s, estimated from analysis of reconstructed $f(m_t)$ spectra of $\Delta^0(1232)$'s, T_0=(79 ± 8 ±1) MeV and (92 ± 13 ± 3) MeV proved to be significantly larger than the corresponding temperatures of protons T_p= (62 ± 2) MeV and (67 ± 2) MeV extracted in Ref. [89] for p+^{12}C and d+^{12}C collisions at 4.2 GeV/c per nucleon, respectively. However, the freeze-out temperatures T_0 of $\Delta^0(1232)$'s estimated in the present work were lower than expected from increasing trend of T_0 with an increase in beam kinetic energy per nucleon observed for $\Delta(1232)$'s generated in central collisions of heavy ions. This was explained by the mainly peripheral character of the analyzed p+^{12}C and d+^{12}C collision events and the relative smallness of the colliding systems.

The spectral temperatures of $\Delta^0(1232)$'s and negative pions in p+^{12}C and d+^{12}C collisions at 4.2 GeV/c per nucleon were extracted from analysis of the corresponding p_t spectra in the framework of Hagedorn Thermodynamic Model. The spectral temperatures of $\Delta^0(1232)$'s and π^- mesons were obtained from fitting their transverse momentum spectra with the one-temperature Hagedorn function both in the experiment and Modified FRITIOF model. The so obtained spectral temperatures of $\Delta^0(1232)$'s proved to be (82 ± 4) MeV and (96 ± 4) MeV in p+^{12}C and d+^{12}C collisions, respectively, and coincided within uncertainties with the corresponding freeze-out temperatures of $\Delta^0(1232)$'s estimated from analysis of $f(m_t)$ spectra of invariant cross sections of $\Delta^0(1232)$'s. The spectral temperatures of $\Delta^0(1232)$'s estimated from Modified FRITIOF model p_t spectra in the framework of Hagedorn Thermodynamic Model agreed within uncertainties with the corresponding temperatures extracted from

the experimental p_t spectra of $\Delta^0(1232)$'s in both p+^{12}C and d+^{12}C interactions. The spectral temperatures of $\Delta^0(1232)$'s and π^- mesons in d+^{12}C collisions at 4.2 *A* GeV/*c* coincided with each other within uncertainties in the experiment as well as in the Modified FRITIOF model. Also the spectral temperatures of $\Delta^0(1232)$'s and negative pions agreed with each other within two standard errors in p+^{12}C collisions.

The new results extracted in the present work on $\Delta^0(1232)$'s generated in p+^{12}C and d+^{12}C collisions at 4.2 GeV/*c* per nucleon may be helpful to interpret the relevant data on resonance production in relativistic heavy ion collisions.

References

[1] K. Nakamura *et al*., (Particle Data Group), "REVIEW OF PARTICLE PHYSICS", *J. Phys. G* **37,** 075021 (2010).

[2] M. Eskef *et al*., (FOPI Collaboration), "Identification of baryon resonances in central heavy-ion collisions at energies between 1 and 2 *A* GeV", *Eur. Phys. J. A* **3**, 335 (1998).

[3] D. Pelte, "In-medium modification of the Δ(1232) resonance at SIS energies", Talk presented at the 15th Winter Workshop on Nuclear Dynamics, Park City, Utah, January 9-16, 1999; arXiv: nucl-ex/9902006v1.

[4] G. E. Brown and M. Rho, "Scaling effective Lagrangians in a dense medium", *Phys. Rev. Lett.* **66**, 2720 (1991).

[5] R. Rapp, "$\pi^+\pi^-$ emission in high-energy nuclear collisions", *Nucl. Phys. A* **725**, 254 (2003).

[6] K. N. Mukhin and O. O. Patarakin, "REVIEWS OF TOPICAL PROBLEMS: Δ isobar in nuclei (review of experimental data)", *Phys. Usp.* **38**, 803 (1995).

[7] E. A. Strokovsky, F. A. Gareev, and Yu. L. Ratis, "Delta-Isobar Excitations of Atomic Nuclei in Charge-Exchange Reactions", *Phys. Part. Nucl*. **24**, 255 (1993).

[8] F. Bertsch and S. Das Gupta, "A guide to microscopic models for intermediate energy heavy ion collisions", *Phys. Rep.* **160**, 189 (1988).

[9] Vladimir Pascalutsa, Marc Vanderhaeghen, and Shin Nan Yang, "Electromagnetic excitation of the Δ(1232)-resonance", *Phys. Rep.* **437**, 125 (2007).

[10] C. Hacker, N. Wies, J. Gegelia, and S. Scherer, "Including the Δ(1232) resonance in baryon chiral perturbation theory ", *Phys. Rev. C* **72**, 055203 (2005).

[11] J. Chiba *et al*., "Coincidence measurements of (*p,n*) reactions at 1.5 GeV/*c* on C and H in the Δ excitation region", *Phys. Rev. Lett.* **67**, 1982 (1991).

[12] T. Hennino *et al*., "Study of decay and absorption of the Δ resonance in nuclei with a 4π detector", *Phys. Lett. B* **283**, 42 (1992).

[13] D. Krpic, G. Skoro, I. Picuric, S. Backovic, and S. Drndarevic, "Baryon resonances in carbon-carbon collisions at 4.2 GeV/*c* per nucleon", *Phys. Rev. C* **65**, 034909 (2002).

[14] Kh. K. Olimov, "Production of baryon resonances in π^-+^{12}C interactions at 40 GeV/*c*", *Phys. Rev. C* **76**, 055202 (2007).

[15] Kh. K. Olimov, S. L. Lutpullaev, B. S. Yuldashev, Y.H. Huseynaliyev, and A.K. Olimov, "Production of Δ(1232) resonances on oxygen nuclei in ^{16}O+p collisions at a momentum of 3.25 GeV/*c* per nucleon", *Eur. Phys. J. A* **44**, 43 (2010).

[16] Kh. K. Olimov, "Production of Delta Isobars on Tantalum Nuclei in CTa Collisions at a Projectile Momentum of 4.2 GeV/*c* per Nucleon", *Phys. At. Nucl.* **73**, 433 (2010).

[17] Kh. K. Olimov S. L. Lutpullaev, K. Olimov, K. G. Gulamov, and J. K. Olimov, "Production of Δ^0 and Δ^{++} resonances in collisions of ^{4}He nuclei with carbon nuclei at 4.2 GeV/*c* per nucleon", *Phys. Rev. C* **75**, 067901 (2007).

[18] Kh. K. Olimov and Mahnaz Q. Haseeb, "Production of Δ^0(1232) resonances in *p* + ^{12}C collisions at a momentum of 4.2 GeV/*c*", *Eur. Phys. J. A* **47**, 79 (2011).

[19] Khusniddin K. Olimov, Mahnaz Q. Haseeb, Alisher K. Olimov, and **Imran Khan**, "Analysis of Δ^0(1232) production in collisions of protons with carbon nuclei at 4.2 GeV/*c*", *Centr. Eur. J. Phys.* **9**, 1393 (2011).

[20] Kh. K. Olimov, Mahnaz Q. Haseeb, **Imran Khan**, A. K. Olimov, and V. V. Glagolev, "Δ^0(1232) production in *d*+^{12}C collisions at 4.2 *A* GeV/*c*", *Phys. Rev. C* **85**, 014907 (2012).

[21] Kh. K. Olimov, Mahnaz Q. Haseeb and **Imran Khan**, "Comparison of Characteristics of Δ^0(1232) Produced in p^{12}C and d^{12}C Collisions at 4.2 *A* GeV/*c*", *Phys. At. Nucl*. **75,** 479 (2012).

[22] **Imran Khan** and Kh. K. Olimov, "Spectral temperatures of Δ^0(1232) resonances produced in p^{12}C and d^{12}C collisions at 4.2 GeV/*c* per nucleon", *Phys. At. Nucl*. **76,** 883 (2013).

[23] G. E. Brown and W. Weise, "Pion scattering and isobars in nuclei", *Phys. Rep.* ***22***, 279 (1975).

[24] G. Gattapan and L. S. Ferreira, "The role of the *Δ* in nuclear physics", *Phys. Rep*. **362**, 303 (2002).

[25] C. Hanhart, "Meson production in nucleon–nucleon collisions close to the threshold", *Phys. Rep*. **397**, 155 (2004).

[26] P. Braun-Munzinger and J. Stachel, "Pion production in heavy ion collisions", *Ann. Rev. Nucl. Part. Sci.* **37**, 97 (1987).

[27] Kenneth Greisen, " End to the Cosmic-Ray Spectrum?", *Phys. Rev. Lett*. **16**, 748 (1966).

[28] A. Mucke, J. P. Rachen, R. Engel, R. J. Protheroe, and T. Stanev, "On photohadronic processes in astrophysical environments", *Publ. Astron. Soc. Austral*. **16**, 160 (1999).

[29] Horst Stöcker and W. Greiner, "High energy heavy ion collisions – probing the equation of state of highly excited hardronic matter", *Phys. Rep*. **137**, 277 (1986).

[30] S. A. Bass, C. Hartnack, H. Stocker, and W. Greiner, "Azimuthal Correlations of Pions in Relativistic Heavy Ion Collisions at 1 GeV/nucleon", *Phys. Rev. C* **51**, 3343 (1995).

[31] D. Armutlisky *et al*., "Multiplicity, Momentum and Angular Distributions of Protons from the Interactions of *p, d, α* and C with Carbon at 4.2 GeV/*c*/Nucleon Momentum", *Z. Phys. A* **328**, 455 (1987).

[32] H. N. Agakishiyev *et al*., "Multiplicity, momentum and angular characteristics of π^- mesons for *p*C, *d*C, *α*C and CC interactions at 4.2 GeV/*c* per nucleon", *Z. Phys. C* **27**, 177 (1985).

[33] Ts. Baatar *et al*., "Analyzing the Features of π^- Mesons and Protons from *A*C Interactions at a Momentum of p = 4.2 GeV/*c* per Projectile Nucleon on the Basis of the FRITIOF Model", *Phys. At. Nucl*. **63**, 839 (2000).

[34] K. K. Gudima and V. D. Toneev, "Particle emission in light and heavy ion reactions", *Nucl. Phys. A* **400**, 173 (1983).

[35] B. Andersson, G. Gustafson, and B. Nilsson-Almqvist, "A model for low p_t hadronic reactions with generalizations to hadron-nucleus and nucleus-nucleus collisions", *Nucl. Phys. B* **281**, 289 (1987).

[36] N. S. Amelin, K. K. Gudima, S. Yu. Sivoklokov, and V. D. Toneev, "Further Development Of A Quark-Gluon-String Model For Describing High-Energy Collisions With A Nuclear Target", *Sov. J. Nucl. Phys*. **52**, 172 (1990).

[37] R. Hagedorn and Johann Rafelski, "Hot Hadronic Matter and Nuclear Collisions", *Phys. Lett. B* **97**, 136 (1980).

[38] R. Hagedorn and J. Ranft, "Statistical thermodynamics of strong interactions at high-energies. 2. Momentum spectra of particles produced in *pp* collisions", *Suppl. Nuovo Cimento* **6**, 169 (1968).

[39] B. Gankhuyag and V. V. Uzhinskii, "Modified FRITIOF code: Negative charged particle production in high-energy nucleus-nucleus interactions", JINR Preprint No. P2-96-419 (Dubna, Russia, 1996).

[40] A. S. Galoyan, G. L. Melkumov, and V. V. Uzhinskii, "Analysis of Charged-Particle Production in Nucleus–Nucleus Interactions near and beyond the Kinematical Limit for Free *NN* Collisions within the FRITIOF Model", *Phys. At. Nucl*. **65**, 1722 (2002).

[41] A. I. Bondarenko, R. A. Bondarenko, A. S. Galoyan, E. N. Kladnitskaya, O. V. Rogachevsky, and V. V. Uzhinskii, "Features of CC Interactions at a Momentum of 4.2 GeV/*c* per Nucleon for Various Degrees of Nuclear Collision Centrality", *Phys. At. Nucl*. **65**, 90 (2002).

[42] A. I. Malakhov, A. N. Sissakian, A. S. Sorin and S. Vokal, "Relativistic Nuclear Physics at the Joint Institute for Nuclear Research", *Physics of Elementary Particles and Nuclei* **38**, 407 (2007).

[43] A. M. Baldin *et al*., "Cumulative meson production", *Yad. Fiz*. **18** , 107 (1973); *Sov. J. Nucl. Phys.* **18**, 53 (1973).

[44] I. B. Issinsky, A. D. Kirillow, A. D. Kovalenko and P. A. Rukoyatkin, "Beams of the Dubna Synchrophasotron and Nuclotron", *Acta Physica Polonica B* **25**, 673 (1994).

[45] Donald H. Perkins, *Introduction to high energy physics*, 4th Edition, (Cambridge University Press, 2000), pp. 366-368.

[46] Gron Tudor Jones, *Archived Bubble Chamber Teaching Materials developed by HST participants*, University of Birmingham (UK), Compiled by Karl Sarnow, Gymnasium Isernhagen (Germany) and Recompiled by Vlado Grejtak (Slovakia); http://teachers.web.cern.ch/teachers/archiv/HST2005/bubble_chambers

[47] A. I. Bondarenko, R. A. Bondarenko, E. N. Kladnitskaya, A. A. Kuznetsov, G. P. Toneeva and B. S. Yuldashev, "The Ensemble of interactions on carbon and hydrogen nuclei obtained using the 2 m propane bubble chamber exposed to the

beams of protons and H-2, He-4, C-12 relativistic nuclei at the Dubna Synchrophasotron", JINR Communications P1-98-292 (Dubna, Russia, 1998).

[48] V. Flaminio *et al.*, "Compilation of cross sections: p and $\bar{p}$ induced reactions", CERN-HERA 84-01 (Geneva, 1984).

[49] V. Flaminio *et al*., "Compilation of cross Section: p and $\bar{p}$ induced reactions", CERN-HERA (Geneva, 1979).

[50] E. Bracci *et al.*, "Compilation of cross sections: p and $\bar{p}$ induced reactions", CERN-HERA 73-01 (Geneva, 1973).

[51] O. Benary *et al*., "*NN* and *ND* Interactions (above 0.5 GeV/c). A Compilation", UCRL-1000 NN (1970).

[52] A. S. Galoyan, E. N. Kladnitskaya, O. V. Rogachevsky, R. Togoo, and V. V. Uzhinskii, "Features of *p*C Interactions at a Momentum of 4.2 GeV/*c* versus the Degree of Centrality of a Collisions between a Proton and a Carbon Nucleus: Kinematical Features of Secondaries", *Phys. At. Nucl.* **67**, 256 (2004).

[53] S. Nagamiya *et al*., "Production of pions and light fragments at large angles in high-energy nuclear collisions", *Phys. Rev. C* **24**, 971 (1981).

[54] R. Malflict and Bernd Schurmann, "Unified microscopic theory of hadron and light fragment inclusive production in relativistic heavy ion collisions", *Phys. Rev. C* **31**, 1275 (1985)

[55] B. P. Adyasevich *et al*., "Universal proton rapidity distributions in high energy nucleus-nucleus collisions", *Phys. Lett. B* **161**, 55 (1985).

[56] N. Angelov *et al*., "Interaction Cross Sections and Negative pion Multiplicities in Nucleus-Nucleus Collisions at 4.2 GeV/*c* Per Nucleon", JINR Preprint No. E1-12548 (Dubna, Russia, 1979).

[57] V. V. Uzhinskii, "MODIFIED CODE FRITIOF. User's Guide", JINR Communications E2-96-192 (Dubna, Russia, 1996).

[58] B. Gankhuyag, "Description of π^- meson and proton characteristics in *np* interactions at $P(n)$=1.25-GeV/*c*–5.1-GeV/*c* within the framework of FRITIOF model", JINR Preprint P2-98-26 (Dubna, Russia, 1998).

[59] K. Abdel Waged and V. V. Uzhinskii, "Model of nuclear disintegration in high-energy nucleus-nucleus interactions", *Phys. At. Nucl*. **60**, 828 (1997).

[60] S. Yu. Shmakov *et al.*, "DIAGEN - Generator of inelastic nucleus-nucleus interaction diagrams", *Computer Physics Communications* **54**, 125 (1989).

[61] M. I. Adamovich *et al*., (EMU-01 Collaboration), **"**Complex analysis of gold interactions with photoemulsion nuclei at 10.7 GeV/nucleon within the framework of cascade and FRITIOF models", *Z. Phys. A* **358**, 337 (1997).

[62] V. Weisskopf, "Statistics and Nuclear Reactions", *Phys. Rev*. **52**, 295 (1937).

[63] V.S. Barashenkov and V. D. Toneev, *Interactions of High-Energy Particles and Nuclei with Nuclei* (Atomizdat, Moscow, 1972).

[64] N. S. Amelin, E. F. Staubo, L. P. Csernai, V. D. Toneev, and K. K. Gudima, "Strangness production in proton and heavy ion collisions at 14.6 *A* GeV", *Phys. Rev*. *C* **44**, 1541 (1991).

[65] R. Stock, "Particle production in high energy nucleus−nucleus collisions", *Phys. Rep*. **135**, 259 (1986).

[66] V. D. Toneev and K. K. Gudima, "Particle Emission In Light And Heavy Ion Reactions", *Nucl. Phys. A* **400**, 173C (1983)

[67] A. S. Botvina, K. K. Gudima, J. Steinheimer, M. Bleicher, and I. N. Mishustin, "Production of spectator hypermatter in relativistic heavy-ion collisions", *Phys. Rev*. *C* **84**, 064904 (2011)

[68] B. Nilsson-Almquist and Evert Stenlund, "Interactions Between Hadrons and Nuclei: The Lund Monte Carlo Model, FRITIOF Version 1.6", *Comput. Phys. Commun*. **43**, 387 (1987).

[69] A. S. Galoyan, E. N. Kladnitskaya, O. V. Rogachevski, R. Togoo, and V. V. Uzhinskii, "Features of *p*C Interactions at a Momentum of 4.2 GeV/*c* versus the Degree of Centrality of Collisions between Protons and Carbon Nuclei: Multiplicity of Secondary Particles", *Phys. At. Nucl*. **66**, 836 (2003)

[70] R. N. Bekmirzaev, E. N. Kladnitskaya, M. M. Muminov, and S. A. Sharipova, "Rapidity distributions of protons in (*p*, *d*, alpha, C) C interactions at 4.2 GeV/*c* per nucleon", *Phys. At. Nucl*. **58**, 1548 (1995).

[71] R. N. Bekmirzaev, E. N. Kladnitskaya and S. A. Sharipova, "Rapidity distributions of π^- mesons in (*p*, *d*, α, C) C interactions at 4.2 GeV/*c* per nucleon", *Phys. At. Nucl*. **58**, 58 (1995).

[72] D. Krpic *et al.*, "Production of $\Delta^{++}(1232)$ in carbon-carbon collisions at 4.2 GeV/*c* per nucleon", *Phys. Rev. C* **46**, 6 (1992).

[73] B. Byckling and K. Kajantie, *Particle Kinematics*, p. 119 (Wiley, London, 1973).

[74] W. Reuter, G. Fricke, K. Merle and H. Miska, "Nuclear charge distribution and rms radius of ^{12}C from absolute elastic electron scattering measurements", *Phys. Rev. C* **26**, 806 (1982).

[75] D. Pelte *et al*., (FOPI Collaboration), "Charged pion production in Au on Au collisions at 1 *A* GeV", *Z. Phys. A* **357**, 215 (1997).

[76] D. Pelte *et al*., (FOPI Collaboration), "Charged pions from Ni on Ni collisions between 1 and 2 *A* GeV", *Z. Phys. A* **359**, 55 (1997).

[77] P. D. Higgins *et al*., "Study of Δ^{++} production in $\pi^- p$ interactions at 100, 200, and 360 GeV/*c*", *Phys. Rev. D* **19**, 731 (1979).

[78] Kh. K. Olimov, "Production of Baryon Resonances in Collisions of ^{4}He Nuclei with Carbon Nuclei at a Momentum of 4.2 GeV/*c* per Nucleon", *Phys. At. Nucl*. **71**, 405 (2008).

[79] W. Weinhold, B. L. Friman, and W. Nörenberg, "Thermodynamics of an interacting πN system", *Acta Phys. Pol. B* **27**, 3249 (1996).

[80] B. Hong *et al*., (FOPI Collaboration), "Abundance of Delta resonances in Ni-58 + Ni-58 collisions between 1*A* GeV and 2 *A* GeV", *Phys. Lett. B* **407**, 115 (1997).

[81] E. L. Hjort *et al*., (EOS Collaboration), "Δ Resonance Production in ^{58}Ni + Cu Collisions at E = 1.97 *A* GeV", *Phys. Rev. Lett*. **79**, 4345 (1997).

[82] K. Olimov, A. A. Yuldashev, and B. S. Yuldashev, "The nature of fast "leading" π^+ mesons in $\pi^- N$ and π^- ^{12}C interactions at 40 GeV/*c*", *JETP Lett*. **32**, 604 (1980).

[83] N. Angelov, O. Balea, and V. Boldea, "Study Of The Production Of Meson Resonances In Pion - Carbon Interactions At P = 40 GeV/*c*", *Sov. J. Nucl. Phys*. **33**, 832 (1981); *Yad.Fiz*. **33,** 1546 (1981).

[84] J. Barrette *et al*., (E814 collaboration), "Measurement of pion enhancement at low transverse momentum and of the Δ resonance abundance in Si-nucleus collisions at AGS energy", *Phys. Lett. B* **351**, 93 (1995).

[85] B. Hong *et al*., (FOPI Collaboration), "Stopping and radial flow in central ^{58}Ni+^{58}Ni collisions between 1 *A* and 2 *A* GeV", *Phys. Rev. C* **57**, 244 (1998).

[86] G. E. Brown, J. Stachel, and G. M. Welke, "Pions from resonance decay in Brookhaven relativistic heavy-ion collisions", *Phys. Lett. B* **253**, 19 (1991).

[87] Lida Chkhaidze, Tamar Djobava, and Lali Kharkhelauri, "Temperatures of Λ Hyperons, K^0 and π^- Mesons Produced in C-C and Mg-Mg Collisions at 4.2 ÷ 4.3 *A* GeV/*c*", *Bulletin of the Georgian National Academy of Sciences* **4**, 41 (2010).

[88] S. Backovic *et al*., "Temperature of negative pions in inelastic (*d*, *α*, C) + (C, Ta) collisions at 4.2 *A* GeV/*c*", *Phys. Rev. C* **46**, 1501 (1992).

[89] L. A. Didenko, V. G. Grishin, and A. A. Kuznetsov, "Investigation of excited nuclear matter in relativistic nucleus-nucleus collisions", *Nucl. Phys. A* **525**, 653c (1991).

[90] P. Braun-Munzinger, J. Stachel, J. P. Wessels, and N. Xu, "Thermal equilibration and expansion in nucleus-nucleus collisions at the AGS", *Phys. Lett. B* **344**, 43 (1995).

[91] P. Braun-Munzinger, J. Stachel, J. P. Wessels, and N. Xu, "Thermal and hadrochemical equilibration collisions at the SPS in nucleus-nucleus collisions", *Phys. Lett. B* **365**, 1 (1996).

[92] M. A. Lisa *et al*., (EOS Collaboration), "Radial Flow in Au + Au Collisions at *E* = (0.25-1.15) *A* GeV", *Phys. Rev. Lett*. **75**, 2662 (1995).

[93] L. Chkhaidze *et al*., "The Temperatures of protons and π^- mesons in central nucleus-nucleus interactions at a momentum of 4.5 GeV/*c* per incident nucleon", *Z. Phys. C* **54**, 179 (1992).

[94] Kh. K. Olimov and Mahnaz Q. Haseeb, "On spectral temperatures of negative pions produced in d^{12}C, ^{4}He^{12}C, and ^{12}C^{12}C collisions at 4.2 *A* GeV/*c*", *Phys. At. Nucl*. **76**, 595 (2013).

[95] W. Weinhold, B. L. Friman, and W. Nörenberg, "Thermodynamics of Δ resonances", *Physics Letters B* **433**, 236 (1998).

List of Publications of PhD thesis
in HEC approved ISI indexed Impact Factor Journals

[1] Khusniddin K. Olimov, Mahnaz Q. Haseeb, Alisher K. Olimov and **Imran Khan**, "Analysis of $\Delta^0(1232)$ production in collisions of protons with carbon nuclei at 4.2 GeV/*c*", *Centr. Eur. J. Phys.* **9**(6), 1393 (2011).
DOI: 10.2478/s11534-011-0048-x, Impact Factor =0.905 (2012).

[2] Kh. K. Olimov, Mahnaz Q. Haseeb, **Imran Khan**, A. K. Olimov and V. V. Glagolev, "$\Delta^0(1232)$ production in $d+^{12}C$ collisions at 4.2 *A* GeV/*c*", *Phys. Rev. C* **85**, 014907 (2012).
DOI: 10.1103/PhysRevC.85.014907, Impact Factor = 3.715 (2012).

[3] Kh. K. Olimov, Mahnaz Q. Haseeb and **Imran Khan**, "Comparison of Characteristics of $\Delta^0(1232)$ Produced in $p^{12}C$ and $d^{12}C$ Collisions at 4.2 *A* GeV/*c*", *Phys. At. Nucl*. **75**(4), 479 (2012).
DOI:10.1134/S1063778812040126, Impact Factor = 0.539 (2012).

[4] **Imran Khan** and Kh. K. Olimov, "Spectral temperatures of $\Delta^0(1232)$ resonances produced in $p^{12}C$ and $d^{12}C$ collisions at 4.2 GeV/*c* per nucleon", *Phys. At. Nucl*. **76,** 883 (2013).
DOI: 10.1134/S1063778813070089, Impact Factor = 0.539 (2012).

List of Oral and Poster Presentations of PhD thesis in various Physics Conferences

[1] **Imran Khan** and Khusniddin K. Olimov, "*Some properties of Δ^0(1232) production in d+^{12}C collisions at 4.2 A GeV/c*", Talk Presented at International Scientific Spring (ISS-2012), March 05-09, 2012, Islamabad, Pakistan, organized jointly by National Centre for Physics (NCP), Islamabad, Pakistan and International Center for Theoretical Physics (ICTP), Trieste, Italy.

[2] Khusniddin K. Olimov, Mahnaz Q. Haseeb, and **Imran Khan**, "*Comparative analysis of the properties of Δ^0(1232) resonances produced in p+^{12}C and d+^{12}C collisions at 4.2 GeV/c per nucleon*", Talk Presented at International Scientific Spring (ISS-2012), March 05-09, 2012, Islamabad, Pakistan, organized jointly by National Centre for Physics (NCP), Islamabad, Pakistan and International Center for Theoretical Physics (ICTP), Trieste, Italy.

[3] **Imran Khan**, Khusniddin K. Olimov and Mahnaz Q. Haseeb, "*Some properties of Δ^0(1232)-resonances produced in p+^{12}C collisions at 4.2 GeV/c*", Poster presented at 37th International Nathiagali Summer College (INSC), 25th June to 7th July, 2012, Nathiagali, Pakistan, organized jointly by Pakistan Atomic Energy Commission (PAEC) and National Centre for Physics (NCP), Islamabad, Pakistan.

[4] Khusniddin K. Olimov and **Imran Khan**, "*About the spectral temperatures of Δ^0(1232) produced in p^{12}C and d^{12}C collisions at 4.2 A GeV/c*", Talk Presented at VI Eurasian Conference, Nuclear Science and Its Application, September 25-28, 2012, Samarkand, Uzbekistan organized by Institute of Nuclear Physics, Uzbekistan Academy of Sciences, Uzbekistan.

[5] **Imran Khan** and Khusniddin K. Olimov, "*Analysis of Δ^0(1232) Production in p+^{12}C and d+^{12}C Collisions at 4.2 GeV/c Per Nucleon*", Talk Presented at 13TH NATIONAL SYMPOSIUM ON FRONTIERS IN PHYSICS, University of Peshawar, Peshawar, Pakistan, December 19-21, 2012 organized jointly by Pakistan Physical Society and University of Peshawar.

[6] **Imran Khan** and Khusniddin K. Olimov, "*Production of $\Delta^0(1232)$ resonances in $p+^{12}C$ and $d+^{12}C$ collisions at 4.2 A GeV/c*", Talk Presented at International Scientific Spring (ISS-2013), March 11-15, 2013, Islamabad, Pakistan, organized jointly by National Centre for Physics (NCP), Islamabad, Pakistan and International Center for Theoretical Physics (ICTP), Trieste, Italy.

[7] **Imran Khan** and Khusniddin K. Olimov, "*About the temperatures of $\Delta^0(1232)$ resonances produced in $p+^{12}C$ and $d+^{12}C$ collisions at 4.2 GeV/c per nucleon*", Talk Presented at 5^{th} International Meeting on Particles and Fields, 25^{th} – 28^{th} March, 2013, Center for High Energy Physics (CHEP), University of the Punjab, Lahore, Pakistan.

Hard Copies of Research Papers of PhD thesis
Published in HEC Recognized ISI indexed Impact Factor International Journals